

A Genetic model for Neurorehabilitation

Ricardo Duarte Custódio

**A dissertation submitted in partial fulfillment of the requirements for the Degree of
Masters in Biomedical Research**

Dissertação para obtenção do grau de Mestre em Investigação Biomédica

at Faculdade de Ciências Médicas | NOVA Medical School of NOVA University Lisbon

9/2019

A genetic model for neurorehabilitation

Ricardo Duarte Custódio
César Mendes, PhD, CEDOC

**A dissertation submitted in partial fulfillment of the requirements for the Degree of
Masters in Biomedical Research**

Dissertação para obtenção do grau de Mestre em Investigação Biomédica

9/2019

INDEX

<i>Index of Figures</i>	6
<hr/> <hr/>	
<i>Acknowledgements</i>	11
<hr/> <hr/>	
<i>Abstract</i>	14
<hr/> <hr/>	
<i>Introduction</i>	15
<hr/> <hr/>	
<i>Motion: the basics</i>	15
<hr/> <hr/>	
<i>Movement coordination</i>	15
<hr/> <hr/>	
<i>Frankenstein's monster, rise: purpose as the soul in eliciting movement</i>	16
<hr/> <hr/>	
<i>Adaptive motor learning</i>	17
<hr/> <hr/>	
<i>Studying movement on the fly</i>	18
<hr/> <hr/>	
<i>Approaches to studying locomotion and adaptive motor learning on the fly</i>	19
<hr/> <hr/>	
<i>Drosophila orthologs of motor adaptation mechanisms</i>	19
<hr/> <hr/>	
<i>Learning and Memory in Drosophila melanogaster</i>	20
<hr/> <hr/>	
<i>Memory phases in Drosophila melanogaster</i> ⁵⁵	22
<hr/> <hr/>	
<i>Aims</i>	24
<hr/> <hr/>	
<i>Materials and methods</i>	25
<hr/> <hr/>	
<i>FlyWalker</i>	25
<hr/> <hr/>	
.....	25
<hr/> <hr/>	
<i>FlyWalker Parameter List and Definitions</i>	26
<hr/> <hr/>	
Gait Parameters.....	26
<hr/> <hr/>	
Step Parameters	26
<hr/> <hr/>	
Spatial Parameters	26
<hr/> <hr/>	
Stability Parameters	27
<hr/> <hr/>	
<i>Fly Handling</i>	28
<hr/> <hr/>	
Fly table	28
<hr/> <hr/>	
Fly Rearing	28
<hr/> <hr/>	
Middle-leg amputation.....	29
<hr/> <hr/>	
Dealing with non- <i>Drosophila melanogaster</i> species	30
<hr/> <hr/>	
<i>Behavioral assays</i>	30
<hr/> <hr/>	
Cycloheximide experiment.....	30

Cycloheximide mixture	30
Rearing.....	30
Test groups	31
Video recordings.....	31
<i>Video Cropping</i>	32
<i>FlyWalker Software Video Analysis</i>	34
<i>Data handling</i>	35
<i>Residual analysis</i>	35
<i>Statistical analysis</i>	36
Results	37
<i>Wild type Drosophila melanogaster Canton-S flies show locomotor recovery in response to double middle-leg amputation</i>	37
Stability parameters	37
Spatial parameters	38
.....	40
Step parameters	40
Gait parameters.....	41
Summary	42
<i>Locomotor recovery from double mid-leg amputation is conserved across two evolutionarily distant Drosophila species</i>	43
Stability parameters	43
Spatial Parameters	45
Step Parameters	46
Summary	48
<i>Dissecting the cAMP cascade of the learning and memory pathway</i>	49
<i>amnesiac</i> ¹	49
Stability parameters	49
Spatial Parameters	50
Step Parameters	51
Summary	53
<i>rutabaga</i> ¹	54
Step Parameters	54

Spatial Parameters	56
Stability Parameters	57
Summary	58
<i>dunce</i> ¹	59
Stability parameters	59
Step parameters	60
Spatial parameters	61
Summary	62
<i>radish</i> ¹	62
Stability parameters	63
Step Parameters	65
Spatial Parameters	66
Summary	67
<i>The effects of cycloheximide on motor learning</i>	68
<i>Effects of Cycloheximide on motor behavior</i>	68
Step parameters	69
Spatial parameters	69
Stability parameters	69
<i>Effects of CHX and EtOH on motor learning</i>	70
Spatial parameters	70
Stability parameters	71
Summary	71
Discussion	72
<i>Drosophila melanogaster, repleta and pseudoobscura: patterns of locomotor recovery</i>	72
<i>Dissecting the cAMP learning and memory cascade: amn¹, rut¹, dnc¹,rsh¹ and de novo protein synthesis</i>	73
Conclusions / future perspectives	77
Bibliography	79

INDEX OF FIGURES

- Figure 1. Memory phases of olfactory memory in *Drosophila melanogaster* ⁵²22
- Figure 2. The Flywalker system. A) Schematic of the fTIR optical LED light sources are located at the edges of an optical glass and light propagates within the glass via internal reflection. Tarsal contacts lead to light scattering detected by a high-speed camera. B) fTIR apparatus with fly tunnel in the center of the optical glass. C) single frame of a fTIR video. the fTIR effect can be seen for three legs in the stance phase (yellow arrows). background light partially illuminates the fly's body (orange dashed ellipse; the center of the body is indicated by an orange cross). D) image generated by the flywalker software. the fly's footprints and body center are tracked throughout the video. present footprints are identified and labeled (yellow arrows). The fly body and trajectory are visualized by a blue line (white arrow). past footprints can also be recorded (red arrows). A scale bar can be introduced. step length is defined as the distance between two consecutive footprints (green arrows).25
- Figure 3. Protocol for the Cycloheximide experiment. The effect of cycloheximide on Canton-S flies was filmed in unamputated (top) and amputated (bottom) conditions at different timepoints, however, only the 72h timepoint was analyzed for this report.31
- Figure 4. *Drosophila melanogaster* wild type Canton-S Stability parameters. A) Body traces for the wild type Canton-S at three timepoints: Unamputated (N=5, n=10), 15 minutes post-amputation (N=5, n=10) and 7 days post-amputation (N=9, n=18). x (0 -> 14000 μm) and y-axis (-2000 -> 2000 μm) are the horizontal and vertical distance travelled by the flies. B) Quantification of wild type Canton-S 's Body Path (μm) via residual analysis vs unamputated control group. C) Quantification of wild type Canton-S's Body Displacement Ratio (body units) via residual analysis vs unamputated control group. D) Quantification of wild type Canton-S's Body Path (μm) via residual analysis vs unamputated control group. Data distribution assessed by D'Agostino Pearson and Shapiro-Wilk normality tests. Multiple comparison tests performed according to patterns of data distribution, either parametric (One-Way ANOVA for normally distributed data; Holm-Sidak's test for multiple comparisons) or non-parametric (Kruskal-Wallis test for abnormally distributed data and Dunn's test for multiple comparisons). Statistical significances resulting from multiple comparison tests are as follows: ****, $P \leq 0,0001$; ***, $P \leq 0,001$; **, $P \leq 0,01$; *, $P \leq 0,05$; ns, $P > 0,05$. Box-plot positioning above or below the x-axis reflects a respective increase or decrease of the analyzed parameter vs the unamputated control group.38
- Figure 5. *Drosophila melanogaster* wild type Canton-S Spatial parameters. A) Wild type Canton-S visual representation of AEP footprint clustering and stance traces for single flies within the median value of AEP footprint clustering for the analysed groups: Unamputated; 15minutes, 72 hours and 7days post-amputation. Body size represents a body unit. B) Quantification of wild type Canton-S's footprint clustering of Anterior Extreme Positions (body units) via residual analysis vs unamputated control group. C) Quantification of wild type Canton-S's footprint clustering of Posterior Extreme Positions (body units) via residual analysis vs unamputated control group. D) Quantification of wild type Canton-S's Average Stance Straightness (body units) via residual analysis vs unamputated control group. E) Quantification of wild type Canton-S's Average Stance Linearity (body units) via residual analysis vs unamputated control group. Data distribution assessed by D'Agostino Pearson and Shapiro-Wilk normality tests. Multiple comparison tests performed according to patterns of data distribution, either parametric (One-Way ANOVA for normally distributed data; Holm-Sidak's test for multiple comparisons) or non-parametric (Kruskal-Wallis test for abnormally distributed data and Dunn's test for multiple comparisons). Statistical significances resulting from multiple comparison tests are as follows: ****, $P \leq 0,0001$; ***, $P \leq 0,001$; **, $P \leq 0,01$; *, $P \leq 0,05$; ns, $P > 0,05$. Box-plot positioning, either above or below the x-axis, reflects a respective increase or decrease of the analyzed parameter vs the unamputated control group.40
- Figure 6. *Drosophila melanogaster* wild type Canton-S Step parameters. A) Quantification of wild type Canton-S's Average Step Length (μm) via residual analysis vs unamputated control group. B) Quantification of wild type Canton-S's Leg Displacement (μm) via residual analysis vs unamputated control group. C) Quantification of wild type Canton-S's Step Frequency (step cycles.s⁻¹) via residual analysis vs unamputated control group. Data distribution assessed by D'Agostino Pearson and Shapiro-Wilk normality tests. Multiple comparison tests performed according to patterns of data distribution, either parametric (One-Way ANOVA for normally distributed data; Holm-Sidak's test for multiple comparisons) or non-parametric (Kruskal-Wallis test for abnormally distributed data and Dunn's test for multiple comparisons). Statistical significances resulting from multiple comparison tests are as follows: ****, $P \leq 0,0001$; ***, $P \leq 0,001$; **, $P \leq 0,01$; *, $P \leq 0,05$; ns, $P > 0,05$. Box-plot positioning above or below the x-axis reflects a respective increase or decrease of the analyzed parameter vs the unamputated control group40
- Figure 7. *Drosophila melanogaster* wild type Canton-S heatmap of all residual data from comparison to unamputated flies of the same genotype. tested locomotor parameters in the following order: Step, Spatial, Gait Parameters and Stability parameters. Data distribution assessed by D'Agostino Pearson and Shapiro-Wilk normality tests. Multiple comparison tests performed according to patterns of data distribution, either parametric (One-Way ANOVA for normally distributed data; Holm-Sidak's test for multiple comparisons) or non-parametric (Kruskal-Wallis test for abnormally distributed data and Dunn's test for multiple comparisons). Bonferroni correction was applied to the multiple comparisons. Statistical significances resulting from multiple comparison tests are as follows: ****, $P \leq 0,0001$ and ***, $P \leq 0,001$, deep red and deep blue; **, $P \leq 0,01$, red and blue; *, $P \leq 0,05$, pale red and pale blue; ns, $P > 0,05$, white.41

Figure 8. *Drosophila repleta* and *pseudoobscura* Stability parameters. A,B) Body traces for *Drosophila repleta* and *pseudoobscura* at three timepoints: Unamputated (N=5, n=10), 15 minutes post-amputation (N=5, n=10) and 7 days post-amputation (N=9, n=18). x (0 ->14000 μm) and y-axis (-2000 -> 2000 μm) are the horizontal and vertical distance travelled by the flies. C,D) Quantification of *Drosophila repleta*'s and *pseudoobscura*'s Body Path (μm) via residual analysis vs unamputated control group. E,F) Quantification of *Drosophila repleta*'s and *pseudoobscura*'s Body Displacement Ratio (body units) via residual analysis vs unamputated control group. G,H) Quantification of *Drosophila repleta*'s and *pseudoobscura*'s Body Displacement Ratio (body units) via residual analysis vs unamputated control group. Data distribution assessed by D'Agostino Pearson and Shapiro-Wilk normality tests. Multiple comparison tests performed according to patterns of data distribution, either parametric (One-Way ANOVA for normally distributed data; Holm-Sidak's test for multiple comparisons) or non-parametric (Kruskal-Wallis test for abnormally distributed data and Dunn's test for multiple comparisons). Statistical significances resulting from multiple comparison tests are as follows: ****, P≤0,0001; ***, P≤0,001; **, P≤0,01; *, P≤0,05; ns, P>0,05. Box-plot positioning above or below the x-axis reflects a respective increase or decrease of the analyzed parameter vs the unamputated control group.....45

Figure 9. *Drosophila repleta* and *pseudoobscura* Spatial parameters. A,B) *Drosophila repleta* and *pseudoobscura* visual representation of AEP footprint clustering and stance traces for single flies within the median value of AEP footprint clustering for the analysed groups: Unamputated; 15minutes, 72 hours and 7days post-amputation. Body size represents a body unit. C,D) Quantification of *Drosophila repleta*'s and *pseudoobscura*'s footprint clustering of Anterior Extreme Positions (body units) via residual analysis vs unamputated control group. E,F) Quantification of *Drosophila repleta*'s and *pseudoobscura*'s Average Stance Straightness (body units) via residual analysis vs unamputated control group. Data distribution assessed by D'Agostino Pearson and Shapiro-Wilk normality tests. Multiple comparison tests performed according to patterns of data distribution, either parametric (One-Way ANOVA for normally distributed data; Holm-Sidak's test for multiple comparisons) or non-parametric (Kruskal-Wallis test for abnormally distributed data and Dunn's test for multiple comparisons). Statistical significances resulting from multiple comparison tests are as follows: ****, P≤0,0001; ***, P≤0,001; **, P≤0,01; *, P≤0,05; ns, P>0,05. Box-plot positioning, either above or below the x-axis, reflects a respective increase or decrease of the analyzed parameter vs the unamputated control group.46

Figure 10. *Drosophila repleta* and *pseudoobscura* Step parameters. A,B) Quantification of *Drosophila repleta*'s and *pseudoobscura*'s Step Frequency (step cycles.s⁻¹) via residual analysis vs unamputated control group. C,D) Quantification of *Drosophila repleta*'s and *pseudoobscura*'s Step Period (milliseconds) via residual analysis vs unamputated control group. E,F) Quantification of *Drosophila repleta*'s and *pseudoobscura*'s Average Stance Duration (seconds) via residual analysis vs unamputated control group. Data distribution assessed by D'Agostino Pearson and Shapiro-Wilk normality tests. Multiple comparison tests performed according to patterns of data distribution, either parametric (One-Way ANOVA for normally distributed data; Holm-Sidak's test for multiple comparisons) or non-parametric (Kruskal-Wallis test for abnormally distributed data and Dunn's test for multiple comparisons). Statistical significances resulting from multiple comparison tests are as follows: ****, P≤0,0001; ***, P≤0,001; **, P≤0,01; *, P≤0,05; ns, P>0,05. Box-plot positioning above or below the x-axis reflects a respective increase or decrease of the analyzed parameter vs the unamputated control group.47

Figure 11. a,b) *Drosophila repleta* and *pseudoobscura* heatmap of all residual data from comparison to unamputated flies of the same genotype. tested locomotor parameters in the following order: Step, Spatial and Stability parameters. Data distribution assessed by D'Agostino Pearson and Shapiro-Wilk normality tests. Multiple comparison tests performed according to patterns of data distribution, either parametric (One-Way ANOVA for normally distributed data; Holm-Sidak's test for multiple comparisons) or non-parametric (Kruskal-Wallis test for abnormally distributed data and Dunn's test for multiple comparisons). Bonferroni correction was applied to the multiple comparisons. Statistical significances resulting from multiple comparison tests are as follows: ****, P≤0,0001 and ***, P≤0,001, deep red and deep blue; **, P≤0,01, red and blue; *, P≤0,05, pale red and pale blue; ns, P>0,05, white.48

Figure 12. *Amnesiac*¹ Stability parameters. A,B) Body traces in the form of lines and heatmap for *Amnesiac*¹ at three timepoints: Unamputated (N=5, n=10), 15 minutes post-amputation (N=5, n=10) and 7 days post-amputation (N=9, n=18). x (0 ->14000 μm) and y-axis (-2000 -> 2000 μm) are the horizontal and vertical distance travelled by the flies. Increase in colour brightness represents coordinates in which more flies passed through. C) Quantification of *Amnesiac*¹'s Body Path (μm) via residual analysis vs unamputated control group. D) Quantification of *Amnesiac*¹'s Body Displacement Ratio via residual analysis vs unamputated control group. E) Quantification of *Amnesiac*¹'s average area of all configurations (body units) via residual analysis vs unamputated control group. Data distribution assessed by D'Agostino Pearson and Shapiro-Wilk normality tests. Multiple comparison tests performed according to patterns of data distribution, either parametric (One-Way ANOVA for normally distributed data; Holm-Sidak's test for multiple comparisons) or non-parametric (Kruskal-Wallis test for abnormally distributed data and Dunn's test for multiple comparisons). Statistical significances resulting from multiple comparison tests are as follows: ****, P≤0,0001; ***, P≤0,001; **, P≤0,01; *, P≤0,05; ns, P>0,05. Box-plot positioning above or below the x-axis reflects a respective increase or decrease of the analyzed parameter vs the unamputated control group.....50

Figure 13. *Amnesiac*¹ Spatial parameters. A) *Amnesiac*¹ visual representation of AEP footprint clustering and stance traces for single flies within the median value of AEP footprint clustering for the analysed groups: Unamputated; 15minutes, 72 hours and 7days post-amputation. Body size represents a body unit. B) Quantification of *Amnesiac*¹'s footprint clustering of Anterior Extreme Positions (body units) via residual analysis vs unamputated control group. C) Quantification of *Amnesiac*¹'s footprint clustering of Posterior Extreme Positions (body units) via residual analysis vs unamputated control group. D) Quantification of

*Amnesiac*¹'s Average Stance Straightness (body units) via residual analysis vs unamputated control group. E) Quantification of *Amnesiac*¹'s Average Stance Linearity (body units) via residual analysis vs unamputated control group. Data distribution assessed by D'Agostino Pearson and Shapiro-Wilk normality tests. Multiple comparison tests performed according to patterns of data distribution, either parametric (One-Way ANOVA for normally distributed data; Holm-Sidak's test for multiple comparisons) or non-parametric (Kruskal-Wallis test for abnormally distributed data and Dunn's test for multiple comparisons). Statistical significances resulting from multiple comparison tests are as follows: ****, P≤0,0001; ***, P≤0,001; **, P≤0,01; *, P≤0,05; ns, P>0,05. Box-plot positioning, either above or below the x-axis, reflects a respective increase or decrease of the analyzed parameter vs the unamputated control group.51

Figure 14. *Amnesiac*¹ Step parameters. A) Quantification of *Amnesiac*¹'s Average swing duration (seconds) via residual analysis vs unamputated control group. B) Quantification of *Amnesiac*¹'s Leg Displacement (µm) via residual analysis vs unamputated control group. C) Quantification of *Amnesiac*¹'s Average Step Length (µmeters) via residual analysis vs unamputated control group. D) Quantification of *Amnesiac*¹'s Stance duration (S) via residual analysis vs unamputated control group. E) Quantification of *Amnesiac*¹'s Step Frequency (step cycles.s⁻¹) via residual analysis vs unamputated control group. F) Quantification of *Amnesiac*¹'s Step period (milliseconds) via residual analysis vs unamputated control group. Data distribution assessed by D'Agostino Pearson and Shapiro-Wilk normality tests. Multiple comparison tests performed according to patterns of data distribution, either parametric (One-Way ANOVA for normally distributed data; Holm-Sidak's test for multiple comparisons) or non-parametric (Kruskal-Wallis test for abnormally distributed data and Dunn's test for multiple comparisons). Statistical significances resulting from multiple comparison tests are as follows: ****, P≤0,0001; ***, P≤0,001; **, P≤0,01; *, P≤0,05; ns, P>0,05. Box-plot positioning above or below the x-axis reflects a respective increase or decrease of the analyzed parameter vs the unamputated control group.52

Figure 15. *Amnesiac*¹ heatmap of all residual data from comparison to unamputated flies of the same genotype. tested locomotor parameters in the following order: Step, Spatial and Stability parameters. Data distribution assessed by D'Agostino Pearson and Shapiro-Wilk normality tests. Multiple comparison tests performed according to patterns of data distribution, either parametric (One-Way ANOVA for normally distributed data; Holm-Sidak's test for multiple comparisons) or non-parametric (Kruskal-Wallis test for abnormally distributed data and Dunn's test for multiple comparisons). Bonferroni correction was applied to the multiple comparisons. Statistical significances resulting from multiple comparison tests are as follows: ****, P≤0,0001 and ***, P≤0,001, deep red and deep blue; **, P≤0,01, red and blue; *, P≤0,05, pale red and pale blue; ns, P>0,05, white.53

Figure 16. *Rutabaga*¹ Step parameters. A) Quantification of *Rutabaga*¹'s Average swing duration (seconds) via residual analysis vs unamputated control group. B) Quantification of *Rutabaga*¹'s Step length (µmeters) via residual analysis vs unamputated control group. C) Quantification of *Rutabaga*¹'s Average swing speed (millimeters per second) via residual analysis vs unamputated control group. Data distribution assessed by D'Agostino Pearson and Shapiro-Wilk normality tests. Multiple comparison tests performed according to patterns of data distribution, either parametric (One-Way ANOVA for normally distributed data; Holm-Sidak's test for multiple comparisons) or non-parametric (Kruskal-Wallis test for abnormally distributed data and Dunn's test for multiple comparisons). Statistical significances resulting from multiple comparison tests are as follows: ****, P≤0,0001; ***, P≤0,001; **, P≤0,01; *, P≤0,05; ns, P>0,05. Box-plot positioning above or below the x-axis reflects a respective increase or decrease of the analyzed parameter vs the unamputated control group.55

Figure 17. *Rutabaga*¹ Spatial parameters. A) *Rutabaga*¹ visual representation of AEP footprint clustering and stance traces for single flies within the median value of AEP footprint clustering for the analysed groups: Unamputated; 15minutes, 72 hours and 7days post-amputation. Body size represents a body unit. B) Quantification of *Rutabaga*¹'s footprint clustering of Anterior Extreme Positions (body units) via residual analysis vs unamputated control group. C) Quantification of *Rutabaga*¹'s footprint clustering of Posterior Extreme Positions (body units) via residual analysis vs unamputated control group. Data distribution assessed by D'Agostino Pearson and Shapiro-Wilk normality tests. Multiple comparison tests performed according to patterns of data distribution, either parametric (One-Way ANOVA for normally distributed data; Holm-Sidak's test for multiple comparisons) or non-parametric (Kruskal-Wallis test for abnormally distributed data and Dunn's test for multiple comparisons). Statistical significances resulting from multiple comparison tests are as follows: ****, P≤0,0001; ***, P≤0,001; **, P≤0,01; *, P≤0,05; ns, P>0,05. Box-plot positioning, either above or below the x-axis, reflects a respective increase or decrease of the analyzed parameter vs the unamputated control group.56

Figure 18. *Rutabaga*¹ Stability parameters. A,B) Body traces in the form of lines and heatmap for *Rutabaga*¹ at three timepoints: Unamputated (N=5, n=10), 15 minutes post-amputation (N=5, n=10) and 7 days post-amputation (N=9, n=18). x (0 ->14000 µm) and y-axis (-2000 -> 2000 µm) are the horizontal and vertical distance travelled by the flies. Increase in colour brightness represents coordinates in which more flies passed through. C) Quantification of *Rutabaga*¹'s average onset ratio (frames) via residual analysis vs unamputated control group. D) Quantification of *Rutabaga*¹'s stability Ratio (frames) via residual analysis vs unamputated control group. Data distribution assessed by D'Agostino Pearson and Shapiro-Wilk normality tests. Multiple comparison tests performed according to patterns of data distribution, either parametric (One-Way ANOVA for normally distributed data; Holm-Sidak's test for multiple comparisons) or non-parametric (Kruskal-Wallis test for abnormally distributed data and Dunn's test for multiple comparisons). Statistical significances resulting from multiple comparison tests are as follows: ****, P≤0,0001; ***, P≤0,001; **, P≤0,01; *, P≤0,05; ns, P>0,05. Box-plot positioning above or below the x-axis reflects a respective increase or decrease of the analyzed parameter vs the unamputated control group.57

- Figure 19.** Rutabaga¹ heatmap of all residual-tested locomotor parameters in the following order: Step, Spatial and Stability parameters. **Data distribution** assessed by D’Agostino Pearson and Shapiro-Wilk normality tests. **Multiple comparison** tests performed according to patterns of data distribution, either parametric (One-Way ANOVA for normally distributed data; Holm-Sidak’s test for multiple comparisons) or non-parametric (Kruskal-Wallis test for abnormally distributed data and Dunn’s test for multiple comparisons). Bonferroni **correction** was applied to the multiple comparisons. **Statistical significances** resulting from multiple comparison tests are as follows: ****, P≤0,0001 and ***, P≤0,001, deep red and deep blue; **, P≤0,01, red and blue; *, P≤0,05, pale red and pale blue; ns, P>0,05, white.58
- Figure 20.** *Dunce*¹ Stability parameters. A,B) Body traces in the form of lines and heatmap for *Dunce*¹ at three timepoints: Unamputated (N=5, n=10), 15 minutes post-amputation (N=5, n=10) and 7 days post-amputation (N=9, n=18). x (0 ->14000 μm) and y-axis (-2000 -> 2000 μm) are the horizontal and vertical distance travelled by the flies. Increase in colour brightness represents coordinates in which more flies passed through. C) Quantification of *Dunce*¹’s Body displacement (μmeters) via residual analysis vs unamputated control group. D) Quantification of *dunce*¹’s Body path (μmeters) via residual analysis vs unamputated control group. E) Quantification of *dunce*¹’s Body Displacement Ratio (body units) via residual analysis vs unamputated control group. Data distribution assessed by D’Agostino Pearson and Shapiro-Wilk normality tests. Multiple comparison tests performed according to patterns of data distribution, either parametric (One-Way ANOVA for normally distributed data; Holm-Sidak’s test for multiple comparisons) or non-parametric (Kruskal-Wallis test for abnormally distributed data and Dunn’s test for multiple comparisons). Statistical significances resulting from multiple comparison tests are as follows: ****, P≤0,0001; ***, P≤0,001; **, P≤0,01; *, P≤0,05; ns, P>0,05. Box-plot positioning above or below the x-axis reflects a respective increase or decrease of the analyzed parameter vs the unamputated control group.60
- Figure 21.** *dunce*¹ Step parameters. A) Quantification of *Dunce*¹’s Step length (μmeters) via residual analysis vs unamputated control group. B) Quantification of *Dunce*¹’s step period (milliseconds) via residual analysis vs unamputated control group. C) Quantification of *Dunce*¹’s step frequency (step cycles per second) via residual analysis vs unamputated control group. D) Quantification of *Dunce*¹’s average swing duration (seconds) via residual analysis vs unamputated control group. E) Quantification of *Dunce*¹’s average stance duration (seconds) via residual analysis vs unamputated control group. Data distribution assessed by D’Agostino Pearson and Shapiro-Wilk normality tests. Multiple comparison tests performed according to patterns of data distribution, either parametric (One-Way ANOVA for normally distributed data; Holm-Sidak’s test for multiple comparisons) or non-parametric (Kruskal-Wallis test for abnormally distributed data and Dunn’s test for multiple comparisons). Statistical significances resulting from multiple comparison tests are as follows: ****, P≤0,0001; ***, P≤0,001; **, P≤0,01; *, P≤0,05; ns, P>0,05. Box-plot positioning above or below the x-axis reflects a respective increase or decrease of the analyzed parameter vs the unamputated control group.61
- Figure 22.** *Dunce*¹ Spatial parameters. A) *Dunce*¹ visual representation of AEP footprint clustering and stance traces for single flies within the median value of AEP footprint clustering for the analysed groups: Unamputated; 15minutes, 72 hours and 7days post-amputation. Body size represents a body unit. B) Quantification of *dunce*¹’s footprint clustering of Anterior Extreme Positions (body units) via residual analysis vs unamputated control group. C) Quantification of *dunce*¹’s footprint clustering of Posterior Extreme Positions (body units) via residual analysis vs unamputated control group. D) Quantification of *dunce*¹’s Average stance straightness (μmeters) via residual analysis vs unamputated control group. Data distribution assessed by D’Agostino Pearson and Shapiro-Wilk normality tests. Multiple comparison tests performed according to patterns of data distribution, either parametric (One-Way ANOVA for normally distributed data; Holm-Sidak’s test for multiple comparisons) or non-parametric (Kruskal-Wallis test for abnormally distributed data and Dunn’s test for multiple comparisons). Statistical significances resulting from multiple comparison tests are as follows: ****, P≤0,0001; ***, P≤0,001; **, P≤0,01; *, P≤0,05; ns, P>0,05. Box-plot positioning, either above or below the x-axis, reflects a respective increase or decrease of the analyzed parameter vs the unamputated control group.62
- Figure 23.** *Dunce*¹ heatmap of all residual data from comparison to unamputated flies of the same genotype tested locomotor parameters in the following order: Step, Spatial and Stability parameters. Data distribution assessed by D’Agostino Pearson and Shapiro-Wilk normality tests. Multiple comparison tests performed according to patterns of data distribution, either parametric (One-Way ANOVA for normally distributed data; Holm-Sidak’s test for multiple comparisons) or non-parametric (Kruskal-Wallis test for abnormally distributed data and Dunn’s test for multiple comparisons). Bonferroni correction was applied to the multiple comparisons. Statistical significances resulting from multiple comparison tests are as follows: ****, P≤0,0001 and ***, P≤0,001, deep red and deep blue; **, P≤0,01, red and blue; *, P≤0,05, pale red and pale blue; ns, P>0,05, white.62
- Figure 24.** *Radish*¹ Stability parameters. A,B) Body traces in the form of lines and heatmap for *Dunce*¹ at three timepoints: Unamputated (N=5, n=10), 15 minutes post-amputation (N=5, n=10) and 7 days post-amputation (N=9, n=18). x (0 ->14000 μm) and y-axis (-2000 -> 2000 μm) are the horizontal and vertical distance travelled by the flies. Increase in colour brightness represents coordinates in which more flies passed through. C) Quantification of *Radish*¹’s Body Path (μm) via residual analysis vs unamputated control group. D) Quantification of *Radish*¹’s Body Displacement Ratio (body units) via residual analysis vs unamputated control group. E) Quantification of *Radish*¹’s Body Displacement Ratio (body units) via residual analysis vs unamputated control group. Data distribution assessed by D’Agostino Pearson and Shapiro-Wilk normality tests. Multiple comparison tests performed according to patterns of data distribution, either parametric (One-Way ANOVA for normally distributed data; Holm-Sidak’s test for multiple comparisons) or non-parametric (Kruskal-Wallis test for abnormally distributed data and Dunn’s test for multiple comparisons). Statistical significances resulting from multiple comparison tests are as

- follows: ****, $P \leq 0,0001$; ***, $P \leq 0,001$; **, $P \leq 0,01$; *, $P \leq 0,05$; ns, $P > 0,05$. Box-plot positioning above or below the x-axis reflects a respective increase or decrease of the analyzed parameter vs the unamputated control group.....64
- Figure 25. *Radish*¹ Step parameters. A) Quantification of *Radish*¹'s average swing speed (millimeters per second) via residual analysis vs unamputated control group. B) Quantification of *Radish*¹ duty factor (frames) via residual analysis vs unamputated control group. C) Quantification of *Radish*¹'s Average step frequency (step cycles per second) via residual analysis vs unamputated control group. Data distribution assessed by D'Agostino Pearson and Shapiro-Wilk normality tests. Multiple comparison tests performed according to patterns of data distribution, either parametric (One-Way ANOVA for normally distributed data; Holm-Sidak's test for multiple comparisons) or non-parametric (Kruskal-Wallis test for abnormally distributed data and Dunn's test for multiple comparisons). Statistical significances resulting from multiple comparison tests are as follows: ****, $P \leq 0,0001$; ***, $P \leq 0,001$; **, $P \leq 0,01$; *, $P \leq 0,05$; ns, $P > 0,05$. Box-plot positioning above or below the x-axis reflects a respective increase or decrease of the analyzed parameter vs the unamputated control group.65
- Figure 26. *radish*¹ Spatial parameters. A) *radish*¹ visual representation of AEP footprint clustering and stance traces for single flies within the median value of AEP footprint clustering for the analysed groups: Unamputated; 15minutes, 72 hours and 7days post-amputation. Body size represents a body unit. B) Quantification of *radish*¹'s footprint clustering of posterior Extreme Positions (body units) via residual analysis vs unamputated control group. Data distribution assessed by D'Agostino Pearson and Shapiro-Wilk normality tests. Multiple comparison tests performed according to patterns of data distribution, either parametric (One-Way ANOVA for normally distributed data; Holm-Sidak's test for multiple comparisons) or non-parametric (Kruskal-Wallis test for abnormally distributed data and Dunn's test for multiple comparisons). Statistical significances resulting from multiple comparison tests are as follows: ****, $P \leq 0,0001$; ***, $P \leq 0,001$; **, $P \leq 0,01$; *, $P \leq 0,05$; ns, $P > 0,05$. Box-plot positioning, either above or below the x-axis, reflects a respective increase or decrease of the analyzed parameter vs the unamputated control group.....66
- Figure 27. *radish*¹ heatmap of all residual data from comparison to unamputated flies of the same genotype. tested locomotor parameters in the following order: Step, Spatial and Stability parameters. Data distribution assessed by D'Agostino Pearson and Shapiro-Wilk normality tests. Multiple comparison tests performed according to patterns of data distribution, either parametric (One-Way ANOVA for normally distributed data; Holm-Sidak's test for multiple comparisons) or non-parametric (Kruskal-Wallis test for abnormally distributed data and Dunn's test for multiple comparisons). Bonferroni correction was applied to the multiple comparisons. Statistical significances resulting from multiple comparison tests are as follows: ****, $P \leq 0,0001$ and ***, $P \leq 0,001$, deep red and deep blue; **, $P \leq 0,01$, red and blue; *, $P \leq 0,05$, pale red and pale blue; ns, $P > 0,05$, white.67
- Figure 28. *Cycloheximide's and Empty vehicle's effect on unamputated flies* heatmap of all residual data from comparison to Canton-S untreated and unamputated flies. tested locomotor parameters in the following order: Step, Spatial and Stability parameters. Data distribution assessed by D'Agostino Pearson and Shapiro-Wilk normality tests. Multiple comparison tests performed according to patterns of data distribution, either parametric (One-Way ANOVA for normally distributed data; Holm-Sidak's test for multiple comparisons) or non-parametric (Kruskal-Wallis test for abnormally distributed data and Dunn's test for multiple comparisons). Bonferroni correction was applied to the multiple comparisons. Statistical significances resulting from multiple comparison tests are as follows: ****, $P \leq 0,0001$ and ***, $P \leq 0,001$, deep red and deep blue; **, $P \leq 0,01$, red and blue; *, $P \leq 0,05$, pale red and pale blue; ns, $P > 0,05$, white.68
- Figure 29. *Cycloheximide's and empty vehicle's effect on locomotor recovery.* heatmap of all residual data from comparison to Canton-S untreated and unamputated flies. tested locomotor parameters in the following order: Step, Spatial and Stability parameters. Data distribution assessed by D'Agostino Pearson and Shapiro-Wilk normality tests. Multiple comparison tests performed according to patterns of data distribution, either parametric (One-Way ANOVA for normally distributed data; Holm-Sidak's test for multiple comparisons) or non-parametric (Kruskal-Wallis test for abnormally distributed data and Dunn's test for multiple comparisons). Bonferroni correction was applied to the multiple comparisons. Statistical significances resulting from multiple comparison tests are as follows: ****, $P \leq 0,0001$ and ***, $P \leq 0,001$, deep red and deep blue; **, $P \leq 0,01$, red and blue; *, $P \leq 0,05$, pale red and pale blue; ns, $P > 0,05$, white.70
- Figure 30. a) The cAMP "learning and memory" pathway. Figure design inspired by Waddell, S & Quinn, W. G., Trends genet., 2001³⁸. B) *rsh* and Rac1 interaction and hypothesis of *rsh* influence on learning and memory. Interaction Between Rac1 and Raf described by zhong, Y. et al., Neuron, 2018⁵⁰.....76

ACKNOWLEDGEMENTS

All the thanks I state here come from the bottom of my heart, from increasing depths as your eyes go through these pages.

I want to thank to all my friends outside of this master's degree, for all the good times we had together, all the hedonism, all the distractions you gave me, all the social skills I acquired through getting to know you all – and a hypothetical god knows I've changed: my friends from “the zone”, my friends from FCUL: Babi, César and Jorge; Quadrado, Baeta, Lucas, Coelho, Rafa, Paixão and Pêgo; we kept together even though some of us are so distant in space or in what we dedicate ourselves to.

I want to thank the friends I made in CEDOC, for teaching me how to look at the world with even inquisitive eyes, and for all the scientific tips you gave me when hardships arose: there are many, but those for whom I *must* spell each letter of your names are Zé Vicente, for showing me that art and science are merely two sides of the same coin; João “Johnny Thunder” Ferreira, for the majestic beard I aspire to one day have and the sapience that comes with, a great example of inquisitiveness in science and life, and also for integrating me and many other master students in the CEDOC community; Hugo Moreiras, who helped me in my private and academic lives with insightful perspectives. With you all, I have had very stimulating conversations about science, art, philosophy, politics and bullshit, and for all the pleasant and unpleasant times, thank you!

To the great teachers we had, who presented themselves not as teachers, but as students who simply knew more than us: Paulo, for choosing me be a part of your master's. Even though I was clearly one of the “wild cards”, you trusted me, be it by despair that the master's wouldn't have enough students, or for seeing that I was not as ordinary as my grades reflected. You really did a great job in picking a class of fine aspiring scientists, and most of all, of fine people. Cláudia, who gave me so much positive reinforcement and confidence throughout this last year. You were the first to truly make me feel like I have a place in science. To Rita, for being such a great scientist, teacher, and person. I truly admire you for how kind and compelling you are, for your work, and especially for showing me that behind every scientist there is a person made of flesh, blood, and *especially* neurons, and that all that we are is as compatible with science as the passion we put in it – even though if at first we don't feel like we fit. For all the lab meetings and your suggestions to my work and for teaching me to look at the figures first and think them through before caving to the temptation of looking at the text. You are – and don't get jealous, César – the teacher I loved the most to meet in our first year of classes, and that didn't change much in this one either.

To all the friends I made in this master's, for our journey together through thick and thin. For all our differences and for our ability to meet in the middle: you accepted and helped me, and together we grew strong as group and as scientists. I hold so much admiration for so many of you, for different reasons that shouldn't go on paper, that all I can say is this: it was a pleasure knowing you and I hope our paths cross frequently.

To the Neurogenetics of Locomotion Lab: to Marta, for helping me in starting this endeavor and for teaching me everything I needed to know to do so; for all the work you left behind, all the optimizations you made in this protocol and for mending the sails on this boat so that I had the smoothest journey you could offer. To my students – and oh, how I pitied you for having to put up with me: Catarina, my first, for all the mistakes I made and you tolerated, and for your curiosity which made correcting them so much easier; and Sofia, for the great interest, pertinent questions and sound logic you showed, and for the super ambitious experiment we made happen; it would have been a real pain to do it all without you. To Ana, Ana and Anna, respectively, for all the punches in the arm when my tongue was far too impertinent; for the great laughs and disposition and the personal hardship we shared and endured together; for showing me how a post-doc should be like, for the script you wrote for me, and for bringing my scientific curiosity to a new level. To Xana, the hero the lab, who always helped me (and so much) and who I now consider a very good friend: you were the one who *really* had to put up with me and you taught me so much that I now consider myself a FlyBoy. To César, for accepting this sketchy individual in your sketchy-DIY-based lab, for helping my brain's expansion inside this thick skull of mine by teaching me so much and for (almost) always answering the annoying knocks on the door. For the chamber of reflection we created, where so many ideas – good and bad – bounced. For the trust you put in me and I ended up being able to put on myself. For making me feel so much at ease in the lab, with my work and with you, so much so that I can call you my friend. Thank you all.

To the ones that matter the most, for which the few words I have – which put a knot on my throat – merely show that there will never be enough.

To Tool for *finally* releasing Fear Inoculum which helped me so much during the writing process.

To Cirilla, who, with its soft fur and purrs, warmed my heart during the loneliest times.

To Shoshanna, the woman who turned a brat into the better man I am today. You pointed me towards a path that fulfills me by knowing me better than I did myself. You taught me how to manage hardships with perspective, cold blood and a warm heart, and with yours, you gave me love I didn't know existed. You made me better and it will be very difficult to ever thank you enough for what we went through together and for all it made me become. Even though, thank you, *ma belle*.

To my parents, Cecilia and João, who, as best they knew, educated the person writing these words. Who sacrificed so much, and who helped me to unimaginable lengths even though I have, at times, been such an asshole. No words can ever express it all; all I have left that may come close is this: I love you. I hope I made, and will keep on making you proud despite all the bad I have in me. I love you, and will again and again....and you Raul, my brother, my best friend, who gave me so much strength in the hardest times, and that, with one sentence, stopped me many times from giving up: “pressure makes diamonds”. I still am not, but if I ever become one, it's because of your words. I love you, my brother.

To avô Tó, for showing me that you do not need to study much to be wise; all you need is patience, a lot of strength and good examples such as yourself. This is for you, as for many times during this process you were in my thoughts. I miss you too much.

“O meu deus é a Natureza.”

António Duarte Gil

“Se podes olhar, vê. Se podes ver, repara.”

José de Sousa Saramago in “Ensaio sobre a cegueira”

ABSTRACT

Coordinated walking behavior in vertebrates and multi-legged invertebrates is controlled by evolutionarily conserved neuronal networks capable of generating movement in a fast, stable, and energy-efficient way. At the same time, it provides the flexibility to adapt to changes in the terrain, load, and under extreme conditions, to changes in internal motor representations resulting from adaptation to injury or disease. Our aim is to understand and characterize the neuronal mechanisms of plasticity that mediate motor adaptation to injury. To do so, we use *Drosophila melanogaster*, an easily manipulatable animal model with a powerful genetic toolkit, and the FlyWalker System that allows quantification of locomotor behavior of freely-walking *Drosophila* with high spatial and temporal resolution.

In order to study motor recovery, we submit flies to a middle-leg amputation and quantify locomotor behavior over the course of time. We found that, although highly uncoordinated, *Drosophila melanogaster* can walk immediately after amputation. Over time, we observe a gradual improvement in coordination and increasingly controlled gate choice, with several parameters returning to control values. Moreover, we found that this behavior is phenocopied in *D. repleta* and *D. pseudoobscura*, two distant *Drosophila* species, hence showing that the phenotype of locomotor recovery after limb injury is evolutionarily conserved in the *Drosophilidae* phylogenetic tree.

We then tested several classic Learning and Memory mutants pertaining to the cAMP signaling pathway for Long Term Memory (*amnesiac*, *rutabaga*, *dunce* and *radish*); these mutants displayed little signs of locomotor recovery – reflected in the absence of gait adaptation, inability to stabilize the body during walking bursts and decreased footprint precision and accuracy; over time these add up, resulting in a locomotor behavior phenotype in which the flies are inaccurate and random in each step taken, and hence walk in an increasingly uncoordinated fashion. Additionally, we tested inhibition of *de novo* protein synthesis using the translation inhibitor Cycloheximide, which yielded no palpable results.

These results indicate that flies can readjust their neuronal-motor circuitry to an injured state, observable through a time-dependent recovery in locomotor performance, and that this behavioral phenotype is evolutionarily conserved throughout the *Drosophilidae* phylogenetic tree. Moreover, general genetically encoded mechanisms relevant for memory and learning (described by classical olfactory learning paradigms) may be involved in this process of locomotor adaptation and recovery – possibly by promoting neuronal plasticity events.

By identifying specific genes and their expression patterns in the nervous system occurring during motor adaptation, we will be able to genetically dissect and target mechanisms of neuronal plasticity involved in locomotor recovery.

INTRODUCTION

MOTION: THE BASICS

Motion is a basic and essential characteristic of animal life and is a product of highly selective pressure: it is both shaped and gives shape to the organism it commands. When movement is purposeful, it generates an immense array of stereotyped behaviors, enabling animals to navigate and interact with its environment. This integration of the capacity for an animal to sense the world and to react to its changing conditions is key in evolution, allowing both hunter and prey to fight for survival.

Substrates can be aquatic, terrestrial and aerial, but even though these do not share the element of navigation, the basic biological mechanisms to generate movement are quite stereotyped across animal species ^{1,2}: a Central Nervous System (CNS) – the brain and spinal cord (or ventral nerve cord (VNC) in invertebrates) – controls muscles supported by an endo- or exoskeleton. It does so through the Peripheral Nervous System (PNS) which 1) induces the *execution* of motor commands via motor neurons; and 2) via sensory neurons constantly feeds the brain with sensorial and autonomic information. In this model there is a constant information feedback flow that crosses two physical “bridges”: the one connecting the CNS and PNS – the spinal cord; the other, neuromuscular junctions, where the PNS synapses onto muscles to induce action and reaction.

MOVEMENT COORDINATION

Coordinated movement and locomotion, be it in mammals or arthropods, is based on evolutionarily conserved neuronal networks and brain structures that generate an array of fast, stable and energetically efficient motor behaviors ³. In the CNS, higher order brain structures and Central Pattern Generators (CPGs) in the spinal/ventral nerve cord ^{4,5} coordinate and control movement in a rhythmic fashion, while still being reactive to the feedback from PNS sensory information – information which can be provenient from proprioceptive sensorial structures⁶ (to perceive tension within the musculoskeletal system) or gathered by the vestibular ⁷, visual ⁸ and olfactory systems. In healthy organisms, all these sensorial queues are assimilated, processed and integrated in the brain, after which motor outputs, in turn, are issued to the spinal cord and effector motor neurons ² to initiate ⁹, sustain or change¹⁰ between motor programs pertinent to a given situation.

Referring specifically to the PNS, its neuronal distribution increases in complexity as the animal’s size increases; this because complex body morphologies require equally complex motor representations in the brain and muscles in order to function efficiently. Accompanying motor neuron distribution in the PNS are sensory neurons which play a role in modulating motor actions. This happens in part because sensory neurons also relay information to the brain regarding executed motor tasks, facilitating more precise motor control, an incredibly important feature in the survival and prospering of an animal.

In the brain, after any action occurs, different neuronal populations spanning various brain regions, are activated when performing a motor task; these keep on being activated to persist or create a new, preferably coherent follow-up movement. Examples go from taking a next step in waking or running to articulating words and sounds.

FRANKENSTEIN'S MONSTER, RISE: PURPOSE AS THE SOUL IN ELICITING MOVEMENT

Even though functionality in physiology and in mechanisms of neurotransmission are critical for movement, it will, unfortunately, not be much more than involuntary or spasmodic if devoid of purpose – this is obtained by integrating received sensory information with that of the animal's internal state, enabling the body to initiate a viable motor command. An extreme example of inability to integrate these types of information may arise when a split-brain surgery (Corpus callosotomy) is performed. In this example the left and right brain hemispheres are partially or fully disconnected (to control epileptic seizures) resulting in curious phenotypical examples of involuntary but coordinated movement¹¹. When facing specific contexts, the two hemispheres – now unable to communicate – can sometimes have conflicting intentions, giving rise to different reactions performed by each side of the body: imagine having your right hemisphere, almost as if with a mind of its own, disagreeing with the shirt “you” want to wear today and slapping your hand for it...and now imagine it *suggesting* a different shirt, too¹²!

Other, more common examples of neuronally originated motor disfunctions regard neurodegenerative diseases such as Huntington's¹³ or Parkinson's¹⁴, in which brain centers important for movement initiation are affected. *Substantia nigra* degeneration can cause symptoms that range from movements generated spontaneously, involuntary and uncoordinatedly – jerks, characteristic of Huntington's disease; to the exact opposite in Parkinson's disease patients, which exhibit difficulty in movement initiation (like taking a first step of a walk cycle) and display severe tremors when still. These examples show that 1) the brain exerts control over the body, 2) various parts of it have different contributions to movement, and 3) the motivation of a movement is as important as its execution – one does not exist without the other, be it voluntarily (as exemplified) or involuntary (as happens with reflex movements). *Purpose* gives both fluidity and coordination to the way bodies move; and it's with it that the musculoskeletal and nervous system's ensemble work shines: a fish will flap its tail harder for faster propulsion and a hare will zigzag running to its rabbit hole for protection, but especially so if they are motivated to escape a hungry fast-growing looming shadow. Three important factors should come clear from this analogy: all these movements, if performed by healthy animals are 1) all **stereotyped** behaviors executed through similar molecular and musculoskeletal mechanisms – although some learnt and trained, whereas others are thought to be innate; 2) highly **fluid, coordinated and energetically efficient**; and 3) **motivated** by context and the internal state of the animal. The motivations in the example above were driven by the looming shadow's *internal* state wanting to satiate hunger, and by the hare and fish's reactions to an *external*, probably dangerous, looming stimulus.

When the nervous and the musculoskeletal system are healthy, the ability animals have can *sense* their internal state and execute specific *reactions* to satisfy it – all the while taking context into consideration – work hand in hand to generate a huge array of **behaviors**. These behaviors allow animals to adapt and prosper in their environments following a similar *modus operandi*: stereotyped behaviors like mating, feeding, the fight, flight or freeze responses, as well as the flexibility to adapt to changes in its environment and even to changes in its own body. All these context dependent behaviors are possible because of a highly selective and responsive nervous system that tightly controls and coordinates the musculoskeletal system. By understanding the fundamental aspects of movement regarding its kinematics, the necessary neuronal circuits behind a behavior, and the genetic programs that give rise to so many coherent and stereotyped phenomena, manipulatable mechanisms may be unveiled and exploited in the near future to hopefully facilitate recovery in cases of perturbed motor behaviors.

ADAPTIVE MOTOR LEARNING

Neuronal plasticity mechanisms exert changes on behavior via kinematic adaptations when learning or re-learning – if in response to dysfunction – new motor skills. This happens by (re)gaining stability (in whichever body parts are involved) and by movement (re)coordination^{15,16}, so that the organism can behave purposefully and functionally while maintaining or returning energetic efficiency and oxygen consumption to baseline levels. In order for this behavioral adaptation to happen the animal must sense the world to adapt to it¹⁷⁻¹⁹, but the mechanisms of adaptation should happen in different components of the organism; the muscles that support the body should become stronger (as happens in physiotherapy) but, and most likely, **neuronal plasticity-driven reorganization**^{20,21,22} should also occur. As we now know, various neuronal populations command different motor outputs – different networks are responsible for the various adopted gaits in fly locomotion¹⁰ and for many other behaviors, linked and mapped to specific neuronal populations of brain circuits, interneurons, descending neurons and motor representations – and since fine motor control is so important for a functional output, it is expected that the reorganization should also be somewhat widespread. An interesting example described by Kliemann *et al.*²³ reports that patients who underwent complete removal of a brain hemisphere when at a young age (from 3 months to 11 years old) develop to be fully functional adults. In these cases the brain's plasticity shines – in order to compensate for half a brain missing and still control the whole body, the connectivity between and inside brain networks is increased, all the while preserving the organization of canonical resting-state networks.

Given that such profound changes in the brain still result in functional motor capacity by recurring to various compensation mechanisms, which are the components that, in a fully developed adult, could be readapted and contribute to a regain in motor function?

The **CPG networks**, areas postulated to exist within the nerve cord and which, by balancing intrinsic and neuronal network properties, elicit and maintain repeating movements such as walking, should undergo neuronal plasticity events to adapt previous and no longer optimal activity²⁴. This should happen when a leg is amputated for example, as previously established gaits are no longer useful; in this case, neuronal restructuring by motor training will help establish new gaits for improved locomotor behavior adapted to a new limb distribution. CPGs are postulated to be connected to nerve cord interneurons and descending neurons (DN) from the brain, which by motor training may also be reshaped.

The **brain**, being the central hub that generates behavioral responses, is also a likely candidate to guide re-coordination of motor control. By relearning previously established motor tasks or by learning new ones – as happens with stroke or amputation patients for example – the brain, through motor training, adapts its control over the body²⁵; this training elicits two different physiological responses. The most obvious is an increase in muscular strength, occurring as more muscle is built and synapses become more efficient at triggering activity; this can happen by either adding new synapses at neuromuscular junction branches, or by increasing neurotransmitter release at specific NMJs to facilitate activation.

Parallel to this, motor training also induces almost immediate physiological plasticity in brain areas relevant for eliciting muscle activity – the motor cortex and spinal cord²⁵ for example – after which an expansion of motor cortex map areas is detected by MRI, and increased motor evoked potential (MEP) amplitudes are recorded after transcranial magnetic stimulation (TMS) of specific motor cortex sites²⁶. In this study, a polymorphism (val66met) in the brain-derived neurotrophic factor (BDNF) gene has been implied as important for the increase in neuronal plasticity in the primary motor cortex following motor training; interestingly, individuals with either the homozygotic or heterozygotic forms of the mutation elicited electrophysiological motor evoked potentials with the same amplitude before and after training

and did not show increased motor cortex map areas displayed by non-mutated individuals²⁶ highlighting its role in neuroplasticity.

Like BDNF, other molecules²⁷ such as Apolipoprotein E²⁸ (APOE) are thought to promote neuronal plasticity, especially in contexts of recovery from neuronal or motor insults (as in ischemic strokes²⁹ or other traumatic brain injuries³⁰). Curiously, BDNF also plays a role in other more generalized, hippocampal-related learning and memory events³¹. This was shown when testing episodic memory and hippocampal activation in the val66met polymorphism context, in which individuals with the mutation had poorer results, seemingly linking neuroplasticity mechanisms and events to overall brain fitness in normal conditions and to contexts of extreme adaptation.

Besides the motor cortex and spinal cord, many other brain areas are implied in movement control and feedback response mechanisms such as the cerebellum, a structure responsible for exerting fine control in movement and thus contributing to its fluidity – various studies point to it as another important candidate in the context of motor adaptation as cerebellar-dependent learning is being established to guide perceptual and movement changes^{32,33}. Additionally, cerebellar-independent learning has also been established to be necessary for feedback control and reinforcement in movement learning^{34,35}.

Neuronal plasticity mechanisms occurring in different brain areas seem to have a role in reshaping preestablished neuronal networks by reinforcing and, perchance, complexifying useful motor representations, and in the meanwhile possibly discarding those that no longer serve a purpose.

STUDYING MOVEMENT ON THE FLY

Using the FlyWalker, a tool for behavioral recording and analysis, Mendes et al. analyzed normal and perturbed locomotion in *Drosophila melanogaster*¹⁰. Analysis of unperturbed locomotion in flies showed that 1) flies, when walking at low, medium or high speeds recur to different neural circuitry to do so; 2) this is reflected by the different gaits they adopt, which change fluidly as speed varies (unlike the abruptness displayed by vertebrates while switching from walking to running). These gaits are: the **wave gait** with five legs on the ground, moving in a wave pattern, as centipedes' legs do, adopted at very low speeds; the **tetrapod gait** with four legs on the ground, used in low and medium speeds and many times adopted when changing direction; and the most commonly used **tripod gait**, adopted at medium to high speeds in which three legs are constantly on the ground – isomeric triangles that flip at each step cycle. Furthermore, they show that 3) walking patterns of flies devoid of proprioception in the legs are less precise at lower speeds, whereas at high speeds self-sensation is slightly overlooked by the organism as footprint alignment has no significative difference from that of wild types.

Regarding general motor adaptation, the authors also showed that flies have the ability to adapt and adopt new locomotor parameters to deal with increased body weight⁷ – much like a kid does when carrying a heavy backpack to go to school. After one week of carrying lighter loads, flies recover the motor performance displayed by their “no load” counterparts (walking speed and several step parameters). However, flies carrying twice their body weight – unable to cope with the extra load – accommodate to it by adopting more stable locomotor patterns (shorter and faster steps with more time spent in stance); both responses serve as evidence of locomotor recovery and, if recovery is unsustainable, of locomotor adaptation. Additionally, the authors once again show that proprioception (in this case driven solely by the chordotonal organ, the legs' weight sensor) is important for this adaptation. These are strong arguments for neuronal plasticity and its strong and long-lasting adaptation mechanisms to varying

external stimuli. As this work shows, plasticity happens not only at a synaptic level but is also translatable in functional behavioral changes.

Here lies another example of the **adaptive motor learning** displayed by motor circuits by undergoing changes to adapt biomechanically³⁶. This phenomenon is fundamental in everyday life, serving a purpose in scenarios of *immediate* accommodation – changes in walking speed³⁷ guided by visual cues³⁸ for example, in which flies slow down by altering inter-leg coordination – helpful in dealing with different environments (e.g. inclination, terrain, or substrate). In addition, there are *long term* changes described and exemplified previously, which occur when learning new motor skills or when adapting to permanent damage to the nervous system (e.g. stroke, spinal cord injury or amputation scenarios^{39–41}).

APPROACHES TO STUDYING LOCOMOTION AND ADAPTIVE MOTOR LEARNING ON THE FLY

In the Neurogenetics of Locomotion lab we study locomotor behavior in the fruit fly *Drosophila melanogaster* by manipulating neuronal populations and directly observing the resulting kinematic changes in behavior. To do so we use the **FlyWalker**, an apparatus built to capture, analyze and categorize four components of locomotion – the **Stability** of the body, **Spatial** distribution of the legs, characteristics of the **Steps** taken and adopted **Gaits** – with a high spatiotemporal resolution (Materials and Methods).^{7,10}

Using this powerful toolkit, we intend to deconstruct locomotor adaptation in response to limb damage. To do so, an amputation model was developed by the lab, and tested and optimized by Marta Santos and César Mendes. This model consists in comparing normal walking behavior, to that displayed by flies submitted to **amputation** of both **middle legs**. It is presupposed that, much like in humans going through physiotherapy and quadruped animals that lose a limb, invertebrates such as *Drosophila* are also capable of locomotor adaptation to cope with such acute damages. These experiments show that flies are indeed capable of adapting to their new four-legged state, and that they do so surprisingly fast and well. In three to seven days, positive changes in spatial and stability parameters can already be observed. Flies start learning how to balance their body in absence of the legs that once gave it stability and start walking in a more coordinated fashion as their footprints, instead of erratically placed, start being more clustered together and the legs start supporting the body in a straighter fashion.

A variety of wild-type *Drosophila melanogaster* strains were tested for locomotor adaptation to amputation (Canton-S, TopBanana, OregonR, DickinsonLab, Canton-S_{TL}) and, with some variation, they all show 1) an ability to **adapt** to the absence of both middle legs by re-learning motor parameters; and 2) that some of these motor parameters **recover** by matching its performance to that displayed by unamputated animals.

Additional studies, performed in other laboratories, with the same purpose of dissecting motor adaptation and the inherent coping mechanisms required for such deeds, show that this phenotype is displayed not only by *Drosophila* but also by other animal models such as the zebrafish⁴², mice⁴³ and humans⁴⁴. Some of these examples show, yet again, the impact of proprioception in adaptive motor learning. However, self-sensation alone does not fully explain how the nervous system regains function and especially how it harnesses its inherent plasticity to reprogram motor behaviors while adaptation occurs. This is the question we are trying to answer by developing a genetic model for neurorehabilitation, with which we intend to aid in identifying genetic players that can modulate motor plasticity, and additionally dissect possible molecular pathways that may contribute to these behavioral changes.

DROSOPHILA ORTHOLOGS OF MOTOR ADAPTATION MECHANISMS

In mammals, as mentioned before, some aspects of motor plasticity have been shown to happen via cerebellar-dependent (changes in movement and body perception) and independent (feedback control and reinforcement in learning) mechanisms. And even though the nervous system in *Drosophila* and other insects is somewhat differently organized, some brain structures have already been described to have similar functions to those of mammals.

The Central Complex (CC) has been described to share some functions with the cerebellum^{45,46} such as fine motor tuning by visually targeting motor actions⁴⁷ and in spatial orientation memory⁴⁸; in these studies, various gene mutations such as those in the protein kinase S6KII (*ignorant*) or in *foraging* have been shown to disturb visual and spatial memory. Ring neurons in the CC's ellipsoid body that act as a neuronal "compass" have a very important role in modulating motor behavior, doing so by establishing of a sense of direction and by creating mental maps^{49,50} and require neuronal plasticity to form functional spatial memories. Additionally, the protocerebral bridge of the CC has also been implied in the acquiring of self-perceptual memory of body size, requiring dCREB2-b – a classical neuroplasticity-promoting transcription factor regulating gene transcription post-learning – so that flies learn their body size and better modulate walking-related behaviors such as seizing an attempt to cross an insurmountable gap on the floor⁵¹.

The Mushroom Bodies (MBs), which will further be dissected in the next chapter, are another good example of orthology: they are described as the insect's hippocampus⁵²⁻⁵⁴, a brain area of extreme importance in learning and memory^{55,56} in mammals and having an extensively described role especially in olfaction and associative learning in flies. Regarding locomotor contribution, the MBs have been implied in the suppression of locomotion to better control it; this was shown by Heisenberg *et al.*⁵⁷ by testing locomotion flies without these structures (by chemical ablation of precursor cells, by expressing a mutation affecting Kenyon cell differentiation, or by expressing tetanus toxin in these same cells). Interestingly, these displayed increased walking activity and indicate a possible role for the mushroom body in walking behavior modulation.

These and other brain structures can exert control over the fly's body by integrating signals and converging them to descending neurons in the VNC, the fly's nerve cord. Many of these descending neurons have even been mapped⁵⁸ and manipulated to directly promote specific motor behaviors such as egg laying (Barry Dickson, Champalimaud Center for the Unknown seminar, unpublished), freezing behavior⁵⁹ or walking bouts REF MB.

From all the given examples of normal locomotion and movement adaptation, one thing becomes increasingly apparent: from flies to humans, all must learn and finetune behaviors through training for motor outputs to be efficient both energetically and purposefully. And while some self-preservation components of behavior are innate, all animals learn how perform most of what the body outputs, from the "least complex" walking to more complex actions like writing or talking. It is from this postulation that the next step in the lab's research emerges: studying classical learning and memory associated genes' function (though dysfunction) and observing their impact on locomotor adaptation.

LEARNING AND MEMORY IN *DROSOPHILA MELANOGASTER*

Some learning and memory related genes are described as “classical” as they have, for over forty years, been dissected in various paradigms to assess the capacity to learn in response to olfactory and spatial cues (which may require vision and orientation). Many of these paradigms of teaching and consequent learning are done by pairing a conditioned stimulus (CS –a specific odorant or visual cue) to an unconditioned stimulus (US – generally one to avoid, such as a foot shock). The rationale is as follows: the animal, normally attracted to a certain smell, starts avoiding it an association with punishment is trained.

This extensive dissection of memory yielded a genetic pathway for its formation^{55,60} in which specific brain regions – characterized by their different gene expression – generate neuronal activity patterns that function as milestones to be reached in order for a memory to be consolidated, the result of which should be a coherent behavioral response long after training.

As stated, the Mushroom Bodies are classified as central hubs of olfactory memory. It integrates dopaminergic unconditioned stimuli with cholinergic conditioned stimuli acting as a coincidence detector. It is through these coincidences that memories gain a useful value – such as the smell of a certain perfume that brings up the memory of your first kiss, or that of rotten shrimp which made you throw up for two days straight – from which attraction, repulsion, caution or other internal states may reemerge when triggered. These memories, however, can only be **recalled** if the organism can **acquire, retain** and **consolidate** the CS+US pairing⁵⁵, so that in the future this association can reemerge by triggering the unconditioned cue (the perfume) when the conditioned stimulus (the kiss or footshock) is absent. On a superficial level, this is the journey of a memory; fortunately, *Drosophila* is an excellent model to escape this superficiality and dive in the complex neuronal circuitry, biochemistry and genetics that underly it. Using *Drosophila*, four distinct – functionally dependent, but genetically independent – memory phases, have been described up to now.

MEMORY PHASES IN DROSOPHILA MELANOGASTER⁵⁵

As Fig. 1 suggests, **short-term memory**⁶¹ (STM) is the first memory phase that becomes active in neurons that subserve its behavioral response. STM is postulated to only be active on the first hour after training – after which it decays – and its activation is thought to be mediated by a sudden rise of cyclic Adenosine Monophosphate (cAMP). cAMP is synthesized by adenylate cyclase (AC) using ATP as its precursor and is degraded by the *dunce*^{62–64}-encoded phosphodiesterase. It was through mutation of *rutabaga*⁶¹, a pan-neuronal AC that STM was initially discovered. *rutabaga* can be activated, generating the sudden cAMP rise in two possible ways: 1) extracellular binding of glutamate to NMDA receptors (NMDAR) make the cell permeable to calcium (Ca²⁺). Ca²⁺ binds to Calmodulin activating it and these, in turn, activate *rutabaga*. 2) directly activated by G protein-coupled receptors (GPCR's), responsive to the neurotransmitters/modulators acetylcholine⁶⁵ (ACh) and eventually serotonin^{66,67,68} (5-HT) and dopamine⁶⁹ (TH).

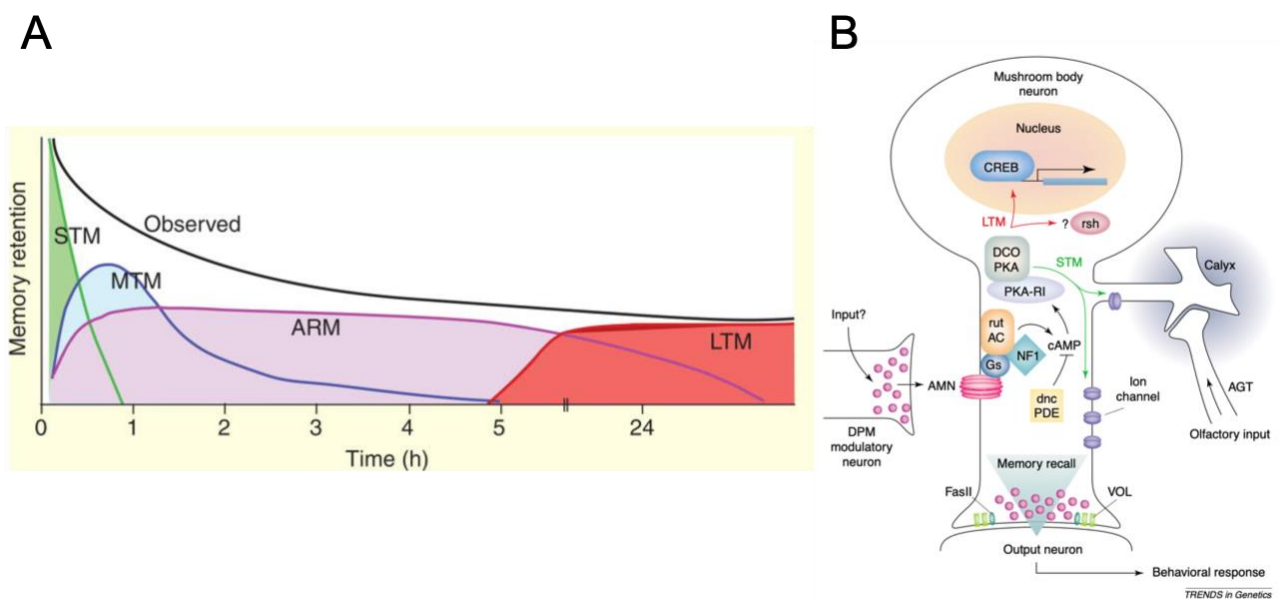


FIGURE 1. A) Memory phases of olfactory memory in *Drosophila melanogaster*⁷⁰. **B)** Cyclic AMP pathway on *Drosophila* mushroom bodies and surrounding cellular structures⁵³.

It is through this second activation route that **middle-term memory** (MTM) – the second memory phase – was discovered. *amnesiac*, the mutation that gave this impression, has been observed with high expression in Dorsal Paired Medial (DPM) neurons (during development) which project to the Mushroom Bodies and activate its ACs^{71,72}. MTM is thought to be active between the first and seventh hours after training, a sensitive time of memory formation which seems to be responsible for reversal learning⁷³ – which facilitates the association of a different conditioned stimulus (e.g. odor) to the same US (footshock). *amnesiac* has additionally been observed in adult MBs and it is described to encode a pre-neuropeptide which seems to be mainly converted to ACh, providing a possible mechanism of sensitization occurring after training.

We now know how some memories can be acquired (STM) and retained for a short time (MTM); how, though, are they consolidated? The cAMP cascade has often been called the memory pathway (Fig. 30A); its initial rise in neurons that are highly active during and after training is thought to promote memory formation via activation of Protein Kinase A (PKA), diverging its signal towards the two missing and independent^{74,75} memory phases: **anesthesia-resistant memory** (ARM, via massed training) and **long-term memory** (LTM, via spaced training). These seem to be brought up by different training paradigms

and are differently effective at memory retention: the first, ARM, by a massed training of 10 uninterrupted sessions lasting up to three days; the latter, LTM, via spaced training consisting of 10 sessions spaced by 15-minute intervals, which lasts up to seven days⁷⁵.

ARM, as the name indicates, is resistant to anesthesia (typically cold shock or by CO₂ administration) and is linked to the mutation on the *radish*⁷⁶⁻⁷⁸ gene. This type of memory seems to act additively with STM and MTM to produce the memory retention curve observed in Fig. 1, reaching its peak after MTM fades, 7 hours after training. Contrary to LTM – which requires *de novo* protein synthesis promoted by nuclear activation of **CRE-CREB** learning-related gene transcription – ARM does not need synthesis to occur; this separation of memory phases makes sense as their effectors are molecular and mechanistically independent as is the memory performance of both. It makes sense for LTM to be the last memory phase to happen, as it leads to and requires gene transcription, thus exerting effects on a longer timescale than that of the *radish*-induced ARM.

These two paradigms, however, are not explicit in as how they occur in normal, untrained conditions, as both can happen at the same time since both are activated by PKA. If this is the case, then the whole STM -> MTM -> ARM -> LTM chain of events may represent checkpoints in memory formation that reinforce each other and, when none are disturbed, result in long lasting memories stored in newly formed synapses.

AIMS

Activity of learning and memory-related genes is a component which we hypothesize to contribute to locomotor adaptation in response to amputation. The four memory phases and associated genes *rutabaga* and *dunce* (STM), *amnesiac* (MTM), *radish* (ARM) and CREB-induced *de novo* protein synthesis (LTM) – due to their intrinsic neuronal plasticity nature and the body of work associating them with learning and memory events – may not act exclusively in the formation of olfactory memory, and could possibly be contributing to the **neurorehabilitation** and whole scale behavioral re-adaptation displayed by our flies when they re-learn how to walk.

In order to better understand locomotor recovery in *Drosophila melanogaster*, and to test our hypothesis that the aforementioned genes pertaining to the cAMP “memory cascade” play a role in locomotor adaptation, we set the following aims:

- To use the FlyWalker software in order to study the kinematic adaptations (Stability, Gait and Step parameters) which occur after amputation in Canton-S (wild type) *Drosophila melanogaster* flies; reanalyze the videos so that, in addition, the recently developed Spatial parameters can also be assessed.
- To show that the phenotype of locomotor adaptation is evolutionarily conserved in phylogenetically distant *Drosophila* species *D. repleta* and *D. pseudoobscura*.
- To study the influence of *amnesiac*, *rutabaga*, *dunce* and *radish* on motor recovery by observing how their loss of function mutants react and adapt to middle-leg amputation, while taking into account the established notion of wild type locomotor recovery.
- To assess if *de novo* protein synthesis is required for neurorehabilitation by testing the locomotor adaptation of Cycloheximide-fed Canton-S flies.

MATERIALS AND METHODS

FLYWALKER

In the Neurogenetics of Locomotion lab we are studying locomotor behavior in the fruit fly *Drosophila melanogaster* by manipulating neuronal populations and directly observing the resulting phenotypic changes in behavior. To do so we use the **FlyWalker**, an apparatus built to capture, analyze and categorize different components of locomotion.

The **hardware** (Fig. 2) is composed by an optical glass with LEDs on its edges and a high speed video camera. Once the lights are turned on, the optical glass' physical properties allow photons to easily travel through it as they are constantly reflected inside the glass, radiating the propagated light – this generates a phenomena termed total internal reflection. However, whenever an object is placed on top of the glass, its point of contact with the surface creates a *frustration* on the light. As the density encountered on “the other side” of the glass is bigger than that of the air, photons, instead of being internally reflected (as they would with air alone), get internally refracted and are scattered towards the

opposite side of the object – this optical effect is termed *frustrated* Total Internal Reflection, *fTIR* for short. It is by exploiting this phenomena that we can film our flies. A video camera placed on the opposite side of the glass captures the light scattered from flies walking freely in the arena, recording it at high speeds – 200 to 250 frames/pictures per second – giving us a high spatiotemporal resolution that allows to capture small nuances in untethered locomotor behavior. These are posteriorly analyzed in our FlyWalker **software**, with which we can categorize four big pillars of locomotion produced by flies freely walking in an arena – for a high spatial resolution. These pillars are composed by various parameters regarding the **Stability** of the body, **Spatial** distribution of the legs, characteristics of the **Steps** taken and adopted **Gaits**.

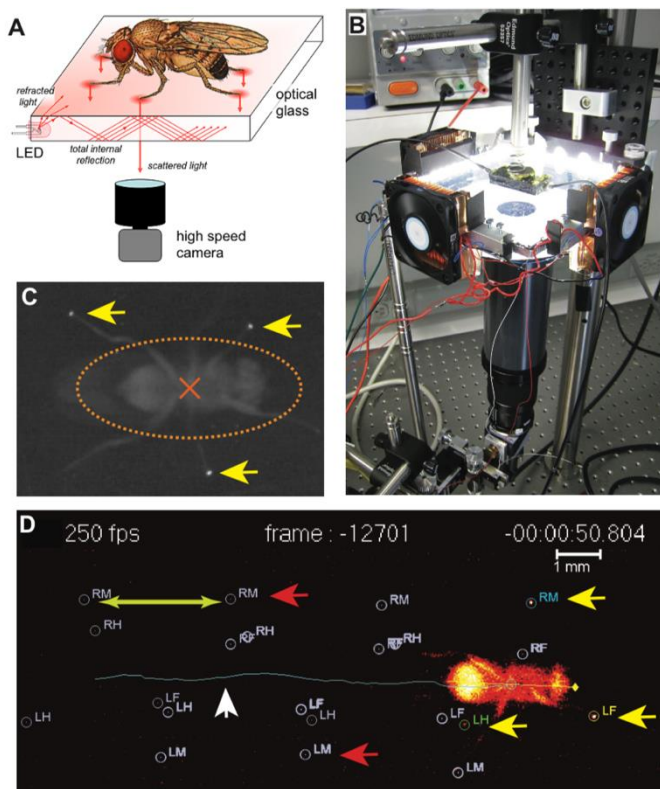


FIGURE 2. The Flywalker system. **A)** Schematic of the fTIR optical LED light sources are located at the edges of an optical glass and light propagates within the glass via internal reflection. Tarsal contacts lead to light scattering detected by a high-speed camera. **B)** fTIR apparatus with fly tunnel in the center of the optical glass. **C)** single frame of a fTIR video. the fTIR effect can be seen for three legs in the stance phase (yellow arrows). background light partially illuminates the fly's body (orange dashed ellipse); the center of the body is indicated by an orange cross. **D)** image generated by the flywalker software. the fly's footprints and body center are tracked throughout the video. present footprints are identified and labeled (yellow arrows). The fly body and trajectory are visualized by a blue line (white arrow). past footprints can also be recorded (red arrows). A scale bar can be introduced. step length is defined as the distance between two consecutive footprints (green arrows).

FLYWALKER PARAMETER LIST AND DEFINITIONS

GAIT PARAMETERS

- **Tripod Index:** Number of frames in which a fly has 3 legs on the ground in a triangular configuration (1 front, 1 middle, 1 hind).
- **Tetrapod Index:** Number of frames in which a fly has 4 legs on the ground in a quadrangular configuration (tripod + 1 leg).
- **Wave index:** Number of frames in which a fly has 5 legs on the ground.
- **Non-canonical Index:** Number of frames in which a fly's leg configurations are neither tripod, tetrapod nor wave.
- **Gait Index:** Average value for a window of frames where: tripod=+1; tetrapod=-1; non-canonical=0. Indicates the most adopted gait in a 5- step walking bout.
- **Tripod Duration** (milliseconds (ms)): Amount of time during which a fly is adopting the tripod gait.
- **Inter-Tripod Duration** (milliseconds (ms)): Time spent, between two tripod step cycles, in other gait configurations.

STEP PARAMETERS

- **Average Step Frequency:** Number of step cycles (of each leg) per second.
- **Average Step Period** (milliseconds (ms)): Time to complete a step cycle (for each leg).
- **Footprint Alignment** (micrometers (μm)): Standard deviation from the average point of adjacent ipsilateral footprints projected onto the displacement axis.
- **Average Swing Speed** (millimeters per second (mm/s)): Speed of the swing phase (average of all legs).
- **Average Step Length** (micrometers (μm)): Distance between two consecutive footprints by the same leg (average of all legs).
- **Leg Displacement** (body units (b.u.)): Average of the displacement of all legs during the swing phase.
- **Swing Duration** (seconds (s)): Time a leg spends on the swing phase (average of all legs).
- **Stance Duration** (seconds (s)): Time a leg spends on the stance phase (average of all legs).
- **Duty-factor:** Percentage of time in a step cycle in which the tarsae are on the ground.

SPATIAL PARAMETERS

- **Anterior Extreme Position (AEP) Footprint Clustering** (body units (b.u.)): Standard deviation from the average position where the leg first contacts the glass after touchdown at the end of swing phase (protraction). Measures the clustering of each step offset of a leg relative to the position of the body. The higher the value, the more scattered the footprints left by the same leg are.
- **Posterior Extreme Position (PEP) Footprint Clustering** (body units (b.u.)): Standard deviation from the average position where the leg last contacts the glass after touchdown at the end of swing phase (protraction). Measures the clustering of each step offset of a leg relative to the position of the body. The higher the value, the more scattered the footprints left by the same leg are.
- **Average Stance Linearity** (micrometers (μm)): Average difference between the stance traces generated by each leg during stance phase and a 5-point smoothed line.

- **Stance Straightness:** Ratio between the distance from AEP to PEP (stance phase) and the path described by the tarsal contacts relative to the body (stance trace).
- **Body Size** (micrometers (μm)): size of the fly.

STABILITY PARAMETERS

- **Stability Index:** Ratio between the number of stable frames and the total number of frames analyzed. A frame is stable when the fly center of mass falls within the polygon of support provided by the legs.
- **Body Displacement** (micrometers (μm)): Displacement a fly's center of mass (distance) during a 5-step (of each leg) walking bout.
- **Body Path** (micrometers (μm)): Path traveled by a fly's center of mass of a fly, in a straight line, during a 5-step (of each leg) walking bout.
- **Body Displacement Ratio:** $\frac{\text{distance walked}}{\text{path taken}}$; a ratio approaching the value of "1" indicates a fly whose center of mass (located at the T2 segment) does not oscillate, walking in a perfectly straight line.
- **Onset Ratio:** Position of the center of mass relative to the area of support of a fly (created by its legs in stance) during the onset of a gait configuration. Relative position of the center of mass within the support tripod at the first frame.
- **Offset Ratio:** Relative position of the center of mass within the support tripod at the last frame.
- **Stability Ratio:** Ratio between the number of stable frames (in which the COM is inside the support polygon) and the total number of frames.
- **Area of All Configurations:** Average of the area of all gait configurations adopted during a 5-step walking bout.

FLY HANDLING

FLY TABLE

Lines	Genetic construct	Observations
Canton-S	Wild type	Bloomington Stock Center
<i>Drosophila pseudoobscura</i>	Wild type	Nuno Soares, Instituto Gulbenkian de Ciência
<i>Drosophila repleta</i>	Wild type	Nuno Soares, Instituto Gulbenkian de Ciência
<i>amnesiac</i> ¹ _{TL}	X; loss of function allele, amorphic allele (EMS)	Troy Littleton Lab
<i>rutabaga</i> ¹ _{TL}	X; loss of function allele (EMS)	Troy Littleton Lab
<i>dunce</i> ¹ _{TL}	X; hypomorphic allele (EMS)	Troy Littleton Lab
<i>radish</i> ¹ _{TL}	X; point mutation	Troy Littleton Lab

FLY REARING

Flies are **stored** at 25°C and kept in plastic vials with standard cornmeal food. The parental generation is left to mate and egg-lay for 2 to 3 days in a low to medium population **density** – 10-20 flies, male and female, depending on the strength of the stock – and are then flipped out of the vial for the F1 generation to grow. Powdered yeast is added to the cornmeal food when the parental generation is placed in the vial and when they are flipped-out, to stimulate both egg-laying in the adults and the growth of the F1 generation. Additionally, distilled water can also be added to the medium if the food is dry after egg-laying.

DISCRETE GENERATIONS

The parental generation is flipped out both to keep **discrete generations** in which the parents and the progeny do not cross between themselves, and to counter overcrowding food vials with fertilized eggs. With limited space and resources the F1 generation becomes significantly smaller in size; this, unfortunately can make FlyWalker's job at auto-tracking videos harder since – at a set resolution, zoom and frame-rate – a smaller fly will be recorded and represented on video at a lower pixel density.

FLY CROSSES

When a line is generated from a **cross** of two different genotypes flies are selected on a ratio of two males for each three female virgins, minimizing both male competition and sexual aggression towards the females. In a cross, each sex represents one of the genotypes – be it a mutation in a chromosome or a part of combinatorial system like UAS-Gal4 or LexA-LexO – and each parent contributes with one copy of the 4 chromosomes that make up the fruit fly, with XX234/XY234 and their pairs respectively representing females and males. Fortunately, these mutations and insertions can easily be tracked throughout the generations with phenotypic balancers or markers (such as curly wings on the second chromosome or “bushy shoulders” on the third) inserted on one of the chromosomes of each given pair. This is advantageous, not only to understand what is being crossed, but also to know if a certain insertion of interest is still present in the genome of flies in stock for a long time. For example, a stock of flies with a nSyb-Gal4 / TM6b third chromosome pair has a Gal4 tissue-specific driver for all neurons in heterozygosity with a TM6b balancer which gives the fly “bushy shoulders (humeral)” on the adults and “tubby” larvae phenotypes the flies with this specific Gal4 driver can be identifiable by these two phenotypes, and it's absence makes it untraceable and with unpredictable expression in the F1 generation if crossed.

VIRGINS

Before crossing flies it is essential to know whether or not the females are **virgins**, maximizing the chances of gathering F1 flies with the desired genotype and, most importantly, allowing for the accurate prediction of all the possible genotypes that can originate. Chastity in *Drosophila melanogaster* can be determined for males and females by the same markers. After hatching from the pupal case, flies display two tell-tale signs that they have not yet reached sexual maturity, signs which fade out in 8 to 16 hours, depending on the temperature at which they are stored (lower temperatures slow metabolism and growth and vice versa). The first one are shrunk wings; they are shrunk right after hatching, inflating to their usual size in a few hours. The meconium, a dark bean-like spot – waste products remaining from digestion of its last meal as a larva during the pupal stage – can be observed though higher segments of the abdomen and once defecated, the fly is considered sexually mature.

SEXING FLIES

The **sex of the flies** can be determined by four morphologic differences: Female flies are usually larger than the male counterpart, and its genitalia (mostly developed from the imaginal disc in the eight abdominal segment) is located in the lower abdomen and has a clear color with a pointed shape; male flies are smaller, have a darker lower abdomen and a dark scab-like genitalia and analia. Additionally, males also possess small hairy structures called sex-combs in the upper tarsal segments of each foreleg which, during mating, are used to mount and grab on to the female fly.

MIDDLE-LEG AMPUTATION

PRE-AMPUTATION

Flies are never to be anesthetized via CO₂ administration if to be amputated and only female flies with one to four days of age are selected for this procedure/ protocol.

AMPUTATION AND ANESTHESIA

Female one to four days-old **flies are selected** for amputation. Protocol optimization done by Marta Santos suggests the use of female flies as their motor recovery is more stereotyped than its male counterpart; female flies are also significantly larger than males (and possibly stronger, considering they can lay up to 100 eggs per day) and because of this, when they are on stage, the camera captures bigger, more pixel-dense pictures which increase the reliability of FlyWalker's auto-track feature. Age in the flies is also relevant, as previous data from the lab indicates a lower efficacy in locomotor recovery as ageing progresses, both in male and female *D. melanogaster*.

After selecting female flies within the appropriate age interval, they are anesthetized before amputation. **Anesthesia** is induced though cold by placing a two flies on a chilled metal surface over an ice-filled box; they are anesthetized in this fashion because normal anesthesia via CO₂ administration has been shown to induce behavioral changes lasting up to 3 days, something undesirable in our particular case. Amputation is performed by cutting both Thoracic-2 legs of the fly (middle legs), in the middle of its femoral segments with the aid of a pair of fine forceps and scissors. It should be taken into notice that, should the cut be to up or down the femur, the fly may either bleed to death (lose too much hemolymph) or be able to use the stump as support. Additionally, the other legs are only to be manipulated if need be, and doing so very gently to avoid damage, which would disturbing recovery.

POST-AMPUTATION

After amputation, two flies are placed in each vial either without food or with it, depending if they are to be tested at 15 minutes, or at 3 or 7 days **post-amputation**. When tested at 7 days post-amp the flies are flipped to a vial of fresh food at the third day. Each vial is labeled with the approximate time of amputation so that filming happens at the appropriate/designated time.

DEALING WITH NON-*DROSOPHILA MELANOGASTER* SPECIES

In addition to wild types and Learning and Memory *Drosophila melanogaster* mutants, flies from other *Drosophila* subspecies were also used for motor-learning and walking recovery experiments/assays. We kept 4 subspecies stocked – *Drosophila virilis*, *americana*, *pseudoobscura* and *repleta* – however, only the last two were submitted to the experimental protocol; *D. americana* and *virilis* are so big that they cannot freely move in FlyWalker's current chamber.

Although there are some similarities in experimenting with other species from the *Drosophilidae* phylogenetic tree – the food and temperature in which they grow and the amputation protocol – there are also some noteworthy differences to be considered. One of these is their size: these different species are all significantly bigger than *D. melanogaster* which implies that they must be kept at lower populational density in the food vials. A possible consequence of their larger size is that, even though the stages of the life-cycle are the same, they take much more time to develop, the most extreme case being *D. virilis* taking approximately 3 weeks to become an adult. Another difference is in sexing them is in / determining their sex: besides the fact that females are larger than males, none of the aforementioned sexual differences present in *D. melanogaster* are reflected in these species – they lack characteristic differences in male and female genitalia and males do not possess sex combs. Fortunately the males' testes are observable through the cuticle due to their large size and striking red or orange colors.

BEHAVIORAL ASSAYS

CYCLOHEXIMIDE EXPERIMENT

In this experiment flies were fed cycloheximide for 3 days at most, and tested under the context of motor learning after bilateral middle-leg amputation.

CYCLOHEXIMIDE MIXTURE

Cyclohexamide was fed at a concentration of 0,015M, dissolved in 2% ethanol (99%), distilled water and sucrose (sugar). The mixture – either with cycloheximide (Experimental group) or 2% ethanol alone (negative control group) – was embedded on filter paper from which the flies drank.

- **CHX vial:** empty vial with a pipette tip containing 200µl [water 176µl; ethanol (EtOH) 2%, sucrose 5% and cycloheximide at 15mM 4 µl]
- **EtOH vial:** empty vial with a tip containing 200µl: EtOH 2%, water 179 µl, sucrose 5%);

REARING

All Canton-S flies were reared at 25°C in normal cornmeal food until 3-5 days after pupation. Flies were either amputated or simply put under cold induced anesthesia before being started on the protocol (Fig.

3. T= 0); this was done to control for the effect of cold-induced anesthesia. As shown in Fig. 3, flies were kept on the protocol for three days in 12h cycles of [10h treatment / 30 mins in regular food / 1h30min starvation] and motor behavior was assessed at the end. During the 10h treatment phase flies were kept on vials devoid of normal cornmeal food, instead feeding from mixture-embedded filter papers which would be refilled on each new 12h cycle.

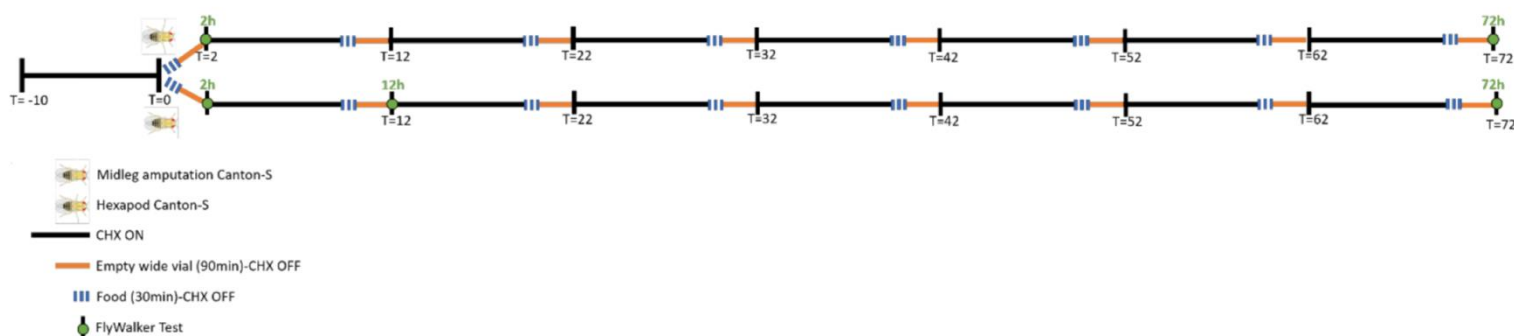


FIGURE 3. Protocol for the Cycloheximide experiment. The effect of cycloheximide on Canton-s flies was filmed in unamputated (top) and amputated (bottom) conditions at different timepoints, however, only the 72h timepoint was analyzed for this report.

TEST GROUPS

In total, 6 groups of Canton-S flies were tested at different timepoints.

In an unamputated context:

- Untreated.
- Vehicle treated for 3 days, tested on the 3rd day.
- Cycloheximide treated for 3 days, tested on the 3rd day (Fig. 3, T= 72h).

In an amputated context:

- Untreated, amputated, tested for motor recovery 72h day post-amputation.
- Vehicle treated, amputated, tested for motor recovery 72h day post-amputation.
- Cycloheximide treated, amputated, tested for motor recovery 72h day post-amputation (Fig. 3, T= 72h).

Other timepoints were filmed (Fig. 3: at T= 0h, with 10 hours of exposure to cycloheximide, T= 2h post-treatment in amputated and unamputated contexts; T= 12h post-treatment in the amputated context) but were not analyzed for motor recovery. The 72h timepoint was used to understand the extent of the difference in locomotor recovery displayed by the vehicle or CHX treated animals.

VIDEO RECORDINGS

Flies to be filmed 3 or 7 days post-amputation are placed in clean empty vials for 30 minutes before to groom, cleaning their tarsi; this both eliminates the occurrence of legs slipping during filming and reduces the footprint food-stains left on the optical glass. Flies to be filmed at 15 minutes post amputation have already been left to groom for 10 to 20 minutes before amputation.

Flies were filmed in similar setups using either a Photron (recording at 250FPS) or Point Grey (recording at 200FPS) high-speed video cameras. Irrespectively of the different cameras and user-interfaces used to

control them, flies were filmed inside the same chamber and in similar mounts that constitute the FlyWalker hardware. Additionally, the videos will be **calibrated** in the FlyWalker Software when to be analyzed. To do so we photograph a Stage Micrometer (Klarmann Rulings, Inc) with the high-speed video camera, and using FIJI, measure the distance between micrometers in pixels.

Before filming, the optic glass is cleaned/wiped with methanol using *cloths* that leave close to no fibers on the glass. Two flies are collected from its vial using a mouth aspirator and are then *breezed* into the chamber. Once they are visible on the computer screen, they are recorded for a maximum of three minutes. They are then aspirated out of the chamber and blown in to its vial and the optical glass is cleaned with methanol in between takes.

After running the first genotype (*radish*) we have opted to start using two flies per take for two reasons: first, for the practicality of filming an N=2 per take; the second reason, an attempt at enhancing the behavioral state of the flies both on scene and off. If a fly is amputated and is scheduled to be filmed 7 days after, then that is simply too much time to be kept alone in a vial with no stimulation whatsoever. Since the readout is of motor-activity, maintaining an ever-so-slightly stimulating social environment during the period of recovery might be the most favorable option. Interestingly, this logic translates well to when the flies are on screen as the simple fact of having two flies walking around means that either 1) they both become more active, or 2) in case that one of them isn't, having a frenetic fly walking around and occasionally bumping in the less active one ends up naturally stimulating it to walk. Another way used to stimulate walking behavior or to unstick a fly from the ceiling or the walls is to gently blow air into the chamber using the mouth aspirator so that they step on the optical glass and initiate walking bouts.

After recording, the video is saved and will be cropped to then be analyzed on the FlyWalker software.

VIDEO CROPPING

When cropping a video, the events of interest we are on the lookout for are walking bursts in straight paths in which a fly takes 4 to 5 step cycles with each leg. We do so by selecting straight walking bursts in which the fly takes up to 6 steps with the same leg, guaranteeing that they take approximately 5 steps with the other legs. It is our intention to analyze exclusively this type of walking behavior as it is natural, frequent and highly stereotyped – depending on the speed, flies predominantly assume either tripod, tetrapod or non-canonical gait configurations – providing a good baseline to compare changes in locomotor behavior in the perspective of motor-learning and memory.

Temporal cropping is performed by going through all videos in the UI of the camera, and observing the behavior of each of the two flies separately (so as not to attribute a certain event to the wrong fly) to select events in which a fly performs a straight walking burst with 4-5 step cycles from each leg. Whence located, that temporal section of the video is cropped out to be further manipulated and the time interval at which it happens is transcribed. This cropping normally results in up to 6 videos per fly from which 2-3 will be used to represent each N; we gather such a big number of videos of each fly to filter the unsatisfactory ones in the next stage of cropping.

Spatial cropping is done using FIJI and the objective is to cut out a small window in which only the one fly is displayed, and rotate the video so that the fly's path is seen from left to right. It is essential that the fly's track leads it out of the cropped out window in the last frames, as in the FlyWalker software these are used to define what constitutes the observable moving object by subtraction of the light emitted by the background from the observable light reflected by the body and legs of the fly.

After spatial cropping, each video will correspond to a series of .PNG image files contained in a folder, in which each picture corresponds to a frame. Considering that the cameras capture videos at a temporal resolution of 200 to 250 frames per second and that videos of unamputated flies are of approximately 100 to 200 frames (less than one second), and that those of amputated flies are of 300 to 500 frames (up to two seconds).

FLYWALKER SOFTWARE VIDEO ANALYSIS

The FlyWalker Software is used to track and quantify a fly's walking behavior from the cropped videos; the quantification comes in the form of auto-generated plots and an Excel spreadsheet that encompasses all the parameters extracted from a video (119 in total). The **auto-generated plots** are generated for each analyzed video and visually represent some of the most important locomotor traits. These encompass features of *gait choice*, *spatial location* and *duration (step parameters)* of each footprint and the track of the fly's center of mass (*stability parameters*) during the walking burst. All information regarding gait, spatial, step and stability parameters of each freely-walking *Drosophila* are automatically registered in an **Excel spreadsheet** and are divided in 119 locomotor parameters, from which the most relevant ones are then compiled (for all the flies of a given genotype and timepoint) and are quantified using Residual analysis.

The tracking is done automatically (**auto-tracking**) and is then manually reviewed and corrected for discrepancies from the video; depending on the settings used in the software, the tracking can be more or less efficient.

Before running the auto-tracking function the software must be **calibrated**. As mentioned in the "Filming" section, a photograph of a Stage Micrometer is taken before filming sessions; with it, the distance of a micrometer (as observed by the camera) is measured and is converted to number of pixels; the value of the average of five of these measurements is calculated and inserted in the "Distance Calibration (pixel/um)" in FlyWalker's Settings.

The most important **settings** to be defined before auto-tracking are the size of the fly – defining the size of the ellipse generated around the fly – and the distance from the fly's head to its center of mass located in its second thoracic segment, where the middle legs connect to the body⁷⁹ – defining where in the ellipse is the fly's True Center (TC). After defining the body, one must juggle with the luminosity intensity that will define the pixel density and will "fill" the ellipse; in this way, the pixel density of the moving object can be tracked through all the images that constitute a video. There are three parameters to modulate the software's sensitivity to light: Higher Body Threshold, Lower Body Threshold (pixel intensity) and Minimum Body Size (pixels).

The Minimum Body Size defines the minimum amount of pixels that account for the body of a fly. This setting is adjusted depending on the light intensity of the LEDs during filming and also on the sensitivity to light of the tracking software, which in turn is defined by the Higher and Lower Body Threshold values. These two define the window of sensitivity to light (pixel intensity) that the tracking software will use to define the body frame by frame, with the Higher Body Threshold being the value maximum Lower Body Threshold being the minimum light intensity that is to be tracked

DATA HANDLING

As mentioned above, after evaluating a video, FlyWalker automatically generates, for each fly, plots that reflect features of all four locomotor categories – gait, stability, step and spatial parameters – as well as an Excel file with the raw data for each of the 119 locomotor parameters. Handling this much data provides us both with an opportunity and a challenge to find a meaning in changes on a given parameter, and in understanding the interactions and influence they have with, and on each other. Approximately 20 flies are filmed for each condition (from which 10 to 15 are viable) and each fly will have two straight walking bursts representing it – each time point then has an $N=10-15$ and $n=20-30$. This will mean that each experiment, counting the controls, will have 40 to 60 flies.

All the **auto-generated** plots are observed, firstly to see if there was any error during the auto and manual tracking of the fly, and secondly to look for locomotor patterns and features that may be interesting – a big variation in the placement of a tarsi, for example, indicating a lack of precision and some randomness in each step taken. This will give us an idea of how a genotype at a certain timepoint is behaving; however it is extremely hard to comprehend and transmit such an amount of data with this type of representation, so further synthesis of visual raw data is necessary, as well as quantification for it.

In order to condense such a large amount of visual data and at the same look for indications of whether a genotype at a determinate time point is regaining locomotor coordination after amputation, we condense the displacement of the fly's center of mass in its straight walking bursts (**body-tracks**). We use a custom script – written in Anaconda Jupyter Notebook by Anna Hobbiss – which fetches the x and y coordinates of the fly's center of mass for their walked paths, and with it visually assess the straightness of their paths. The script forces the body tracks to start at the same point in space and, by calculating the angle of the tracks, rotates them so they align with the x-axis so they start at the same point and face the same direction. The script also creates a heatmap from the aligned body-traces, representing the frequency of the flies bodies in a given position in their path; a heatmap with the brightest points along the x-axis reflects an extremely stable group of flies. With these amassed visual representations, we can observe how straight, stable and long the tracks are, and generally assess a given genotype's adaptation over-time.

RESIDUAL ANALYSIS

R-Studio is used to perform the residual analysis and residual data is saved on Excel files. Plotting of residual data (boxplots) and statistics are performed on GraphPad Prism. Residual analysis is used for each motor parameter. With it, the experimental groups (amputated) are compared to the trendline formed by the control's (unamputated) datapoints in function of the speed. Speed, normally a dependent variable, is treated as independent; in this way the experimental groups' data points will be compared to control flies walking at the same speed within the trendline. Since the compared flies are matched by speed, this also eliminates its effect on multiple motor parameters (the leg's swing speed for example). The distance between the experimental datapoint and the control's trendline is the datapoint's residual value and, in the boxplots shown throughout the manuscript, the Y axis represents the **difference to the control** (control at $Y=0$), at different timepoints, of performance of various locomotor parameters. This difference can be positive or negative, depending on the motor parameter. For example, in Figure 4B (Body path) this difference is positive, meaning that flies at 15 minutes post-amputation dislocated their bodies more than those unamputated to walk the same distance; in Figure 4C however (Body displacement ratio), this difference to unamputated is negative since the ratio of distance/path is negative too – uncoordinated flies will walk a longer path to displace the same distance. In Heatmaps are generated to visualize all analyzed parameters and groups from an experiment.

STATISTICAL ANALYSIS

Statistical analysis is performed on GraphPad Prism 6. Data is tested for normality using D'Agostino Pearson and Shapiro-Wilk normality tests. Statistical analysis for **normally distributed** data is done using a parametric One-Way ANOVA and Holm-Sidak's test for multiple comparisons. Statistical analysis for **abnormally distributed data** is done using a non-parametric Kruskal-Wallis test and Dunn's test for multiple comparisons. The script for the heatmaps' statistical color code was written by Alexandra Medeiros in sPyder (from the Anaconda package), and reflects the same logic as mentioned above for the boxplots: warm colors represent an increase of the statistical difference to control, and cold ones vice-versa.

RESULTS

WILD TYPE *DROSOPHILA MELANOGASTER* CANTON-S FLIES SHOW LOCOMOTOR RECOVERY IN RESPONSE TO DOUBLE MIDDLE-LEG AMPUTATION

To address the hypothesis of locomotor adaptation in *Drosophila melanogaster*, wild type Canton-S flies were submitted to a double middle-leg amputation protocol (Marta Santos, César Mendes, unpublished). Four groups of flies were tested for locomotor performance using the FlyWalker system for behavioral analysis; from which three of them were submitted to the amputation protocol and tested at different timepoints. The groups are the following: Unamputated flies, amputated flies whose locomotor behavior was filmed 15 minutes after the amputation (to assess the immediate effects of the amputation protocol), 72 hours and 7 days post-amputation (to evaluate locomotor recovery throughout time). In order for them to achieve locomotor recovery, they should readapt various locomotor parameters from the four groups the FlyWalker is now capable of assessing – **gait**, **stability**, **spatial** and **step** – so that their walking behavior is visibly better approaching walking behavior exhibited by unamputated flies.

STABILITY PARAMETERS

To understand our method of assessing locomotor adaptation and recovery let's first look at some stability parameters. These focus on the stability of the fly's body while performing straight walking bouts of 5 steps from each leg.

Figure 4A represents one of the most basic and immediate ways of qualitatively addressing locomotor adaptation in our flies: the bulk body traces of the walked paths, representing the trace left by the flies' center of mass while walking (COM, located in the second thoracic segment⁷⁹).

The **body traces** represented in the figure are those of Unamputated flies, as well as of those filmed 15 minutes and 7 days after amputation. From the body traces of unamputated flies, we realize how little the COM is displaced when they walk in straight bouts, whereas in flies filmed 15 minutes after amputation a clear perturbation in straightness is obvious – the absence of the middle legs which once aided in stabilizing the body's displacement shows as the COM is swung to the sides as they attempt to walk straight. To adapt and recover amputated flies must learn how to deal with the excessive lateral displacement of the body, which occurs, as observed on the 7 days post-amputation timepoint – body traces are more clustered along the x-axis and even though the COM still swings, it seems to be much more controlled.

These qualitative observations are reflected in the quantification of several stability parameters via **residual analysis** (the difference between the experimental groups' datapoints from those of the control, comparing flies walking at matching speeds).

The **body path** in Figure 4B for example, shows that amputation significantly increases the flies' body paths (Unamp. vs 15min post-amp.: $P \leq 0,0001$) and that after 7 days they shorten the path's length back to control levels while taking the same number steps (Unamp. vs 15min post-amp.: $P > 0,05$); this parameter shows **adaptation** (over 7 days) and **recovery** (comparison to the control) in locomotor behavior.

The **body displacement ratio** (Fig. 4C) – the ratio of the distance/path (a straight line joining the initial and final positions of the COM) – shows locomotor adaptation (15min vs 7d post-amp.: $P \leq 0,01$) without recovery (Unamp. vs 7d post-amp.: $P \leq 0,0001$). As for the last parameter that consistently shows locomotor recovery, the

area of all configurations (Fig. 4D), we can observe both adaptation (15min vs 7d post-amp.: $P \leq 0,0001$) to the amputated state and a recovery of performance back to unamputated levels (15min vs 7d post-amp.: $P > 0,05$). This parameter calculates the area of the shape formed by the legs contacting the ground, and while amputation initially leads to its increase, possibly in an attempt to maximize body stability by stretching the legs, it decreases back to control levels as the body starts stabilizing overtime.

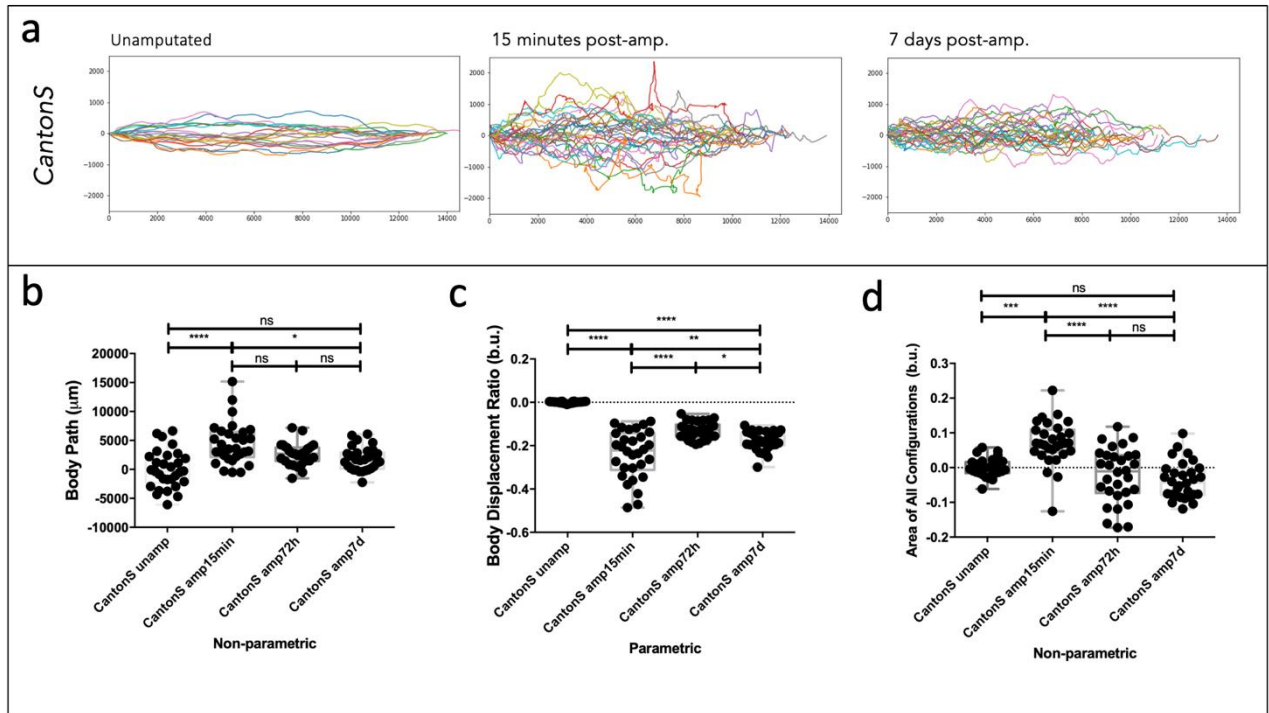
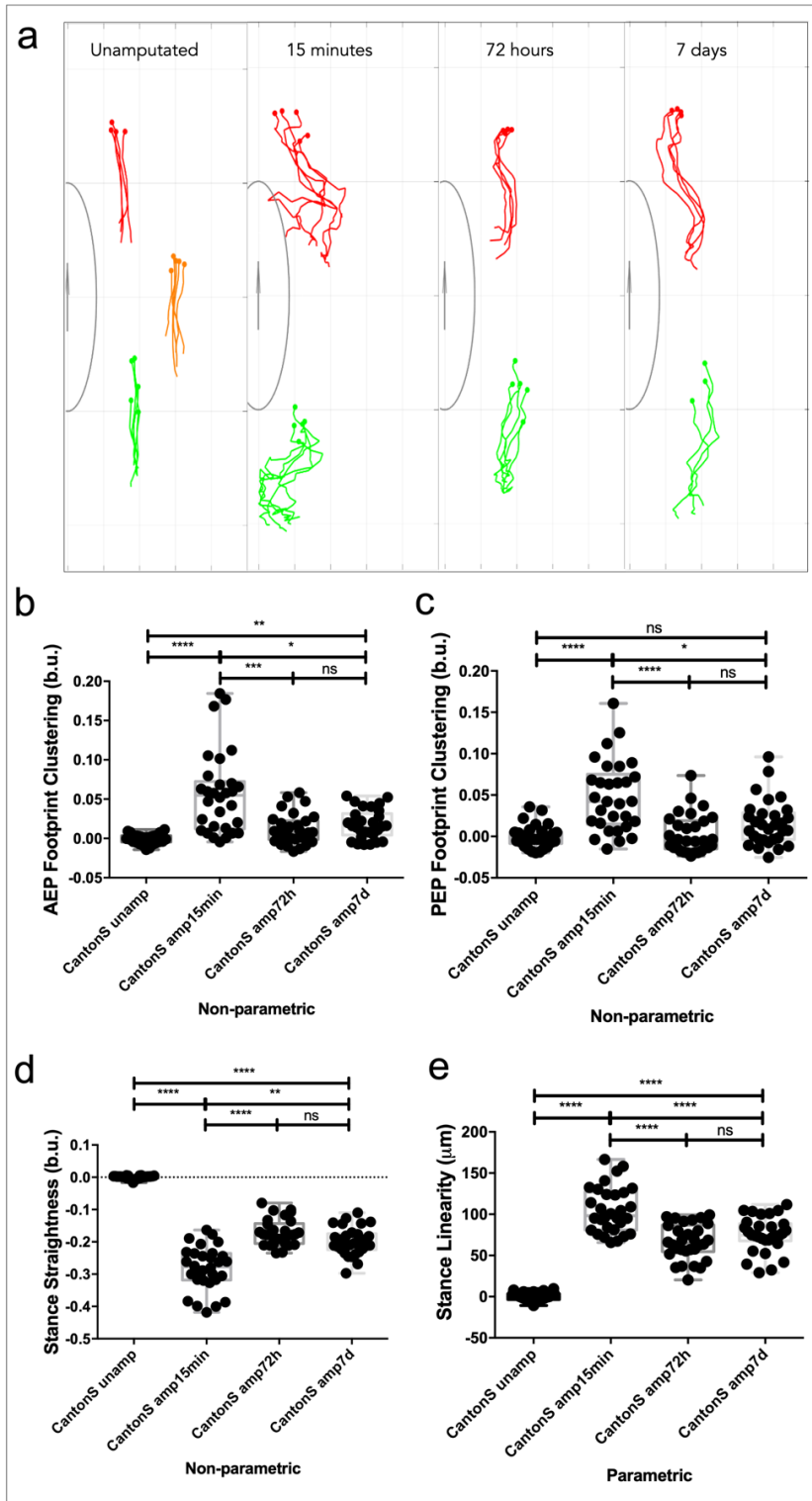


FIGURE 4. *Drosophila melanogaster* wild type Canton-S Stability parameters. **A)** Body traces for the wild type Canton-S at three timepoints: Unamputated (N=5, n=10), 15 minutes post-amputation (N=5, n=10) and 7 days post-amputation (N=9, n=18). x (0 - >14000 µm) and y-axis (-2000 -> 2000 µm) are the horizontal and vertical distance travelled by the flies. **B)** Quantification of wild type Canton-S 's Body Path (µm) via residual analysis vs unamputated control group. **C)** Quantification of wild type Canton-S's Body Displacement Ratio (body units) via residual analysis vs unamputated control group. **D)** Quantification of wild type Canton-S's Body Path (µm) via residual analysis vs unamputated control group. **Data distribution** assessed by D'Agostino Pearson and Shapiro-Wilk normality tests. **Multiple comparison** tests performed according to patterns of data distribution, either parametric (One-Way ANOVA for normally distributed data; Holm-Sidak's test for multiple comparisons) or non-parametric (Kruskal-Wallis test for abnormally distributed data and Dunn's test for multiple comparisons). **Statistical significances** resulting from multiple comparison tests are as follows: ****, $P \leq 0,0001$; ***, $P \leq 0,001$; **, $P \leq 0,01$; *, $P \leq 0,05$; ns, $P > 0,05$. **Box-plot positioning** above or below the x-axis reflects a respective increase or decrease of the analyzed parameter vs the unamputated control group.

SPATIAL PARAMETERS

Qualitative interpretations can also be done for the spatial parameters of Anterior Extreme Position footprint clustering and stance straightness parameters (Fig. 5A). The plot represents one fly per group;



these represented in the figure are flies within the median value of AEP footprint clustering. From this data we observe that both parameters positively evolve over a 7 day period, shown by footprints that are much clustered in the 3rd and 7th days of recovery – indicating coordination in step placement – and as the stance traces left by the legs while displacing the body forwards become straighter. Quantification of these parameters resulted in the same conclusions. **AEP footprint clustering** (Fig. 5B), while greatly suffering due to the amputation of the middle legs (Unamp vs 15min post-amp.: $P \leq 0,0001$) shows motor adaptation (15min vs 72h post-amp.: $P \leq 0,001$; 15min vs 7d post-amp.: $P \leq 0,05$) and recovery to the sustained damage (Unamp vs 7d post-amp.: $P \leq 0,01$). The **Posterior Extreme Position footprint clustering** (Fig. 5C) parameter (position of the legs before it enters the swing phase to take another step) shows the same phenotype with a greater degree of recovery (Unamp vs 7d post-amp.: $P > 0,05$).

The **stance straightness** (Fig. 5D), even though not recovering to control levels (Unamp vs 7d post-amp.: $P \leq 0,0001$), shows adaptation during the 7 day period (15min vs 72h post-amp.: $P \leq 0,0001$; 15min vs 7d post-amp.: $P \leq 0,01$) as does the **stance linearity** (Fig. 5E) (difference of the stance traces from a smoothed line joining AEPs and PEPs) (15min vs 72h post-amp.: $P \leq 0,0001$; 15min vs 7d post-amp.: $P \leq 0,0001$).

FIGURE 5. *DROSOPHILA MELANOGASTER* WILD TYPE CANTON-S SPATIAL PARAMETERS. A) WILD TYPE CANTON-S VISUAL REPRESENTATION OF AEP FOOTPRINT CLUSTERING AND STANCE TRACES FOR SINGLE FLIES WITHIN THE MEDIAN VALUE OF AEP FOOTPRINT CLUSTERING FOR THE ANALYSED GROUPS: UNAMPUTATED; 15MINUTES, 72 HOURS AND 7DAYS POST-AMPUTATION. BODY SIZE REPRESENTS A BODY UNIT. **B)** QUANTIFICATION OF WILD TYPE CANTON-S'S FOOTPRINT CLUSTERING OF ANTERIOR EXTREME POSITIONS (BODY UNITS) VIA RESIDUAL ANALYSIS VS UNAMPUTATED CONTROL GROUP. **C)** QUANTIFICATION OF WILD TYPE CANTON-S'S FOOTPRINT CLUSTERING OF POSTERIOR EXTREME POSITIONS (BODY UNITS) VIA RESIDUAL ANALYSIS VS UNAMPUTATED CONTROL GROUP. **D)** QUANTIFICATION OF WILD TYPE CANTON-S'S AVERAGE STANCE STRAIGHTNESS (BODY UNITS) VIA RESIDUAL ANALYSIS VS UNAMPUTATED CONTROL GROUP. **E)** QUANTIFICATION OF WILD TYPE CANTON-S'S AVERAGE STANCE LINEARITY (BODY UNITS) VIA RESIDUAL ANALYSIS VS UNAMPUTATED CONTROL GROUP. **DATA DISTRIBUTION** ASSESSED BY D'AGOSTINO PEARSON AND SHAPIRO-WILK NORMALITY TESTS. **MULTIPLE COMPARISON** TESTS PERFORMED ACCORDING TO PATTERNS OF DATA DISTRIBUTION, EITHER PARAMETRIC (ONE-WAY ANOVA FOR NORMALLY DISTRIBUTED DATA; HOLM-SIDAK'S TEST FOR MULTIPLE COMPARISONS) OR NON-PARAMETRIC (KRUSKAL-WALLIS TEST FOR ABNORMALLY DISTRIBUTED DATA AND DUNN'S TEST FOR MULTIPLE COMPARISONS). **STATISTICAL SIGNIFICANCES** RESULTING FROM MULTIPLE COMPARISON TESTS ARE AS FOLLOWS: ****, $P \leq 0,0001$; ***, $P \leq 0,001$; **, $P \leq 0,01$; *, $P \leq 0,05$; ns, $P > 0,05$. **BOX-PLOT POSITIONING**, EITHER ABOVE OR BELOW THE X-AXIS, REFLECTS A RESPECTIVE INCREASE OR DECREASE OF THE ANALYZED PARAMETER VS THE UNAMPUTATED CONTROL GROUP.

STEP PARAMETERS

From 8 step parameters, three show signs of recovery and one of them does so to unamputated control levels: the **step length** (Fig. 6A) (Unamp vs 7d post-amp.: $P > 0,05$) increases by the 3rd and 7th days as the legs are swung at greater distances. **Leg displacement** (Fig. 6B) also shows signs of both adaptation (15min vs 72h post-amp.: $P \leq 0,01$; 15min vs 7d post-amp.: $P \leq 0,01$) and recovery (Unamp vs 7d post-amp.: $P \leq 0,001$) although the latter does not happen to a great degree. Lastly, the **step frequency** (Fig. 6C) shows a slight approximation to control levels (Unamp vs 7d post-amp.: $P \leq 0,001$).

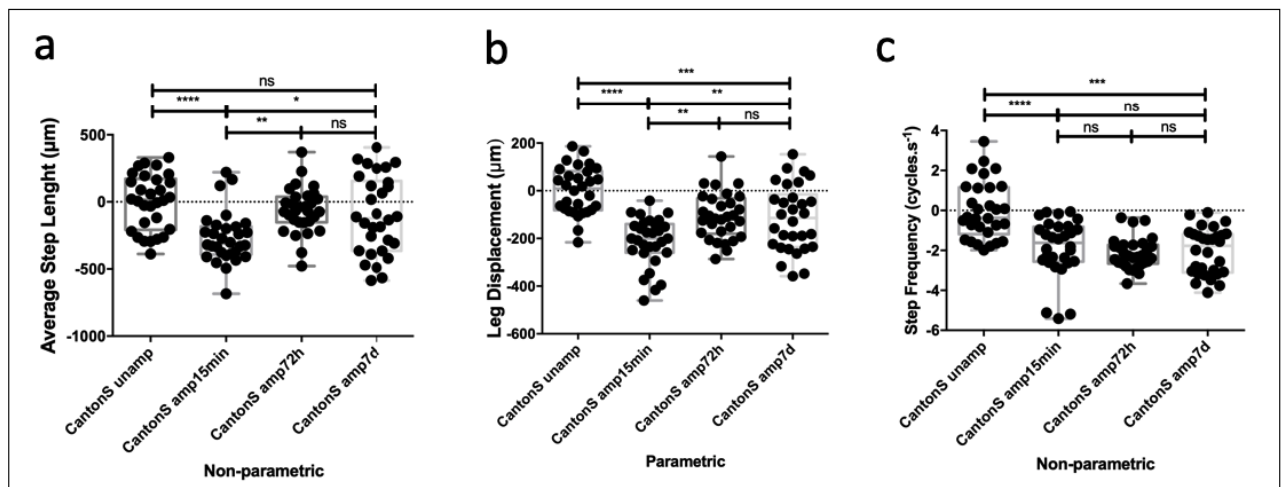


FIGURE 6. *Drosophila melanogaster* wild type Canton-S Step parameters. A) Quantification of wild type Canton-S's Average Step Length (μm) via residual analysis vs unamputated control group. **B)** Quantification of wild type Canton-S's Leg Displacement (μm) via residual analysis vs unamputated control group. **C)** Quantification of wild type Canton-S's Step Frequency (step cycles.s⁻¹) via residual analysis vs unamputated control group. **Data distribution** assessed by D'Agostino Pearson and Shapiro-Wilk normality tests. **Multiple comparison** tests performed according to patterns of data distribution, either parametric (One-Way ANOVA for normally distributed data; Holm-Sidak's test for multiple comparisons) or non-parametric (Kruskal-Wallis test for abnormally distributed data and Dunn's test for multiple comparisons). **Statistical significances** resulting from multiple comparison tests are as follows: ****, $P \leq 0,0001$; ***, $P \leq 0,001$; **, $P \leq 0,01$; *, $P \leq 0,05$; ns, $P > 0,05$. **Box-plot positioning** above or below the x-axis reflects a respective increase or decrease of the analyzed parameter vs the unamputated control group

GAIT PARAMETERS

Canton-S flies do not display any recovery in the analyzed gait parameters as shown in the heatmap of (Fig. 7), which shows the increase (red) and decrease (blue) in statistical difference from the unamputated control. In it, seven gait parameters are shown: **Pace**, **Trot**, **Non-canonical**, **Gait** and **Wave Indexes**, as well as the **Inter-tripod transition time** and **Tripod duration**. Trot and Pace are gaits performed by quadruped animals; from these we see that Canton-S flies do not adopt these gaits as none differ over time. Non-canonical index – a pseudo-gait that reflects uncoordinated leg placement – does not show recovery as it is always shown to be increased vs the unamputated animals.

The other parameters are irrelevant for the question in study. Absence of the middle legs mean that neither wave nor tripod gaits occur; absence of the tripod gait also means that they will have no duration nor transition time. The gait index reflects the index between Pace and Trot gaits, which as mentioned above, are not adopted. Because of this the gait parameters will not be analyzed regarding motor adaptation and recovery.

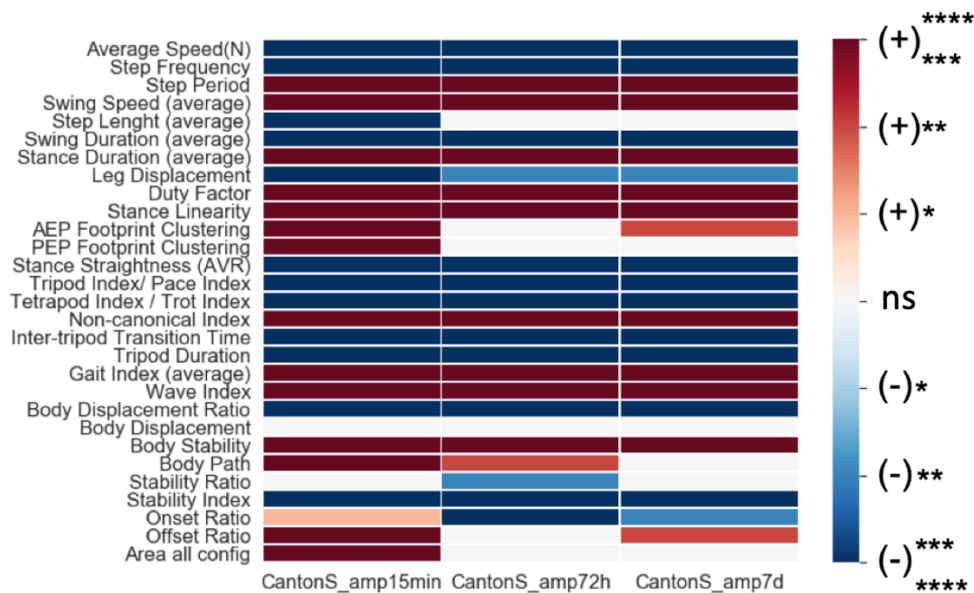


FIGURE 7. *Drosophila melanogaster* wild type Canton-S heatmap of all residual data from comparison to unamputated flies of the same genotype. tested locomotor parameters in the following order: Step, Spatial, Gait Parameters and Stability parameters. **Data distribution** assessed by D’Agostino Pearson and Shapiro-Wilk normality tests. **Multiple comparison** tests performed according to patterns of data distribution, either parametric (One-Way ANOVA for normally distributed data; Holm-Sidak’s test for multiple comparisons) or non-parametric (Kruskal-Wallis test for abnormally distributed data and Dunn’s test for multiple comparisons). Bonferroni **correction** was applied to the multiple comparisons. **Statistical significances** resulting from multiple comparison tests are as follows: ****, $P \leq 0,0001$ and ***, $P \leq 0,001$, deep red and deep blue; **, $P \leq 0,01$, red and blue; *, $P \leq 0,05$, pale red and pale blue; ns, $P > 0,05$, white.

SUMMARY

From this data we can conclude that wild type *Drosophila melanogaster* Canton-S flies:

- 1) recover locomotor in response to middle-leg amputation during an adaptation period of 7 days;
- 2) at the 3rd day post-amputation they already show clear signs of recovery;
- 3) this phenotype occurs by relearning how to perform various walking parameters, from which Spatial and Stability parameters seem to be the modulated the most; Step parameters show little adaptation, whereas Gait parameters seem to be incompatible with the amputation context.

From the Heatmap we can conclude that nine locomotor parameters (step length, leg displacement, AEP and PEP footprint clustering, body displacement, body path, stability ratio, offset ratio and area of all configurations) recover locomotor performance by approaching or in some cases, reaching control levels.

LOCOMOTOR RECOVERY FROM DOUBLE MID-LEG AMPUTATION IS CONSERVED ACROSS TWO EVOLUTIONARILY DISTANT DROSOPHILA SPECIES

After the positive results of locomotor adaptation that occur post middle-leg amputation in various *Drosophila melanogaster* wild type lines including Canton-S, we sought to test if this phenotype was reproducible in the evolutionarily distant *Drosophila* species *Drosophila pseudoobscura* and *Drosophila repleta*. With this experiment, we aimed to understand whether there is any evolutionary conservation of our behavioral readout which, in case of a positive result, adds robustness of our genetic model for neurorehabilitation.

For simplicity, both subspecies will be shown side by side.

STABILITY PARAMETERS

The first component which is a good indicator of locomotor recovery is the straightness of a fly's walking burst. To analyze this, we first compile the fly's Body Traces, a basic visual assay used to compare two most relevant groups to assess recovery – those filmed 15 minutes, with the least time to adapt, and 7 days post-amputation, with the most time to adapt. This data is unprocessed and is merely a compilation of the body's x and y positions of the fly's center of mass (COM) in the walked path.

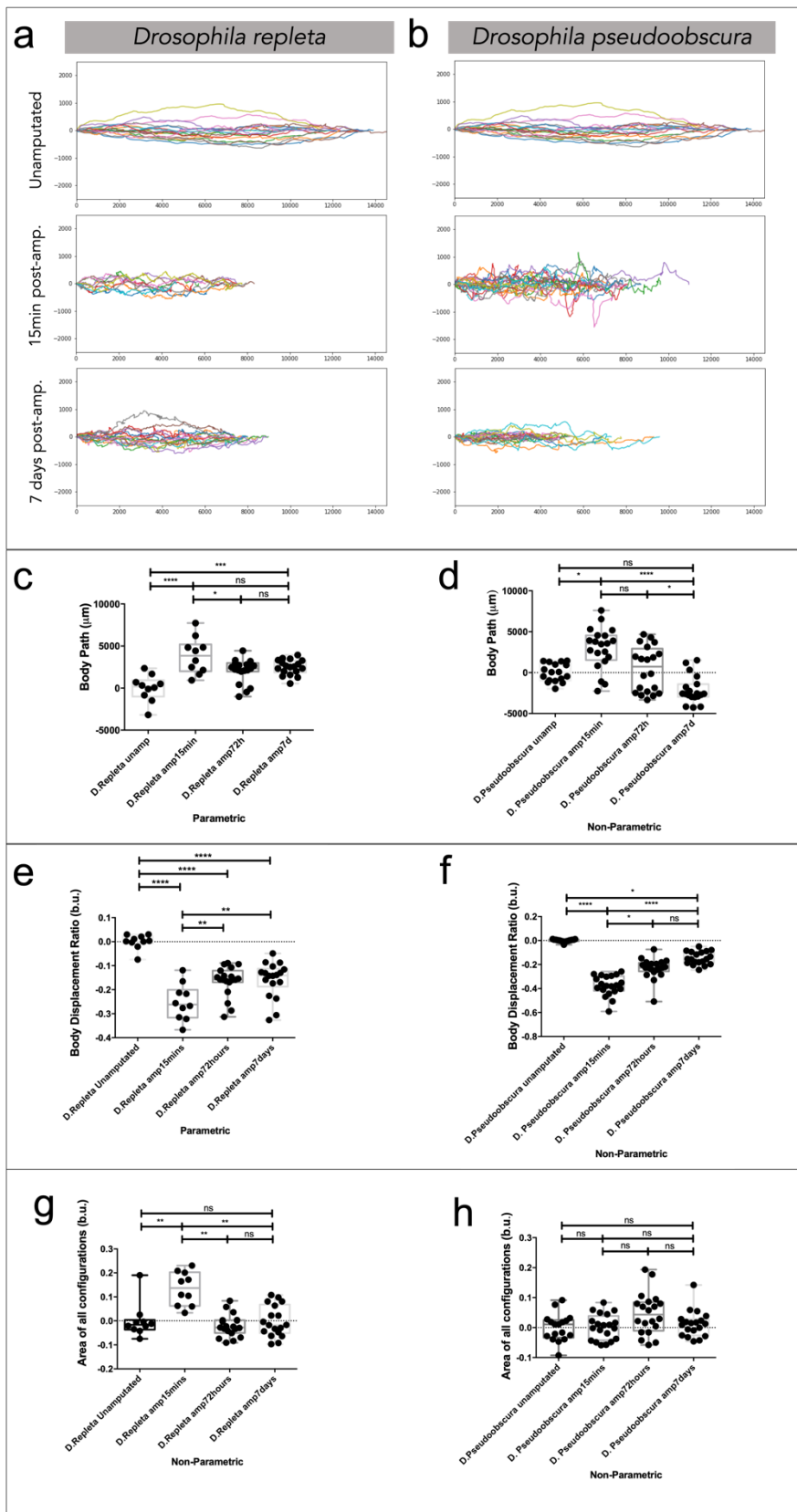
As can be appreciated in Figure 8A and B, we observe that the fly's COM corresponding to the timepoint at 15min post-amputation in *D. pseudoobscura* (N=10, n=20) is wobbly, meaning that there is a big amplitude of the COM's y position along the x axis – the distance traveled in 5 steps. The same cannot be said regarding *D. repleta* (N=5, n=10) on the "15min" timepoint. When comparing the straightness of these walking bursts to those of the "7days" timepoint, a clear straightening of the paths can be observed, in *D. pseudoobscura*: the oscillation of the y position of the COMs is more constrained, indicating the flies now exert more control over their bodies.

Diving in the residual data for stability parameters – corroborating and further adding to the claim in the last paragraph – observation of the **body path** parameter of the two subspecies at the various tested conditions and timepoints shows us that:

1) *D. pseudoobscura* have decreased body path at 7 days of recovery, fully reaching and even surpassing that of the unamputated condition – this implies their body is less dislocated less while giving the same number of steps (Fig. 8C); additionally, it shows that this recovery happens progressively over the course of 7 days, which can be said due to the consistency of the trend to return to unamputated levels – a constant evolution from the timepoint at "15mins", to that of "3 days", reaching its best performance in this motor parameter at "7 days".

2) *D. repleta*, even though not as consistently as *D. pseudoobscura* also recover walking stability over time from middle leg amputation as the evolution of its **body path** (Fig. 8D) indicates when comparing the statistically significant difference of the timepoint at 15 mins to the control (Unamp vs 15min post-amp.: $P \leq 0,0001$) to that of the 7 days to the control (Unamp vs 7d post-amp.: $P \leq 0,001$). Additionally, an evolution can be seen from 15mins to 3 days ($P \leq 0,05$), and a persistence of the body path from the 3 days to 7 days ($P > 0,05$).

Two other stability parameters consistently show signs of recovery or adaptation in both *Drosophila* subspecies: Body Displacement Ratio and Area of All Configurations.



Regarding the **Body's Displacement Ratio** – the ratio between the COM's covered distance and that of the path walked in a perfect straight line – residual data is consistent with the degree of recovery stated above; both subspecies show locomotor recovery, however, *D. pseudoobscura* does so to a greater degree than that of *D. repleta*. As observed in Figures 8E and F, *D. pseudoobscura* is significantly close to the unamputated control (Unamp vs 7d post-amp.: $P \leq 0,05$) and significantly distant from the 15mins post-amputation group (Unamp vs 7d post-amp.: $P \leq 0,0001$). As for *D. repleta*, even though statistical proximity from the unamputated control is non-existent (Unamp vs 7d post-amp.: $P \leq 0,0001$), its body displacement ratio is significantly better than that filmed immediately after amputation at the third and seventh days of recovery (Unamp vs 72h post-amp.: $P \leq 0,01$; Unamp vs 7d post-amp.: $P \leq 0,01$).

Regarding the **Area of All Configurations** – the area of support for which the tarsi on the floor make up the vertices – shows no statistically significant alteration throughout the time spectrum for *D. pseudoobscura* (Unamp vs 15min post-amp.: $P > 0,05$; Unamp vs 7d post-amp.: $P > 0,05$), and shows a return to unamputated control levels for *D. repleta* (Unamp vs 15min post-amp.: $P \leq 0,01$; Unamp vs 7d post-amp.: $P > 0,05$) (Fig. 8G,H).

Other stability parameters such as the Offset Ratio, Body Displacement and Body Stability also indicate signs of recovery, although inconsistently for both subspecies and *Drosophila melanogaster's* Canton-S line.

FIGURE 8. *Drosophila repleta* and *pseudoobscura* Stability parameters. **A,B)** Body traces for *Drosophila repleta* and *pseudoobscura* at three timepoints: Unamputated (N=5, n=10), 15 minutes post-amputation (N=5, n=10) and 7 days post-amputation (N=9, n=18). x (0 ->14000 μ m) and y-axis (-2000 -> 2000 μ m) are the horizontal and vertical distance travelled by the flies. **C,D)** Quantification of *Drosophila repleta*'s and *pseudoobscura*'s Body Path (μ m) via residual analysis vs unamputated control group. **E,F)** Quantification of *Drosophila repleta*'s and *pseudoobscura*'s Body Displacement Ratio (body units) via residual analysis vs unamputated control group. **G,H)** Quantification of *Drosophila repleta*'s and *pseudoobscura*'s Body Displacement Ratio (body units) via residual analysis vs unamputated control group. **Data distribution** assessed by D'Agostino Pearson and Shapiro-Wilk normality tests. **Multiple comparison** tests performed according to patterns of data distribution, either parametric (One-Way ANOVA for normally distributed data; Holm-Sidak's test for multiple comparisons) or non-parametric (Kruskal-Wallis test for abnormally distributed data and Dunn's test for multiple comparisons). **Statistical significances** resulting from multiple comparison tests are as follows: ****, $P \leq 0,0001$; ***, $P \leq 0,001$; **, $P \leq 0,01$; *, $P \leq 0,05$; ns, $P > 0,05$. **Box-plot positioning** above or below the x-axis reflects a respective increase or decrease of the analyzed parameter vs the unamputated control group.

SPATIAL PARAMETERS

All FlyWalker spatial parameters systematically show improvement on behavioral adaptation to walking on four points of contact. As observed on (Fig. 9A,B) – consisting on a single fly within the median value for each group – representing both Anterior Extreme Position Footprint Clustering (tarsal point of contact on the onset of a step) and Stance Straightness (path described by the leg when supporting the body during the step) respectively show 1) a time dependent increase in the clustering of the steps, indicating a gain of coordination during the recovery period; and 2) increase in straightness of steps, indicating that, throughout time, flies can better rely on their existing legs to efficiently support their body.

Quantification of these two parameters via residual analysis supports visual observation of the mentioned plots. **D. repleta** show statistical significance in recovery of **AEP Footprint Clustering** – 15mins vs 7days ($P \leq 0,05$) – and when comparing the difference of the unamputated control to the 15 min timepoint ($P \leq 0,0001$) vs the control to the 7 days timepoint ($P \leq 0,001$) (Fig. 9C,D). **D. pseudoobscura**, as happens with stability parameters, show a greater degree of recovery than *D. repleta*: there is minimal statistical difference when comparing the unamputated control with the 7 days timepoint ($P \leq 0,05$), and when comparing the recovery from amputation **repleta** (15min vs 7d post-amp.: $P \leq 0,001$).

Regarding **stance straightness**, the same adaptation and degree of recovery is consistent in both subspecies, with **D. pseudoobscura** still being the most pronounced (15min vs 7d post-amp.: $P \leq 0,0001$) (Fig. 9E). **D. repleta**, however shows best the evolution of recovery (15min vs 72h post-amp.: $P \leq 0,05$; 15min vs 7d post-amp.: $P \leq 0,001$) (Fig. 9F).

The two other spatial parameters are the Posterior Extreme Position Footprint clustering (PEP footprint clustering: clustering of the tarsal points of contact on the offset of a step) and stance linearity (difference between the path described by the leg when supporting the body during a step, from a straight line connecting the AEPs and PEPs – how close to a straight line they are).

Regarding the **PEP Footprint Clustering** (Fig. 11A,B) the roles are reversed regarding recovery: between **D. repleta** (Unamp vs 7d post-amp.: $P > 0,05$) and **D. pseudoobscura** (Unamp vs 7d post-amp.: $P \leq 0,0001$; 15min vs 7d post-amp.: $P \leq 0,001$), the first shows no statistical difference from unamputated flies – bear in mind, however, that its scale is much smaller than that of its *pseudoobscura* counterpart.

As for the **stance linearity**, **D. repleta** (Fig. 11A,B) (Unamp vs 7d post-amp.: $P > 0,05$; 15min vs 7d post-amp.: $P \leq 0,0001$) also excels compared **D. pseudoobscura** (Fig. 11A,B) (Unamp vs 7d post-amp.: $P \leq 0,05$; 15min vs 7d post-amp.: $P \leq 0,001$), although both display a great degree of adaptation and recovery.

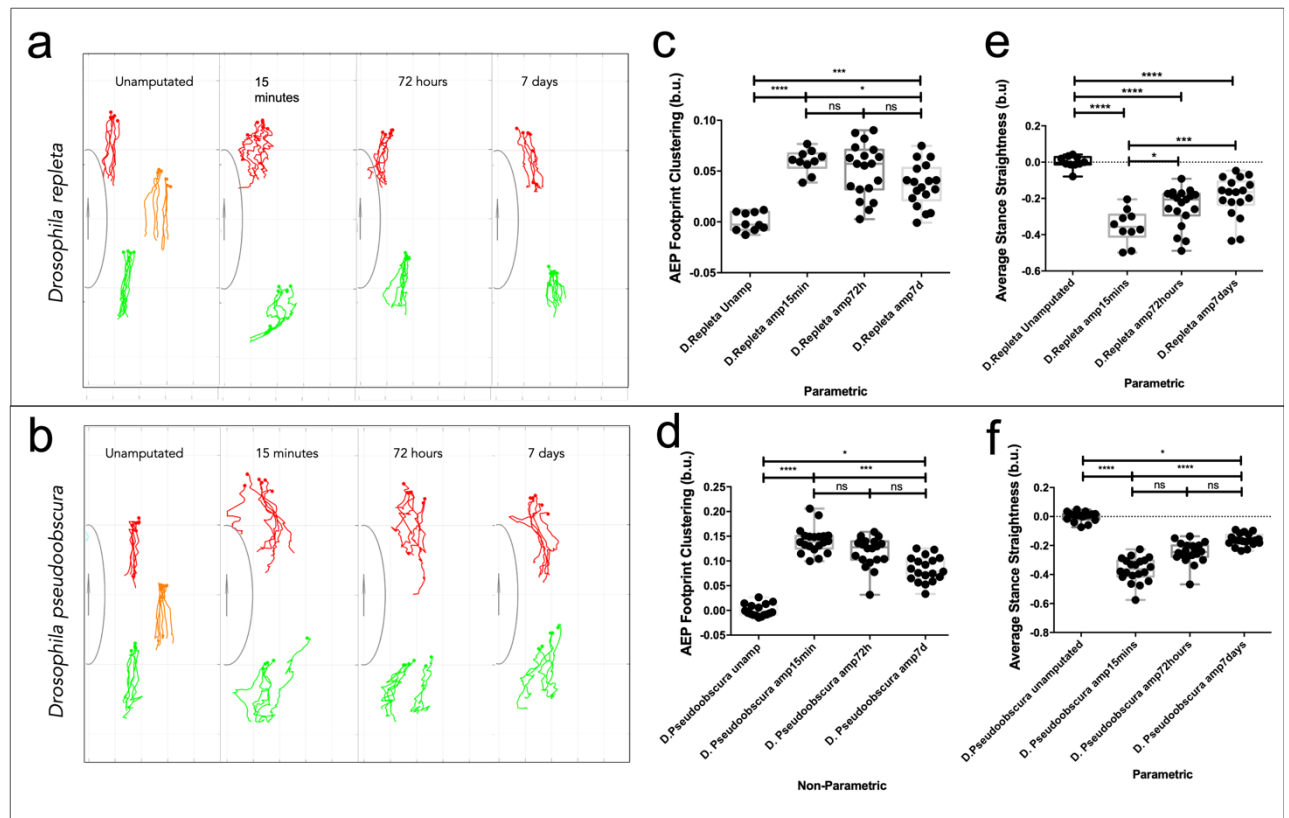


FIGURE 9. *Drosophila repleta* and *pseudoobscura* Spatial parameters. **A,B)** *Drosophila repleta* and *pseudoobscura* visual representation of AEP footprint clustering and stance traces for single flies within the median value of AEP footprint clustering for the analysed groups: Unamputated; 15minutes, 72 hours and 7days post-amputation. Body size represents a body unit. **C,D)** Quantification of *Drosophila repleta*'s and *pseudoobscura*'s footprint clustering of Anterior Extreme Positions (body units) via residual analysis vs unamputated control group. **E,F)** Quantification of *Drosophila repleta*'s and *pseudoobscura*'s Average Stance Straightness (body units) via residual analysis vs unamputated control group. **Data distribution** assessed by D'Agostino Pearson and Shapiro-Wilk normality tests. **Multiple comparison** tests performed according to patterns of data distribution, either parametric (One-Way ANOVA for normally distributed data; Holm-Sidak's test for multiple comparisons) or non-parametric (Kruskal-Wallis test for abnormally distributed data and Dunn's test for multiple comparisons). **Statistical significances** resulting from multiple comparison tests are as follows: ****, $P \leq 0,0001$; ***, $P \leq 0,001$; **, $P \leq 0,01$; *, $P \leq 0,05$; ns, $P > 0,05$. **Box-plot positioning**, either above or below the x-axis, reflects a respective increase or decrease of the analyzed parameter vs the unamputated control group.

STEP PARAMETERS

Three step parameters show consistent improvement in both *Drosophila* subspecies: Step Frequency – the number of step cycles per second; Step Period – the time to complete a cycle, consisting on the stance and swing of a leg; and Stance Duration – the time the legs contact the floor. In all these parameters, *D. pseudoobscura* once again excels in recovery ratio, although very closely followed by *D. repleta*.

Regarding **step frequency**, both subspecies show recovery at 3 days post-amputation and maintain the phenotype up to 7 days post-amputation (72h vs 7d post-amp.: $P > 0,05$); however, when compared to the unamputated control, *D. pseudoobscura* takes the same number of step cycles per second (Fig. 10A) (Unamp. vs 7d post-amp.: $P > 0,05$), whereas *D. repleta* performs slightly worse (Fig. 10B) (Unamp. vs 7d post-amp.: $P \leq 0,05$). In terms of recovery from the amputation itself, *D. pseudoobscura* recovers to a greater extent than *D. repleta* (respectively, 15min vs 7d post-amp.: $P \leq 0,0001$; 15min vs 7d post-amp.: $P \leq 0,05$). This last comparison is mirrored in their **step periods** (Fig. 10C,D), although when they are compared to the unamputated control, both show a return to control values, neither having significant statistical difference from it –

this means that both subspecies take as much time completing a swing and a stance as if they had not been submitted to amputation, indicating a complete recovery of walking behavior in this parameter.

Regarding their **stance duration** (Fig. 10E,F), *D. pseudoobscura* also returns to control values (Unamp. vs 7d post-amp.: $P > 0,05$) and its recovery period shows statistical significance (15min vs 7d post-amp.: $P \leq 0,01$), whereas *D. repleta* still requires more time in the stance phase of a step at 7 days post amputation compared to its unamputated control ($P \leq 0,05$) and recover to a lesser degree (15min vs 7d post-amp.: $P \leq 0,05$).

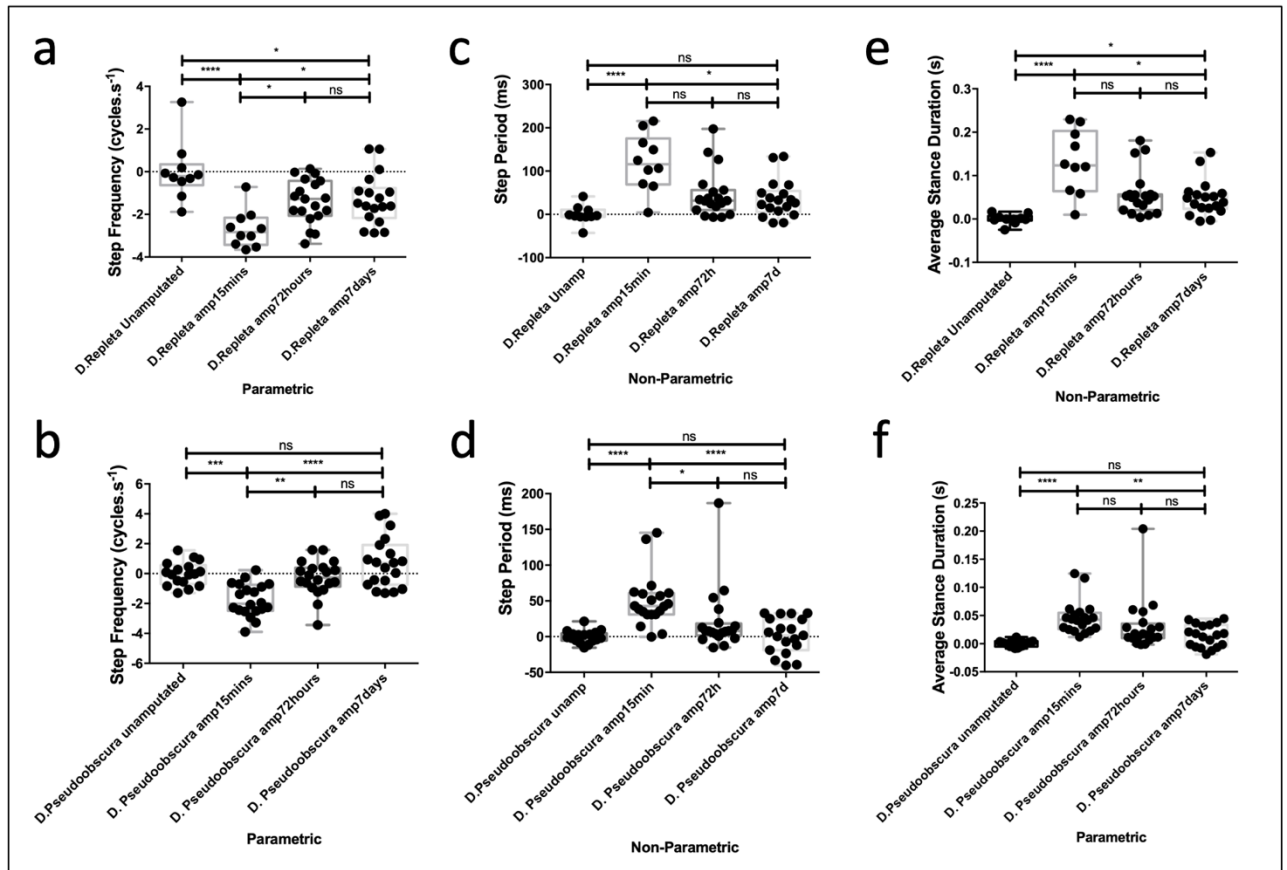


FIGURE 10. *Drosophila repleta* and *pseudoobscura* Step parameters. **A,B**) Quantification of *Drosophila repleta*'s and *pseudoobscura*'s Step Frequency (step cycles.s⁻¹) via residual analysis vs unamputated control group. **C,D**) Quantification of *Drosophila repleta*'s and *pseudoobscura*'s Step Period (milliseconds) via residual analysis vs unamputated control group. **E,F**) Quantification of *Drosophila repleta*'s and *pseudoobscura*'s Average Stance Duration (seconds) via residual analysis vs unamputated control group. **Data distribution** assessed by D'Agostino Pearson and Shapiro-Wilk normality tests. **Multiple comparison** tests performed according to patterns of data distribution, either parametric (One-Way ANOVA for normally distributed data; Holm-Sidak's test for multiple comparisons) or non-parametric (Kruskal-Wallis test for abnormally distributed data and Dunn's test for multiple comparisons). **Statistical significances** resulting from multiple comparison tests are as follows: ****, $P \leq 0,0001$; ***, $P \leq 0,001$; **, $P \leq 0,01$; *, $P \leq 0,05$; ns, $P > 0,05$. **Box-plot positioning** above or below the x-axis reflects a respective increase or decrease of the analyzed parameter vs the unamputated control group.

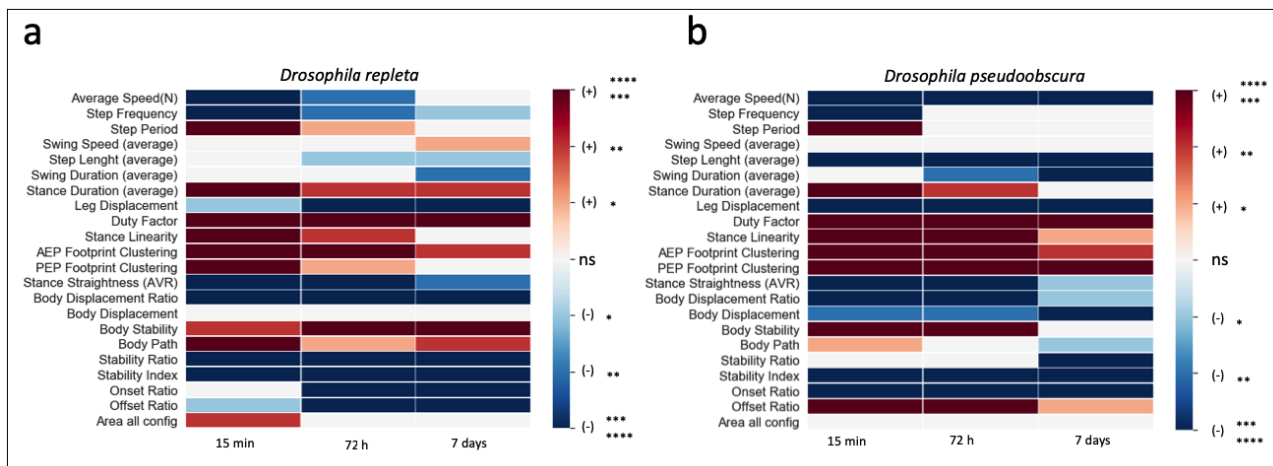


FIGURE 11. A,B) *Drosophila repleta* and *pseudoobscura* heatmap of all residual data from comparison to unamputated flies of the same genotype. tested locomotor parameters in the following order: Step, Spatial and Stability parameters. **Data distribution** assessed by D’Agostino Pearson and Shapiro-Wilk normality tests. **Multiple comparison** tests performed according to patterns of data distribution, either parametric (One-Way ANOVA for normally distributed data; Holm-Sidak’s test for multiple comparisons) or non-parametric (Kruskal-Wallis test for abnormally distributed data and Dunn’s test for multiple comparisons). Bonferroni **correction** was applied to the multiple comparisons. **Statistical significances** resulting from multiple comparison tests are as follows: ****, $P \leq 0,0001$ and ***, $P \leq 0,001$, deep red and deep blue; **, $P \leq 0,01$, red and blue; *, $P \leq 0,05$, pale red and pale blue; ns, $P > 0,05$, white.

SUMMARY

Summing up the data regarding Stability, Spatial and Step parameters (Fig. 11A,B)) of amputated walking behavior on *Drosophila pseudoobscura* and *repleta* strongly suggest that these, like their Canton-S *Drosophila melanogaster* counterpart, can efficiently deal with the amputation of both middle legs, doing so by adapting various locomotor parameters which grants them the ability to walk using only four legs.

Recapitulating, these two *Drosophila* subspecies systematically adapted three of the nine analyzed **Stability parameters** (Body displacement ratio, Body path and Area of all configurations), and non-systematically *D. repleta* and *D. pseudoobscura* respectively showed improvement in four (Body Displacement) and five (Body Stability and Offset Ratio) of these motor parameters.

Of the **Step parameters**, recovery on three of them – out of eight – are again shared between both (step frequency, step period and stance duration); it is worth adding that *D. pseudoobscura* sees no change to its Swing Speed with the amputation, leaving no room for improvement.

Very interestingly all four **Spatial parameters** recover in both subspecies, showing an immense adaptive power and revealing a possible strategy in adapting to this type of injury.

DISSECTING THE cAMP CASCADE OF THE LEARNING AND MEMORY PATHWAY

AMNESIAC¹

We start the dissection of the “Learning and Memory” pathway by one of its initiators – the Middle-term Memory associated *amnesiac*¹ pre-neuropeptide – a known activator of the cAMP cascade via GPCR binding and which directly promotes its synthesis via Adenylate Cyclase.

In order to assess its function in locomotor adaptation, we submitted mutant *amn*¹ flies to the mid-leg amputation protocol and assessed its motor performance when unamputated and at 15-minutes, 72 hours and 7 days after amputation (Marta Santos, César Mendes, unpublished).

STABILITY PARAMETERS

Visual interpretation of the bulk body traces of these flies shows (Fig. 12A,B) no significant changes in body path. Via residual data quantification however, their **body paths** show a significative improvement, consistent with motor recovery; this is demonstrated in (Fig. 12C) in the difference of both 3- and 7-days post-amputation, from its 15 minutes counterpart ($P \leq 0,001$ and $P \leq 0,0001$, respectively), although not to the unamputated control; this indicates there is no recovery but slight level of adaptation occurs regarding the distance of straight walking bouts needed to take 5 steps from each leg.

Two other *amn*¹'s *body-related parameters* also display signs of motor recovery: the **body displacement ratio** (Fig. 12D) – yielding the same statistical differences as the body paths; and **body displacement parameters** – with no significative difference from the unamputated control at 7-days post-amputation and with a significative difference ($P \leq 0,05$) from its 15-mins post-amputation counterpart.

Regarding their **stability ratio** (Fig. 15) and **stability index** (Fig. 15), *amn*¹ mutants display the same amount of adaptation: significantly distant from its unamputated counterpart at 7-days post-amputation ($P \leq 0,0001$) with slight adaptation of both parameters overtime (15mins vs 7 days post-amp.: $P \leq 0,05$). This pattern of slight adaptation is again repeated to the same degree on the **Onset** and **Offset Ratios**.

Regarding the flies' support area, indicated by the **Area of All Configurations** (Fig. 12E) , we observe the same pattern in recovery as mentioned above: Unamputated vs 7 days post-amputation has a $P \leq 0,0001$ (no statistical proximity to control flies). Adaptation is also slight: flies tested 15mins after amputation recover very little in 7 days ($P \leq 0,05$).

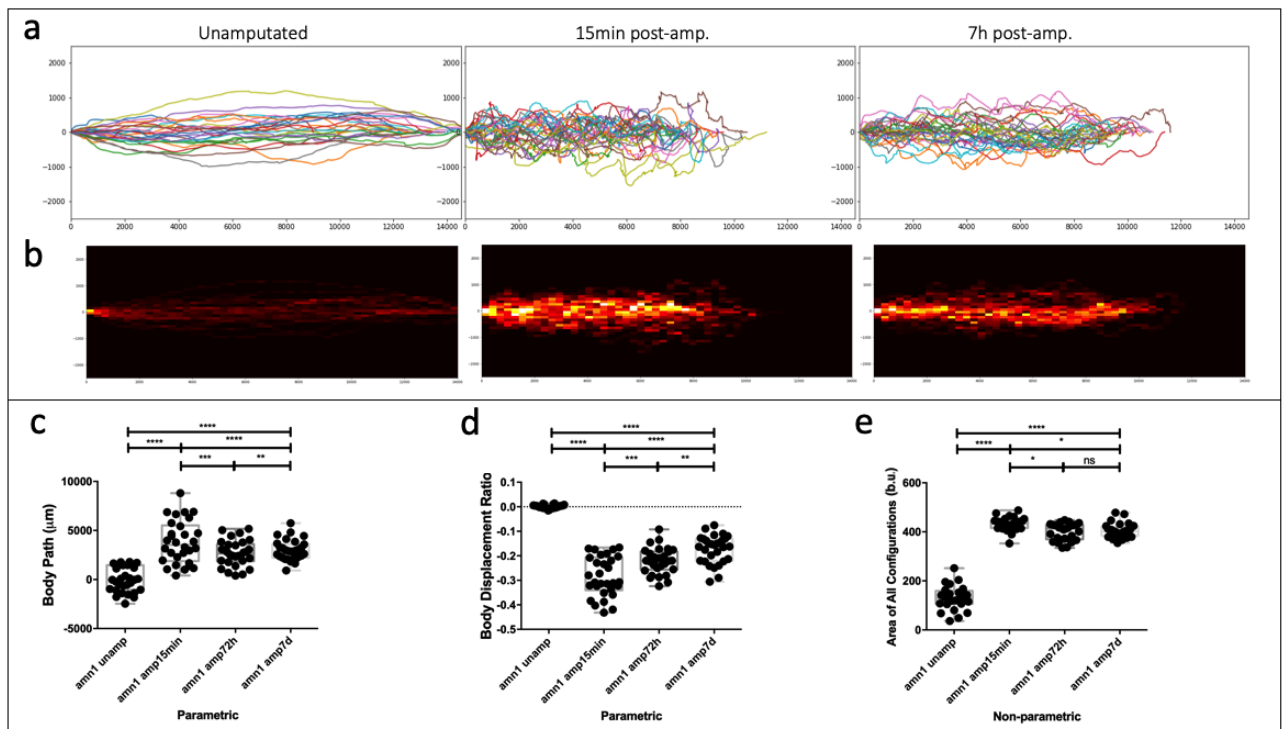


FIGURE 12. *Amnesiac*¹ Stability parameters. **A,B)** Body traces in the form of lines and heatmap for *Amnesiac*¹ at three timepoints: Unamputated (N=5, n=10), 15 minutes post-amputation (N=5, n=10) and 7 days post-amputation (N=9, n=18). *x* (0 → 14000 µm) and *y*-axis (-2000 → 2000 µm) are the horizontal and vertical distance travelled by the flies. Increase in **colour brightness** represents coordinates in which more flies passed through. **C)** Quantification of *Amnesiac*¹'s Body Path (µm) via residual analysis vs unamputated control group. **D)** Quantification of *Amnesiac*¹'s Body Displacement Ratio via residual analysis vs unamputated control group. **E)** Quantification of *Amnesiac*¹'s average area of all configurations (body units) via residual analysis vs unamputated control group. **Data distribution** assessed by D'Agostino Pearson and Shapiro-Wilk normality tests. **Multiple comparison** tests performed according to patterns of data distribution, either parametric (One-Way ANOVA for normally distributed data; Holm-Sidak's test for multiple comparisons) or non-parametric (Kruskal-Wallis test for abnormally distributed data and Dunn's test for multiple comparisons). **Statistical significances** resulting from multiple comparison tests are as follows: ****, P≤0,0001; ***, P≤0,001; **, P≤0,01; *, P≤0,05; ns, P>0,05. **Box-plot positioning** above or below the *x*-axis reflects a respective increase or decrease of the analyzed parameter vs the unamputated control group.

SPATIAL PARAMETERS

Similar to the recovery patterns on many Stability parameters, most Spatial Parameters – **stance linearity** (Fig. 13E), **AEP** (Fig. 13B) and **PEP footprint clustering** (Fig. 13C) – show only a small degree of adaptation to the amputated state (15mins vs 7days post-amp.: P ≤ 0,05). From these, only the stance linearity shows recovery (Unamp vs 15min post-amp.: P ≤ 0,0001 ; Unamp vs 7d post-amp.: P ≤ 0,001); neither AEP nor PEP footprint clustering get close to the performance of the unamputated controls at the 7th day post-amputation (Unamp vs 7d post-amp.: P ≤ 0,0001). The **average stance straightness** (Fig. 13D) is the sole spatial parameter that shows high levels of adaptation (15mins vs 7days post-amp.: P ≤ 0,0001) which, however, it is not reflected on the degree of recovery (Unamp vs 7d post-amp.: P ≤ 0,0001).

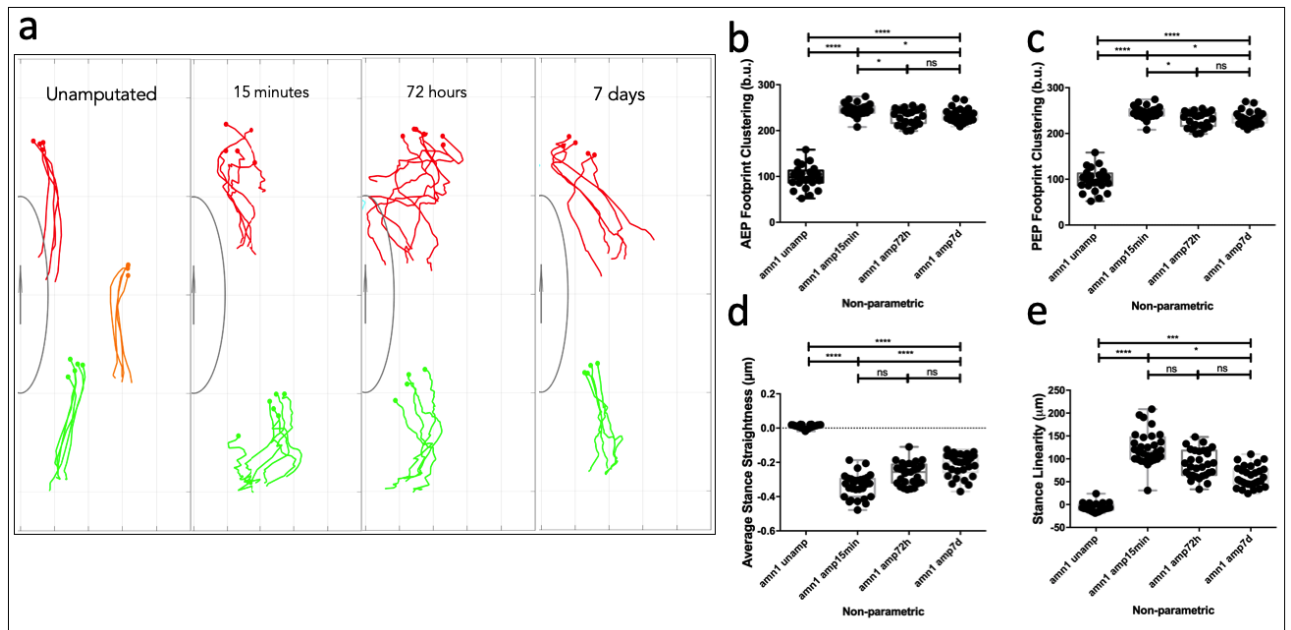


FIGURE 13. *Amnesiac*¹ Spatial parameters. **A)** *Amnesiac*¹ visual representation of AEP footprint clustering and stance traces for single flies within the median value of AEP footprint clustering for the analysed groups: Unamputated; 15minutes, 72 hours and 7days post-amputation. Body size represents a body unit. **B)** Quantification of *Amnesiac*¹'s footprint clustering of Anterior Extreme Positions (body units) via residual analysis vs unamputated control group. **C)** Quantification of *Amnesiac*¹'s footprint clustering of Posterior Extreme Positions (body units) via residual analysis vs unamputated control group. **D)** Quantification of *Amnesiac*¹'s Average Stance Straightness (body units) via residual analysis vs unamputated control group. **E)** Quantification of *Amnesiac*¹'s Average Stance Linearity (body units) via residual analysis vs unamputated control group. **Data distribution** assessed by D'Agostino Pearson and Shapiro-Wilk normality tests. **Multiple comparison** tests performed according to patterns of data distribution, either parametric (One-Way ANOVA for normally distributed data; Holm-Sidak's test for multiple comparisons) or non-parametric (Kruskal-Wallis test for abnormally distributed data and Dunn's test for multiple comparisons). **Statistical significances** resulting from multiple comparison tests are as follows: ****, $P \leq 0,0001$; ***, $P \leq 0,001$; **, $P \leq 0,01$; *, $P \leq 0,05$; ns, $P > 0,05$. **Box-plot positioning**, either above or below the x-axis, reflects a respective increase or decrease of the analyzed parameter vs the unamputated control group.

STEP PARAMETERS

Regarding Step Parameters, six out of eight adapt, from which three return to unamputated levels: **swing duration**, **leg displacement** and **step length**. Initially, average **swing duration** did not suffer much from the amputation itself (Unamp. vs 15min post-amp.: $P > 0,05$), decreasing however, at 3 days post-amputation (15mins vs 72h post-amp.: $P \leq 0,001$); this decrease in the swing duration reverts, returning to control levels on the seventh day of adaptation (15mins vs 7days post-amp.: $P \leq 0,01$; Unamp. vs 7days post-amp.: $P > 0,05$) (Fig. 14A). **Leg displacement** is significantly decreased as a result of amputation, being maintained up to 3 days post-amputation (Unamp. vs 15min post-amp.: $P \leq 0,001$; 15mins vs 72h post-amp.: $P > 0,05$), reverting to control levels at 7 days of adaptation (Unamp. vs 7d post-amp.: $P > 0,05$; 15mins vs 72h post-amp.: $P \leq 0,01$) (Fig. 14B). At the seventh day post-amputation, **Step length** returns to control values (Unamp. vs 7d post-amp.: $P > 0,05$) from the slight decrease it suffers (Unamp. vs 15mins post-amp.: $P \leq 0,05$), by having a peak of adaptivity from the 3rd to the 7th day post-amputation (72h vs 7d post-amp.: $P \leq 0,001$) (Fig. 14C).

Other Step Parameters that show recovery, however slight as it may be, are the **stance duration**, **step period** and **step frequency**, none of which are statistically close to the unamputated control (Unamp. vs 7d post-amp.: $P \leq 0,0001$) (Fig. 14D,E,F). **Stance duration** is slightly decreased by the 3rd day of adaptation, maintaining this level of recovery up to the last timepoint assessed (15mins vs 72h post-amp.: $P \leq 0,05$; 72h vs 7d post-amp.: $P > 0,05$). **Step frequency** and **step period** both worsen in performance resultant from amputation;

less step cycles per second – step frequency – and take more time for to be completed – step period (Unamp. vs 7d post-amp.: $P \leq 0,0001$). Regarding their recovery overtime, flies end up taking more step cycles per second by the 3rd day and maintain this performance to the very end (15mins vs 72h post-amp.: $P \leq 0,0001$; 72h vs 7d post-amp.: $P > 0,05$); in the meanwhile, their step period is decreased at the 3rd day, maintaining this performance to the last (15mins vs 72h post-amp.: $P \leq 0,01$; 72h vs 7d post-amp.: $P > 0,05$).

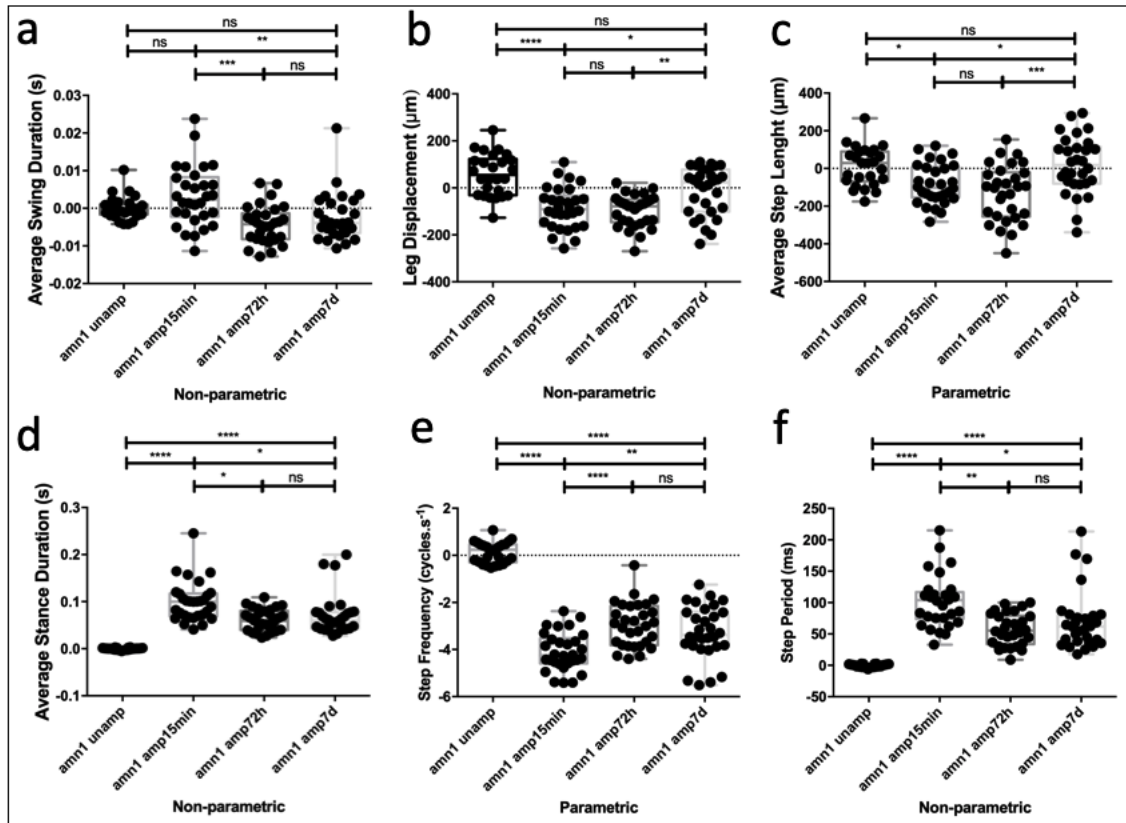


FIGURE 14. *amnesiac 1* Step parameters. **A)** Quantification of *Amnesiac 1*'s Average swing duration (seconds) via residual analysis vs unamputated control group. **B)** Quantification of *Amnesiac 1*'s Leg Displacement (μm) via residual analysis vs unamputated control group. **C)** Quantification of *Amnesiac 1*'s Average Step Length (μmeters) via residual analysis vs unamputated control group. **D)** Quantification of *Amnesiac 1*'s Stance duration (S) via residual analysis vs unamputated control group. **E)** Quantification of *Amnesiac 1*'s Step Frequency ($\text{step cycles}\cdot\text{s}^{-1}$) via residual analysis vs unamputated control group. **F)** Quantification of *Amnesiac 1*'s Step period (milliseconds) via residual analysis vs unamputated control group. **Data distribution** assessed by D'Agostino Pearson and Shapiro-Wilk normality tests. **Multiple comparison** tests performed according to patterns of data distribution, either parametric (One-Way ANOVA for normally distributed data; Holm-Sidak's test for multiple comparisons) or non-parametric (Kruskal-Wallis test for abnormally distributed data and Dunn's test for multiple comparisons). **Statistical significances** resulting from multiple comparison tests are as follows: ****, $P \leq 0,0001$; ***, $P \leq 0,001$; **, $P \leq 0,01$; *, $P \leq 0,05$; ns, $P > 0,05$. **Box-plot positioning** above or below the x-axis reflects a respective increase or decrease of the analyzed parameter vs the unamputated control group.

SUMMARY

Observing Figure 15 of general motor adaptation we conclude that four parameters show it. Recovery occurs in three step parameters (step length, swing duration and leg displacement), whereas one stability parameter (body displacement) shows adaptation.

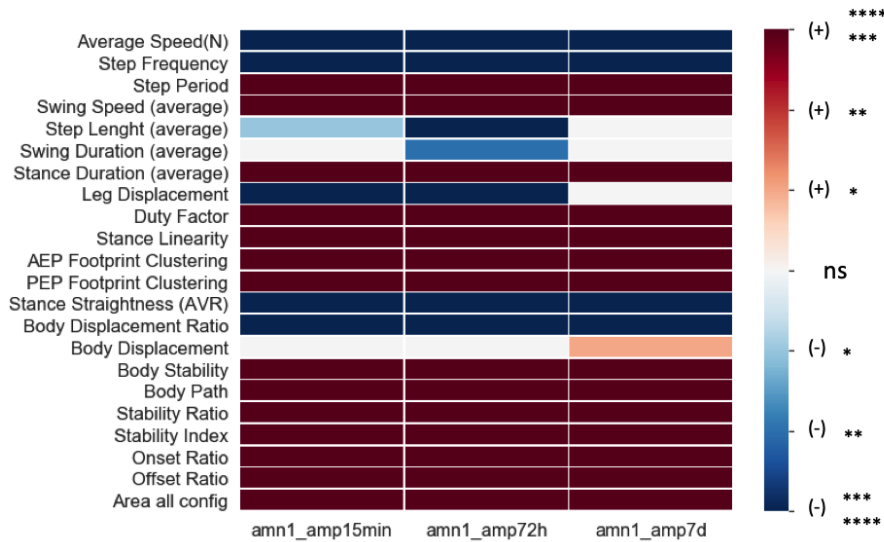


FIGURE 15. *amnesiac*¹ heatmap of all residual data from comparison to unamputated flies of the same genotype. tested locomotor parameters in the following order: Step, Spatial and Stability parameters. **Data distribution** assessed by D’Agostino Pearson and Shapiro-Wilk normality tests. **Multiple comparison** tests performed according to patterns of data distribution, either parametric (One-Way ANOVA for normally distributed data; Holm-Sidak’s test for multiple comparisons) or non-parametric (Kruskal-Wallis test for abnormally distributed data and Dunn’s test for multiple comparisons). Bonferroni **correction** was applied to the multiple comparisons. **Statistical significances** resulting from multiple comparison tests are as follows: ****, P≤0,0001 and ***, P≤0,001, deep red and deep blue; **, P≤0,01, red and blue; *, P≤0,05, pale red and pale blue; ns, P>0,05, white.

RUTABAGA¹

The next mutant we sought to study is that of *rutabaga* (Marta Santos, César Mendes, unpublished), a pan-neuronal adenylate cyclase thought to promote Short-term memory. *rut*¹ is responsive to activation – via the intracellular rise in Ca²⁺-Calmodulin concentration or through GPCR direct activation – by synthesizing cAMP from ATP, initiating the cAMP cascade and thus promoting memory formation and exerting .

STEP PARAMETERS

The **average swing duration** is the sole parameter in this category which, at the 7th day post-amputation, sees a return of motor performance to the levels of the unamputated control unamputated (Unamp. vs 7d post-amp.: P>0,05) (Fig. 16A) recovering from its continuous increase up to the third day of recovery – the legs display a “reach out” behavior to grab on to the substrate as the body is falling in the opposite direction. It does so by adapting two other parameters, the **step length** and the **swing speed**.

At 15mins post-amputation the **swing duration** increases whereas the **step length** decreases – this a normal behavior at this timepoint and is concurrent with the instability the flies must be experiencing (Fig. 16A,B) (respectively: Unamp. vs 15min post-amp.: P≤0,01; Unamp. vs 15min post-amp.: P≤0,0001).

At 72h post-amputation this instability is still reflected in both parameters showing no signs of motor recovery: the **step length** has a slight increase from its 15mins counterpart, while the **swing duration** continues to increase when compared to the unamputated control (respectively: 15min vs 72h post-amp.: P≤0,05; Unamp. vs 72h post-amp.: P≤0,001) – the flies take a longer time during the swing phase for the leg to take small steps. The inefficacy keeps on getting more pronounced.

It is at the 7th day post-amputation that, by manipulating the swing speed, the flies are able to significantly adapt their swing duration to control levels (Unamp. vs 7d post-amp.: P≤0,01). While the **step length** is maintained at the levels of the 72h timepoint (still swinging the legs in smaller distances than the controls), the **swing duration** is decreased to unamputated control levels because the flies increase their **swing speed** (Fig. 16A,C) (respectively: 72h vs 7d post-amp.: P>0,05; Unamp. vs 7d post-amp.: P>0,05) – so, while the step length remains smaller and almost unchanged over time due to the amputation, flies adapt the speed at which they project their legs (increase it) in order to decrease the duration of this swing phase. Although they cannot take long steps as they did before, they adapt the speed and length of the stride to adapt to this unchangeable variable.

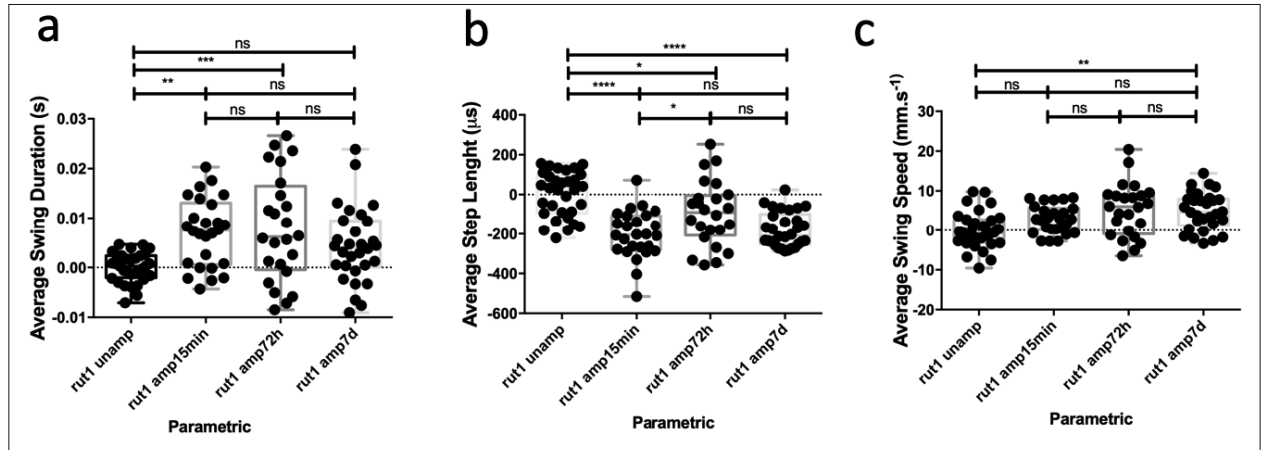


FIGURE 16. *rutabaga 1* Step parameters. **A)** Quantification of *Rutabaga 1*'s Average swing duration (seconds) via residual analysis vs unamputated control group. **B)** Quantification of *Rutabaga 1*'s Step length (µmeters) via residual analysis vs unamputated control group. **C)** Quantification of *Rutabaga 1*'s Average swing speed (millimeters per second) via residual analysis vs unamputated control group. **Data distribution** assessed by D'Agostino Pearson and Shapiro-Wilk normality tests. **Multiple comparison** tests performed according to patterns of data distribution, either parametric (One-Way ANOVA for normally distributed data; Holm-Sidak's test for multiple comparisons) or non-parametric (Kruskal-Wallis test for abnormally distributed data and Dunn's test for multiple comparisons). **Statistical significances** resulting from multiple comparison tests are as follows: ****, $P \leq 0,0001$; ***, $P \leq 0,001$; **, $P \leq 0,01$; *, $P \leq 0,05$; ns, $P > 0,05$. **Box-plot positioning** above or below the x-axis reflects a respective increase or decrease of the analyzed parameter vs the unamputated control group.

SPATIAL PARAMETERS

Regarding Spatial parameters **AEP footprint clustering** is the sole showing signs of adaptation during the seven days the flies have to do so. Its recovery is only noticeable from the third to the seventh day post-amputation, although it is hardly efficient in improving motor performance, as it gets nowhere close to the levels displayed by its unamputated controls – this can be observed via quantification in (Fig. 17B) (72h vs 7d post-amp.: $P \leq 0,05$; Unamp. vs 7d post-amp.: $P \leq 0,0001$) and in (Fig. 17A) in which a fly within the median value for AEP footprint clustering is depicted; the lack of clustering of the points of contact during the onset of a step is clear, so is the lack of straightness from traces left by the legs displacing the body. Both these parameters reveal incoordination in tarsal placement and suggest that this action is not occurring in a controlled, but in a random fashion – the tarsi are placed wherever they hit, probably due to an inability to stabilize the body during the as-straight-as-possible (but hardly straight at all) walking bursts. To further stress this inability, **PEP footprint clustering** (Fig. 17C) residual analysis actually shows this parameter getting worse from the timepoint at 15mins post-amputation to the third day of recovery (15mins vs 72h post-amp.: $P \leq 0,05$). If at 72h post-amputation the AEPs don't show the increase reflected on the PEPs, the data suggests that the body is so unbalanced during stances, that its displacement causes the tarsi to get dislocated from its initial onset position; the legs do not seem to have enough strength to hold on to the substrate nor to stabilize the body in a stable position.

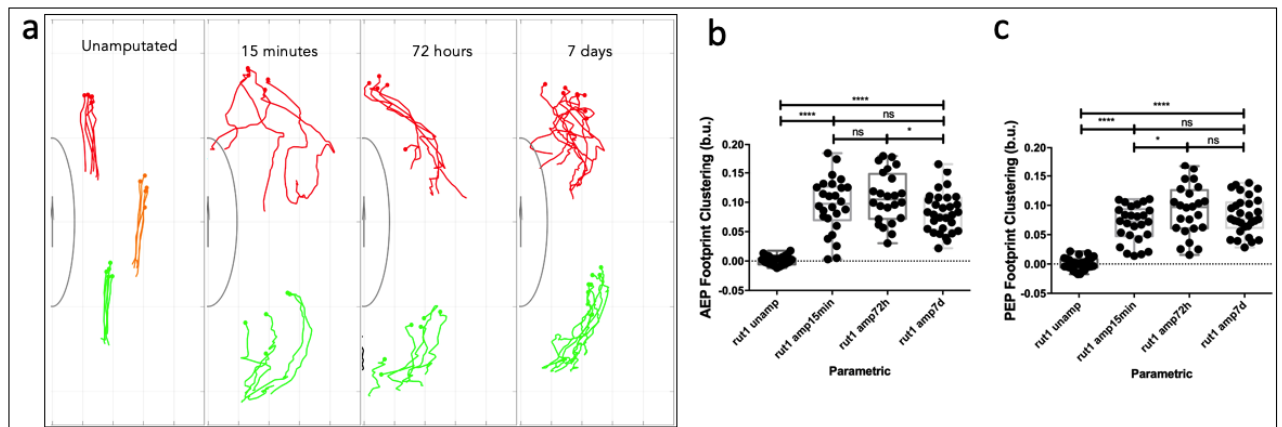


FIGURE 17. *rutabaga*¹ Spatial parameters. **A)** *Rutabaga*¹ visual representation of AEP footprint clustering and stance traces for single flies within the median value of AEP footprint clustering for the analysed groups: Unamputated; 15minutes, 72 hours and 7days post-amputation. Body size represents a body unit. **B)** Quantification of *Rutabaga*¹'s footprint clustering of Anterior Extreme Positions (body units) via residual analysis vs unamputated control group. **C)** Quantification of *Rutabaga*¹'s footprint clustering of Posterior Extreme Positions (body units) via residual analysis vs unamputated control group. **Data distribution** assessed by D'Agostino Pearson and Shapiro-Wilk normality tests. **Multiple comparison** tests performed according to patterns of data distribution, either parametric (One-Way ANOVA for normally distributed data; Holm-Sidak's test for multiple comparisons) or non-parametric (Kruskal-Wallis test for abnormally distributed data and Dunn's test for multiple comparisons). **Statistical significances** resulting from multiple comparison tests are as follows: ****, $P \leq 0,0001$; ***, $P \leq 0,001$; **, $P \leq 0,01$; *, $P \leq 0,05$; ns, $P > 0,05$. **Box-plot positioning**, either above or below the x-axis, reflects a respective increase or decrease of the analyzed parameter vs the unamputated control group.

STABILITY PARAMETERS

This brings us to our last category of motor parameters: Stability. Three parameters in total show improvement in performance, one of them even returning to control levels; the average stability, onset and offset ratios; body displacement however, gets worse over time (Unamp. vs 7d post-amp.: $P \leq 0,01$).

Regarding the **average onset and offset ratios**, which reflect the position of the fly's center of mass during the onset and offset of an area of support formed by the legs (the higher the ratio, the more centered the COM is on the area of support), we see an approximation to control levels in on the **onset** at 7 days post-amputation (Fig. 18B) (72h vs 7d post-amp.: $P \leq 0,0001$) consistent with the increase in AEP footprint clustering, whereas during the **offset**, *rutabaga* flies can fully stabilize their COM, showing no difference from their unamputated counterparts (Fig. 19) (Unamp. vs 7d post-amp.: $P > 0,05$). Similar in both cases there is a big decrease in performance at 72h (Unamp. vs 72h post-amp.: $P \leq 0,0001$), after which both adapt to different extents, as mentioned above.

Regarding the **average stability ratio**, and consistent with the changes observed in the onset and offset ratios, this parameter suffers a significant decrease at 72h post-amputation, recovering on the 7th day (Fig. 18C) (Unamp. vs 72h post-amp.: $P \leq 0,0001$; Unamp. vs 7d post-amp.: $P \leq 0,01$).

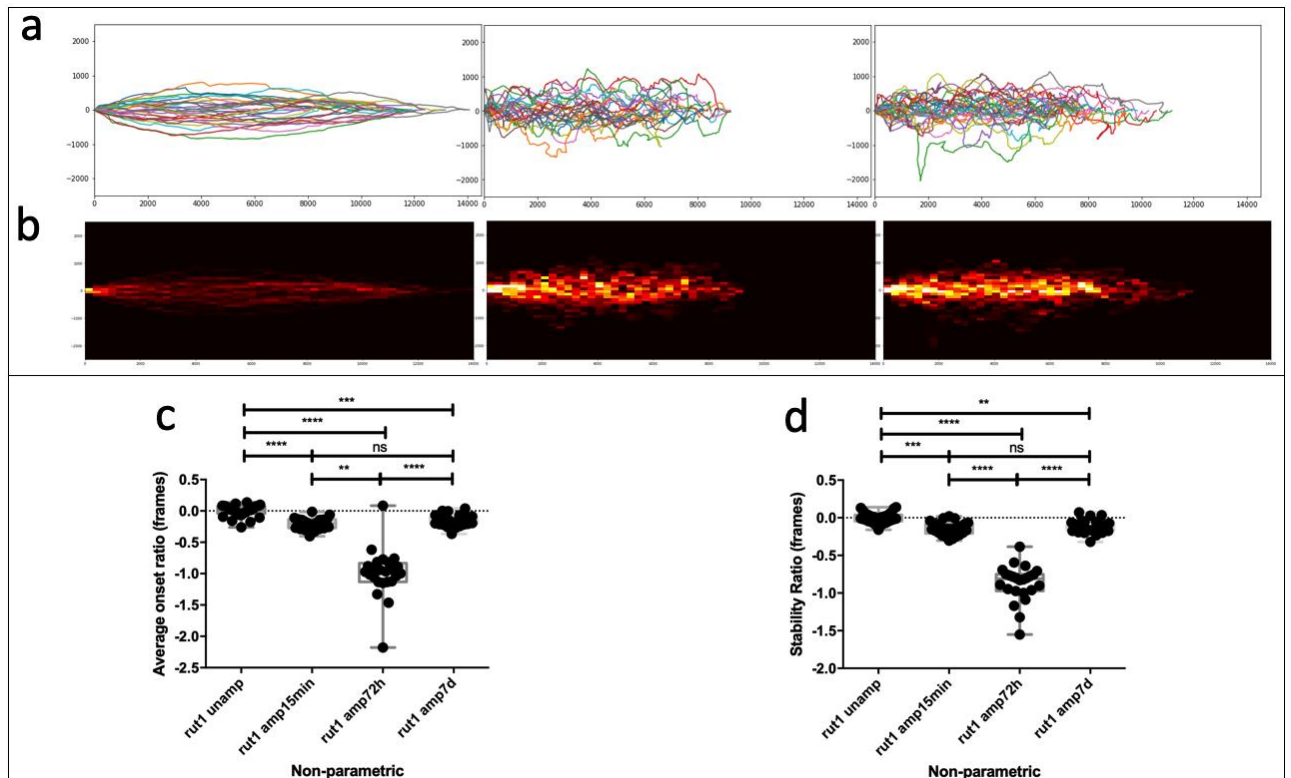


FIGURE 18. *rutabaga 1* Stability parameters. **A,B)** Body traces in the form of lines and heatmap for *Rutabaga 1* at three timepoints: Unamputated (N=5, n=10), 15 minutes post-amputation (N=5, n=10) and 7 days post-amputation (N=9, n=18). *x* (0 -> 14000 μm) and *y*-axis (-2000 -> 2000 μm) are the horizontal and vertical distance travelled by the flies. Increase in **colour brightness** represents coordinates in which more flies passed through. **C)** Quantification of *Rutabaga 1*'s average onset ratio (frames) via residual analysis vs unamputated control group. **D)** Quantification of *Rutabaga 1*'s stability Ratio (frames) via residual analysis vs unamputated control group. **Data distribution** assessed by D'Agostino Pearson and Shapiro-Wilk normality tests. **Multiple comparison** tests performed according to patterns of data distribution, either parametric (One-Way ANOVA for normally distributed data; Holm-Sidak's test for multiple comparisons) or non-parametric (Kruskal-Wallis test for abnormally distributed data and Dunn's test for multiple comparisons). **Statistical significances** resulting from multiple comparison tests are as follows: ****, $P \leq 0,0001$; ***, $P \leq 0,001$; **, $P \leq 0,01$; *, $P \leq 0,05$; ns, $P > 0,05$. **Box-plot positioning** above or below the *x*-axis reflects a respective increase or decrease of the analyzed parameter vs the unamputated control group.

SUMMARY

Rutabaga, being a pan-neuronally expressed protein with such a widespread role in the cell, was expected to – and indeed does – show a big behavioral effect on recovery upon middle-leg amputation. Observing (Fig. 19) we notice that many parameters are greatly affected by the procedure and do not show alterations overtime. Those that do, do so to a slight degree in case of recovery (swing duration), whereas others perform equal to the control at 15 minutes post-amputation and decay in performance as time goes by (body displacement and swing speed). Indeed, only the offset ratio shows levels equal to the control after the adaptation period.

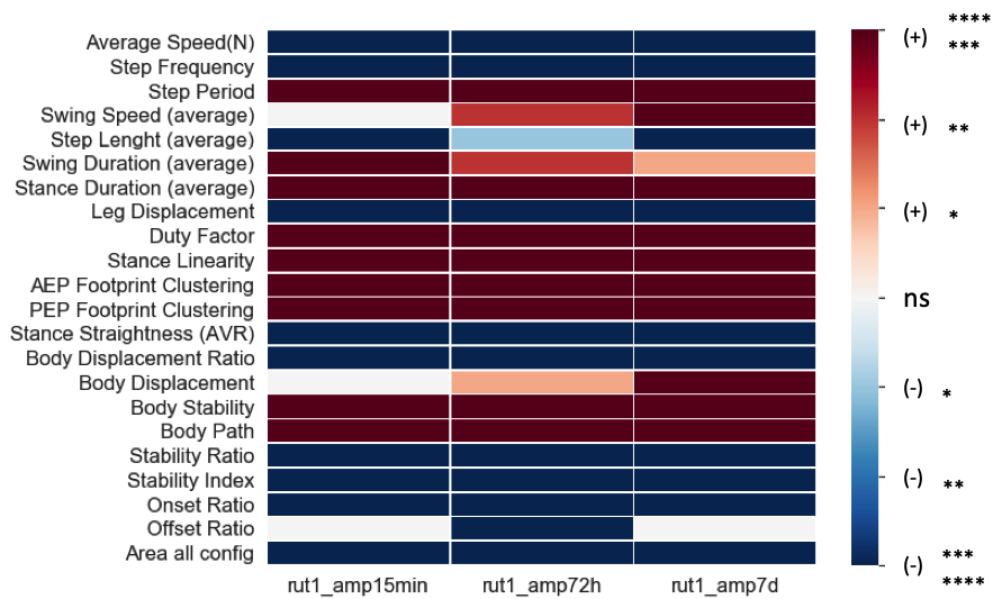


Figure 19. *rutabaga*¹ heatmap of all residual-tested locomotor parameters in the following order: Step, Spatial and Stability parameters. **Data distribution** assessed by D’Agostino Pearson and Shapiro-Wilk normality tests. **Multiple comparison** tests performed according to patterns of data distribution, either parametric (One-Way ANOVA for normally distributed data; Holm-Sidak’s test for multiple comparisons) or non-parametric (Kruskal-Wallis test for abnormally distributed data and Dunn’s test for multiple comparisons). Bonferroni **correction** was applied to the multiple comparisons. **Statistical significances** resulting from multiple comparison tests are as follows: ****, P≤0,0001 and ***, P≤0,001, deep red and deep blue; **, P≤0,01, red and blue; *, P≤0,05, pale red and pale blue; ns, P>0,05, white.

DUNCE¹

In the cAMP cascade we are studying, *dnc1* is a cAMP-specific phosphodiesterase which degrades the *rutabaga* synthesized cAMP; because of the counterbalance it exerts it also has a role, along with *rut1*, in STM.

Since this cAMP regulation is non-existent in our *dnc1* mutant flies, one expects this pathway to be extremely upregulated due to the rise in cAMP in the affected cells, which could in theory improve recovery by potentiating both LTM and ARM.

STABILITY PARAMETERS

Observation of the body traces (Fig. 20A) of *dunce* mutants reveals that, when unamputated, these flies are very capable of walking in a straight fashion as would be expected. Once amputated, and although the body traces by themselves may not prove sufficiently conclusive, we can see a trend in narrowing of the walked paths in the 15min and 7d timepoints; additionally their respective body trace heatmaps show the same occurrence even more evidently (Fig. 20B). Three motor parameters can be sought to clarify the gain in stability: the body displacement, body path and body displacement ratio – three of the four stability parameters that show a positive trend in recovery.

Quantification via residual analysis shows that the **body displacement** (Fig. 20C) does not suffer immediate changes caused by amputation (Unamp. vs 15min post-amp.: $P > 0,05$) but does so extensively at the third day of recovery (15min vs 72h post-amp.: $P \leq 0,0001$) – this change however, is actually positive as it shows that the body is displaced *less* and is steadier than the control. This changes at the 7th day of recovery, as the body displacement at this timepoint becomes similar to that of unamputated flies (Unamp. vs 7d post-amp.: $P > 0,05$).

Regarding the **body path** (Fig. 20D), quantification shows that, even though it does not return to levels displayed by unamputated flies (Unamp. vs 7d post-amp.: $P \leq 0,0001$), there is also adaptation and some motor recovery. The body path is immediately affected by amputation (Unamp. vs 15min post-amp.: $P \leq 0,0001$) and during the recovery period it both greatly improves (15min vs 72h post-amp.: $P \leq 0,001$) and then gets slightly worst (15min vs 7d post-amp.: $P > 0,05$); this, however does not necessarily that there is no recovery, as comparison between the 3rd and 7th days of recovery shows that there is only a slight deviation. This brings to the spotlight a (as of this moment) unanswerable question: would we continue to see a detriment in recovery, had we a later timepoint?

The **body displacement ratio** (Fig. 20E) is the last body stability parameter that – although much less palpable – still shows signs of adaptation. This parameter, as previously mentioned, is the ratio between the distance walked in 5 steps (of the same leg) and its path. This ratio is significantly hampered at 15mins post-amputation (Unamp. vs 15min post-amp.: $P \leq 0,0001$) as the distance walked is far smaller than the path the fly's COM traversed from the initial position to its final. This effect is only slightly reverted at the 3rd day (15min vs 72h post-amp.: $P \leq 0,05$) and is maintained at the same level at the 7th (72h vs 7d post-amp.: $P > 0,05$), showing no recovery if compared to the unamputated control (Unamp. vs 7d post-amp.: $P \leq 0,0001$).

The offset ratio also shows some signs of adaptation as it evolves in a small degree from the effect caused by the amputation (Unamp. vs 15min post-amp.: $P \leq 0,001$) in the last day of recovery (Unamp. vs 7d post-amp.: $P \leq 0,01$).

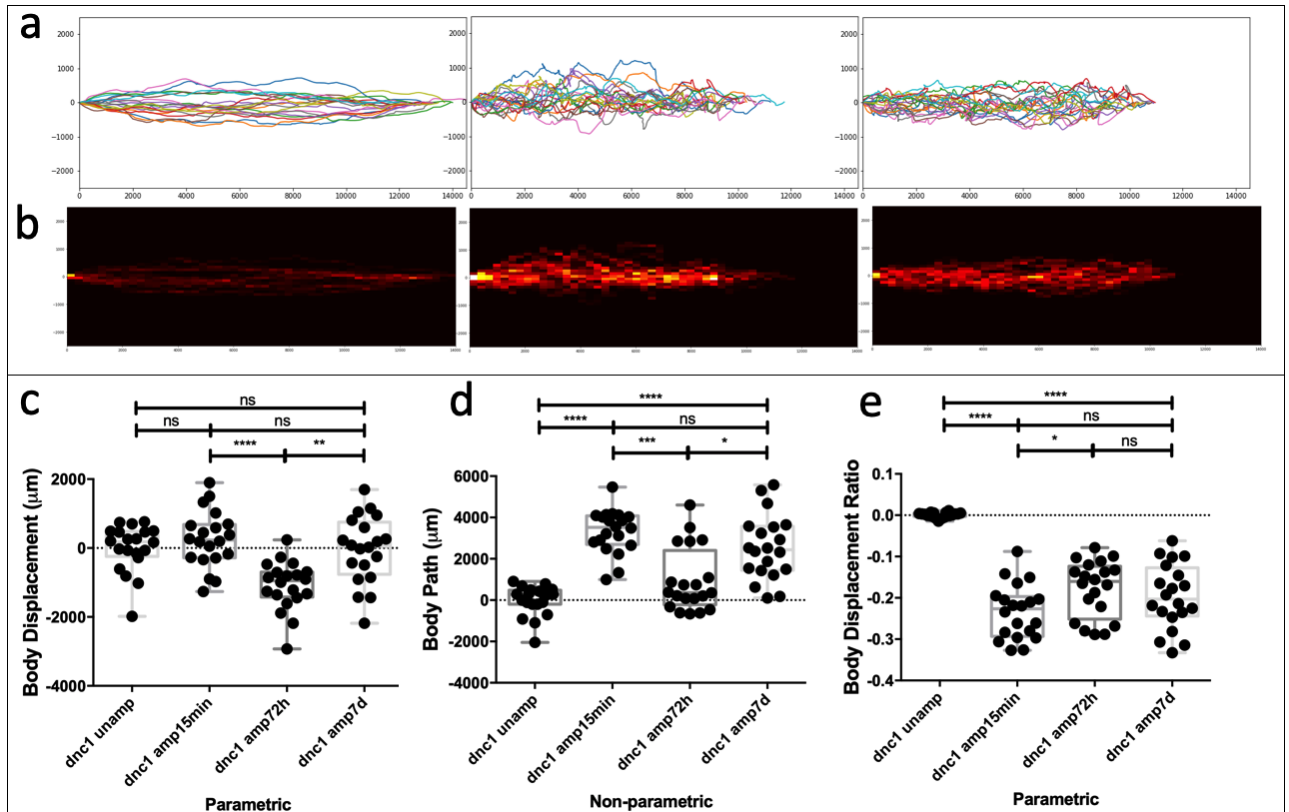


FIGURE 20. *dunce*⁻¹ Stability parameters. **A,B)** Body traces in the form of lines and heatmap for *Duncce*⁻¹ at three timepoints: Unamputated (N=5, n=10), 15 minutes post-amputation (N=5, n=10) and 7 days post-amputation (N=9, n=18). *x* (0 → 14000 µm) and *y*-axis (-2000 → 2000 µm) are the horizontal and vertical distance travelled by the flies. Increase in **colour brightness** represents coordinates in which more flies passed through. **C)** Quantification of *Duncce*⁻¹'s Body displacement (µmeters) via residual analysis vs unamputated control group. **D)** Quantification of *dunce*⁻¹'s Body path (µmeters) via residual analysis vs unamputated control group. **E)** Quantification of *dunce*⁻¹'s Body Displacement Ratio (body units) via residual analysis vs unamputated control group. **Data distribution** assessed by D'Agostino Pearson and Shapiro-Wilk normality tests. **Multiple comparison** tests performed according to patterns of data distribution, either parametric (One-Way ANOVA for normally distributed data; Holm-Sidak's test for multiple comparisons) or non-parametric (Kruskal-Wallis test for abnormally distributed data and Dunn's test for multiple comparisons). **Statistical significances** resulting from multiple comparison tests are as follows: ****, P≤0,0001; ***, P≤0,001; **, P≤0,01; *, P≤0,05; ns, P>0,05. **Box-plot positioning** above or below the *x*-axis reflects a respective increase or decrease of the analyzed parameter vs the unamputated control group.

STEP PARAMETERS

Dunce1 shows a small adaptation in many step parameters (5/8) from which two behave as the unamputated controls on the 7th day of recovery: the step length and swing duration.

The **step length** (Fig. 21A) does not perform much differently when amputated; at the 7th day of recovery its levels are on par with the control suffering only a small decrease on the third day of testing. As for the **step period** and **frequency**, both get drastically affected by the amputation – they take longer to happen as the number of step cycles per second is decreased (Fig. 21B,C) (Unamp. vs 15min post-amp.: P≤0,0001). Both improve on the 3rd day (respectively: 15min vs 72h post-amp.: P≤0,05; 15min vs 72h post-amp.: P≤0,0001) and are stabilized up to the last day of recovery (72h vs 7d post-amp.: P>0,05).

Both components of the step – swing and stance – also adapt to the absence of the middle legs. The **average swing duration** and **swing speed** both return to control levels on the 3rd day – the swing phase lasts less time and the legs move faster (Fig. 21D,E) (15min vs 72h post-amp.: P≤0,0001); this phenotype is

maintained on the 7th day and its performance is on par with the control's (72h vs 7d post-amp.: $P>0,05$; Unamp vs 7d post-amp.: $P>0,05$).

The **stance duration** also recovers on the 3rd day, decreasing (15min vs 72h post-amp.: $P\leq 0,05$) and is slightly maintained up to the 7th day (15min vs 7d post-amp.: $P\leq 0,05$; 72h vs 7d post-amp.: $P>0,05$); it does not however return to control levels.

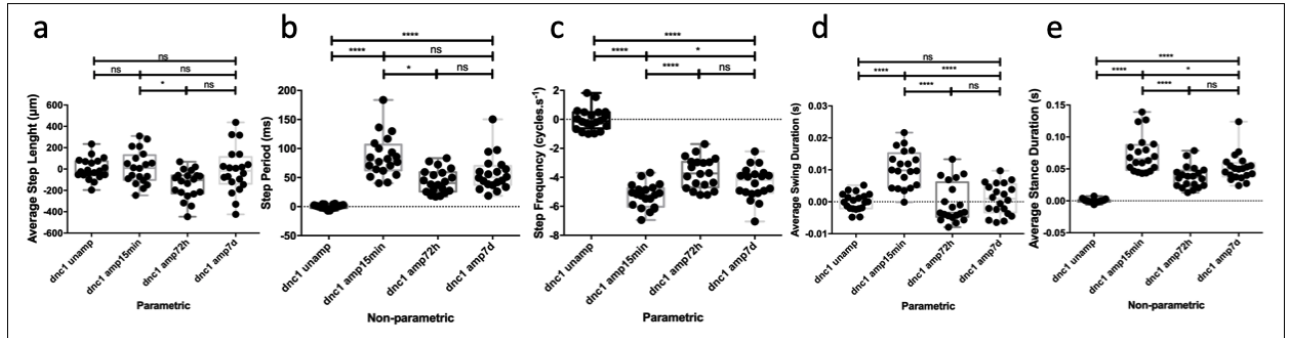


FIGURE 21. *dunce*¹ Step parameters. A) Quantification of *Duncce*¹'s Step length (μ meters) via residual analysis vs unamputated control group. **B)** Quantification of *Duncce*¹'s step period (milliseconds) via residual analysis vs unamputated control group. **C)** Quantification of *Duncce*¹'s step frequency (step cycles per second) via residual analysis vs unamputated control group. **D)** Quantification of *Duncce*¹'s average swing duration (seconds) via residual analysis vs unamputated control group. **E)** Quantification of *Duncce*¹'s average stance duration (seconds) via residual analysis vs unamputated control group. **Data distribution** assessed by D'Agostino Pearson and Shapiro-Wilk normality tests. **Multiple comparison** tests performed according to patterns of data distribution, either parametric (One-Way ANOVA for normally distributed data; Holm-Sidak's test for multiple comparisons) or non-parametric (Kruskal-Wallis test for abnormally distributed data and Dunn's test for multiple comparisons). **Statistical significances** resulting from multiple comparison tests are as follows: ****, $P\leq 0,0001$; ***, $P\leq 0,001$; **, $P\leq 0,01$; *, $P\leq 0,05$; ns, $P>0,05$. **Box-plot positioning** above or below the x-axis reflects a respective increase or decrease of the analyzed parameter vs the unamputated control group.

SPATIAL PARAMETERS

From observing AEP Footprint clustering and Stance straightness plots we can observe a trend in clustering of the AEPs, PEPs and increased straightness occurring as time goes by. From quantification via residual analysis we can see that some of these trends check out, whereas others are nothing but that – trends. Three motor parameters regarding the legs' distribution in space show signs of recovery, albeit small: the AEP and PEP footprint clustering and stance straightness, whereas the linearity of the stance traces observed in (Fig. 22A) even though showing a trend towards improvement, do not reflect this in statistical terms – the traces are still quite disparate to the projected smoothed traces joining the AEPs and PEPs, used to calculate this parameter.

The **stance straightness** (Fig. 22D) of the steps shows signs of locomotor adaptation during the first three days of recovery (15min vs 72h post-amp.: $P\leq 0,05$) after which it stalls (72h vs 7d post-amp.: $P>0,05$), keeping a big difference from the unamputated control (Unamp. vs 7d post-amp.: $P\leq 0,0001$).

The **PEP footprint clustering** (Fig. 22C) shows this exact same trend, differing only in the statistical difference of the recovery during the first three days (15min vs 72h post-amp.: $P\leq 0,01$). As for the **AEP footprint clustering** (Fig. 22B), while no statistical significance is verified during recovery, there is some when comparing the initial and final timepoints of recovery to unamputated flies, in which the latter shows

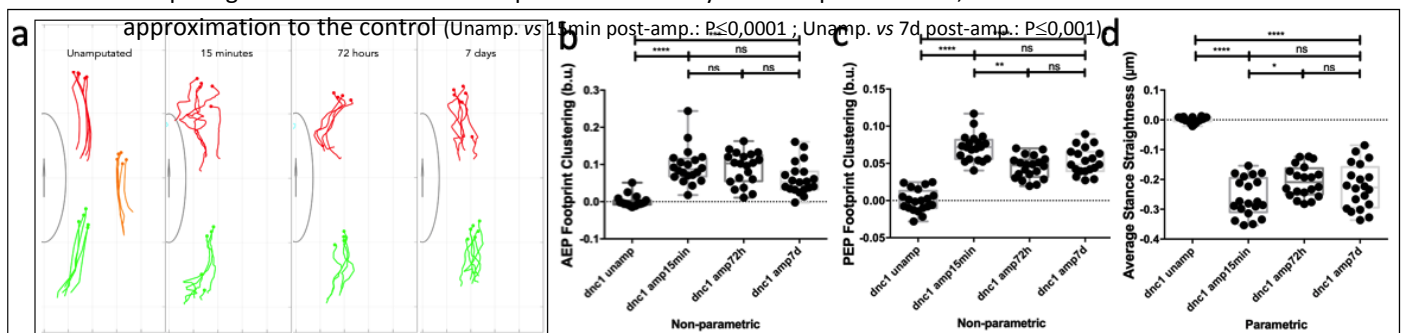


FIGURE 22. *dunce*¹ Spatial parameters. **A)** *Dunce*¹ visual representation of AEP footprint clustering and stance traces for single flies within the median value of AEP footprint clustering for the analysed groups: Unamputated; 15minutes, 72 hours and 7days post-amputation. Body size represents a body unit. **B)** Quantification of *dunce*¹'s footprint clustering of Anterior Extreme Positions (body units) via residual analysis vs unamputated control group. **C)** Quantification of *dunce*¹'s footprint clustering of Posterior Extreme Positions (body units) via residual analysis vs unamputated control group. **D)** Quantification of *dunce*¹'s Average stance straightness (µmeters) via residual analysis vs unamputated control group. **Data distribution** assessed by D'Agostino Pearson and Shapiro-Wilk normality tests. **Multiple comparison** tests performed according to patterns of data distribution, either parametric (One-Way ANOVA for normally distributed data; Holm-Sidak's test for multiple comparisons) or non-parametric (Kruskal-Wallis test for abnormally distributed data and Dunn's test for multiple comparisons). **Statistical significances** resulting from multiple comparison tests are as follows: ****, P≤0,0001; ***, P≤0,001; **, P≤0,01; *, P≤0,05; ns, P>0,05. **Box-plot positioning**, either above or below the x-axis, reflects a respective increase or decrease of the analyzed parameter vs the unamputated control group.

SUMMARY

The (Fig. 23) for the *dunce1* mutant reveals that five locomotor parameters display **recovery** in performance. In terms of stability, the swing speed, step length and swing duration do so. Regarding step and spatial parameters, only one of each recover: the offset ratio and body displacement respectively.

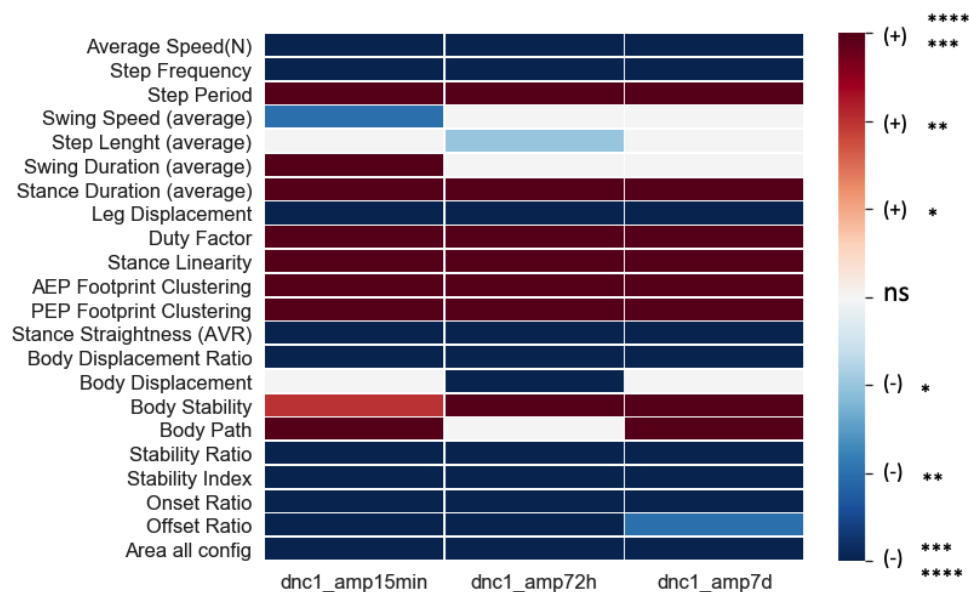


FIGURE 23. *Dunce*¹ heatmap of all residual data from comparison to unamputated flies of the same genotype tested locomotor parameters in the following order: Step, Spatial and Stability parameters. **Data distribution** assessed by D'Agostino Pearson and Shapiro-Wilk normality tests. **Multiple comparison** tests performed according to patterns of data distribution, either parametric (One-Way ANOVA for normally distributed data; Holm-Sidak's test for multiple comparisons) or non-parametric (Kruskal-Wallis test for abnormally distributed data and Dunn's test for multiple comparisons). Bonferroni **correction** was applied to the multiple comparisons. **Statistical significances** resulting from multiple comparison tests are as follows: ****, P≤0,0001 and ***, P≤0,001, deep red and deep blue; **, P≤0,01, red and blue; *, P≤0,05, pale red and pale blue; ns, P>0,05, white.

*RADISH*¹

radish is the most downstream player of the pathway we are studying. It is a small GTPase which has been shown to bind to Rac1^{68,80,81}, a regulator of the cell's actin cytoskeleton and an already demonstrated key player in memory and learning; experiments modulating it show that its upregulation leads to increased forgetting of learnt tasks in mice and *Drosophila*. *Radish* is categorized as a protein-synthesis-independent mechanism for memory consolidation, more specifically for Anesthesia Resistant Memory – anesthesia is a classic memory disruptor.

By studying this mutant, we want to understand if ARM is required for motor recovery, and if so, learn how the exclusive participation of LTM (protein-synthesis dependent) in consolidation aids our phenotype.

STABILITY PARAMETERS

Six stability parameters positively adapt to amputation during the 7 days of recovery, three of which do so to the levels exhibited by the unamputated controls: the body path, average onset ratio and the area of all configurations; the last two also improve in wild type flies.

As shown by the **body traces** figure (Fig. 24A,B) and quantified via residual analysis (Fig. 24C), the **body path** of the flies is significantly affected by the middle-leg amputation (Unamp. vs 15min. post-amp.: $P \leq 0,0001$). By the third day of recovery, maintaining performance up to the last day of testing, it has already recovered to control levels (Unamp. vs 72h post-amp.: $P > 0,05$; Unamp. vs 7d post-amp.: $P > 0,05$).

Although this parameter does not recover to control levels (Unamp. vs 7d post-amp.: $P \leq 0,0001$), this same trend is repeated in the **body stability** (Fig. 24D). After the big hit it takes from the amputation, the fly's bodies become more stable at the 3rd day of testing (15min vs 72h post-amp.: $P \leq 0,0001$) and somewhat maintain this stability up to the very end of the testing period (72h vs 7d post-amp.: $P > 0,05$; 15min vs 7d post-amp.: $P \leq 0,001$). This trend and degree of recovery is mirrored almost exactly in the **body displacement ratio** (Fig. 24E), with the only difference being the degree of recovery from the 15min timepoint to the 3rd day, which is slightly smaller (15min vs 72h post-amp.: $P \leq 0,001$).

While the **onset ratio** (Fig. 24F) does not suffer from the amputation, and even maintains performance up to the last timepoint (Unamp vs 15min post-amp.: $P > 0,05$; Unamp vs 7d post-amp.: $P > 0,05$), the overall **stability ratio** (Fig. 24G) (which encompasses the onset and offset phases of the stance) changes significantly at the 15min timepoint and shows signs of recovery at the 7th day (Unamp vs 15min post-amp.: $P \leq 0,0001$; Unamp vs 7d post-amp.: $P \leq 0,01$).

Regarding the last stability parameter that shows motor adaptation – and does so to the levels of the control (Unamp. vs 7d post-amp.: $P > 0,05$) – the **area of all configurations** (Fig. 24H) is slightly affected by the amputation and continues increasing up to the third day of recovery (Unamp vs 15min post-amp.: $P \leq 0,05$; Unamp vs 72h post-amp.: $P \leq 0,0001$). It decreases from thereon out up to the last day of recovery, as the legs do not need to be stretched out to be able to support the body (72h vs 7d post-amp.: $P \leq 0,001$).

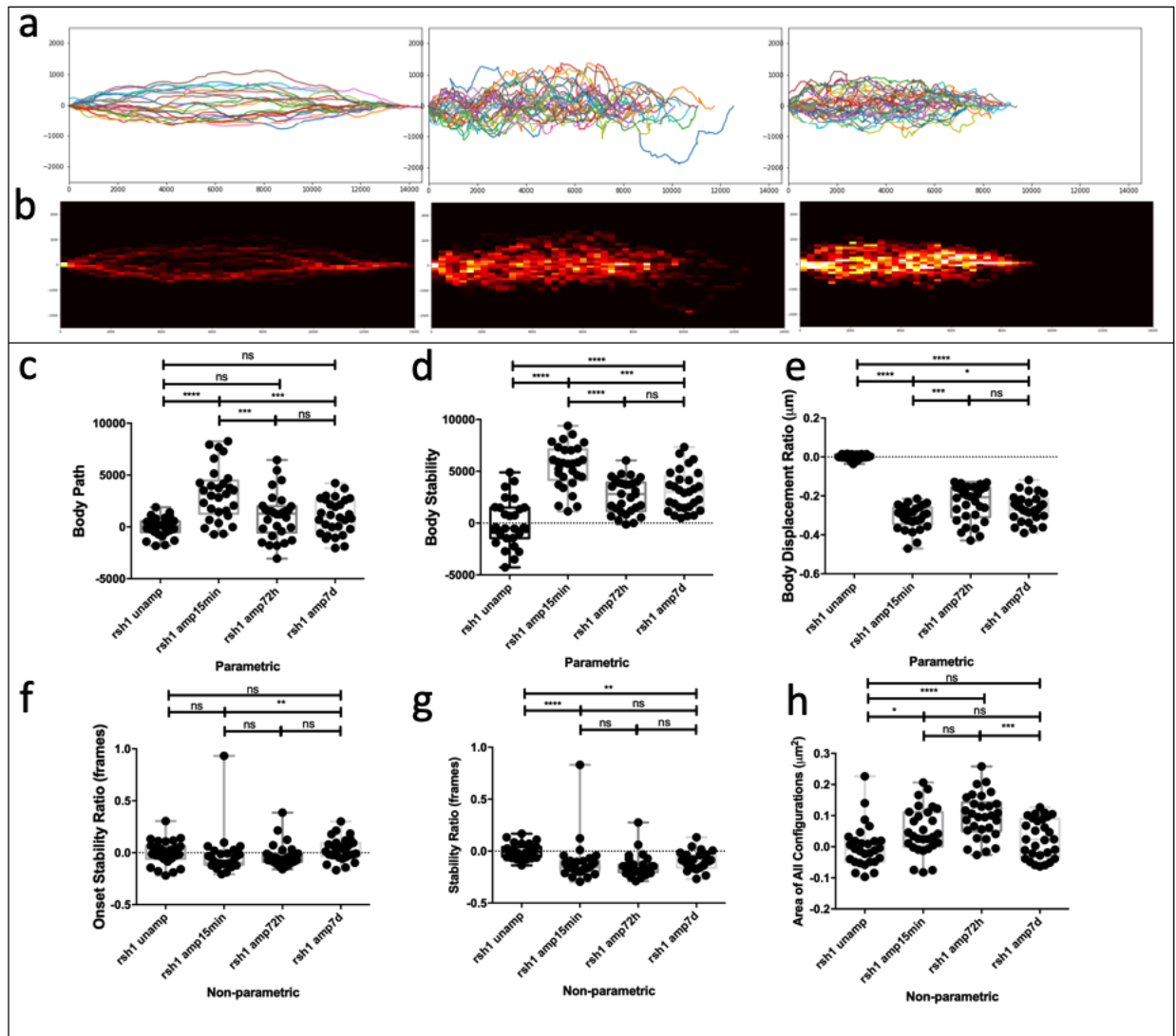


FIGURE 24. *Radish*¹ Stability parameters. **A,B)** Body traces in the form of lines and heatmap for *Dunce*¹ at three timepoints: Unamputated (N=5, n=10), 15 minutes post-amputation (N=5, n=10) and 7 days post-amputation (N=9, n=18). *x* (0 -> 14000 µm) and *y*-axis (-2000 -> 2000 µm) are the horizontal and vertical distance travelled by the flies. Increase in **colour brightness** represents coordinates in which more flies passed through. **C)** Quantification of *Radish*¹'s Body Path (µm) via residual analysis vs unamputated control group. **D)** Quantification of *Radish*¹'s Body Displacement Ratio (body units) via residual analysis vs unamputated control group. **E)** Quantification of *Radish*¹'s Body Displacement Ratio (body units) via residual analysis vs unamputated control group. **Data distribution** assessed by D'Agostino Pearson and Shapiro-Wilk normality tests. **Multiple comparison** tests performed according to patterns of data distribution, either parametric (One-Way ANOVA for normally distributed data; Holm-Sidak's test for multiple comparisons) or non-parametric (Kruskal-Wallis test for abnormally distributed data and Dunn's test for multiple comparisons). **Statistical significances** resulting from multiple comparison tests are as follows: ****, P≤0,0001; ***, P≤0,001; **, P≤0,01; *, P≤0,05; ns, P>0,05. **Box-plot positioning** above or below the *x*-axis reflects a respective increase or decrease of the analyzed parameter vs the unamputated control group.

STEP PARAMETERS

The sole step parameter at control levels is the average **swing speed** (Fig. 25A), which maintained despite the amputation (Unamp. vs 15min post-amp.: $P > 0,05$; Unamp. vs 7d post-amp.: $P > 0,05$).

Two parameters however, become increasingly distant from control levels: the **step frequency** (Fig. 25C) (number of cycles per second) and the **duty factor** (Fig. 25B) (percentage of a step cycle in which the foot is on the ground); the step frequency decreases as recovery goes by (Unamp. vs 15min post-amp.: $P \leq 0,0001$; 72h vs 7d post-amp.: $P \leq 0,05$) while the duty factor increases (15min vs 72h post-amp.: $P \leq 0,001$; 15min vs 7d post-amp.: $P \leq 0,0001$) – flies do less step cycles per second by spending more time in the stance phase, most likely to stabilize the body.

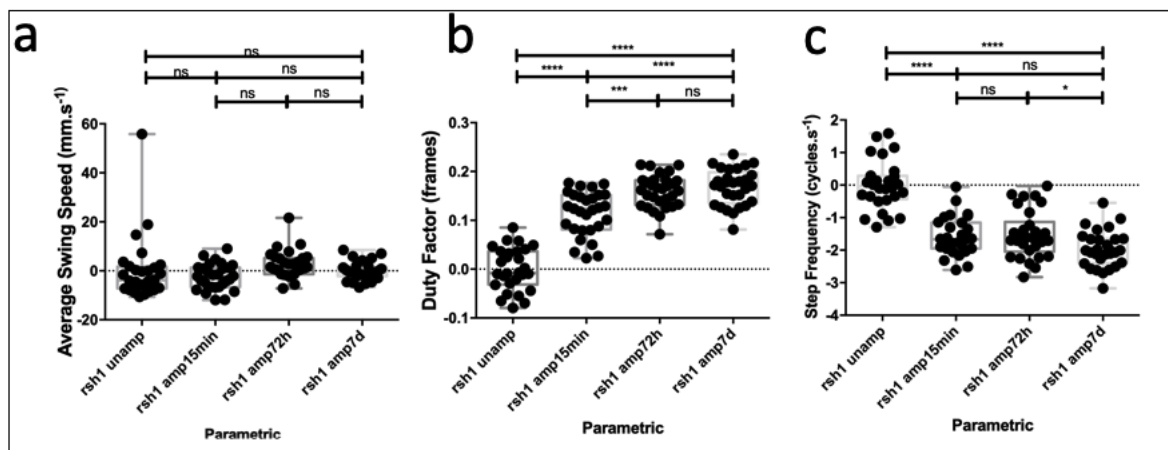


FIGURE 25. Radish ¹ Step parameters. **A)** Quantification of Radish ¹'s average swing speed (millimetres per second) via residual analysis vs unamputated control group. **B)** Quantification of Radish ¹ duty factor (frames) via residual analysis vs unamputated control group. **C)** Quantification of Radish ¹'s Average step frequency (step cycles per second) via residual analysis vs unamputated control group. **Data distribution** assessed by D'Agostino Pearson and Shapiro-Wilk normality tests. **Multiple comparison** tests performed according to patterns of data distribution, either parametric (One-Way ANOVA for normally distributed data; Holm-Sidak's test for multiple comparisons) or non-parametric (Kruskal-Wallis test for abnormally distributed data and Dunn's test for multiple comparisons). **Statistical significances** resulting from multiple comparison tests are as follows: ****, $P \leq 0,0001$; ***, $P \leq 0,001$; **, $P \leq 0,01$; *, $P \leq 0,05$; ns, $P > 0,05$. **Box-plot positioning** above or below the x-axis reflects a respective increase or decrease of the analyzed parameter vs the unamputated control group.

SPATIAL PARAMETERS

Only the **PEP footprint clustering** (Fig. 26B) shows moderate approximation to the control during the adaptation period; no other spatial parameters seem to be worthy of mention as none show change from the 15min timepoint.

The PEP footprint clustering shows the expected alterations result of amputation: an increase on the spatial dispersion of tarsal contacts on the floor (Unamp vs 15min post-amp.: $P \leq 0,0001$). After that, an obvious trend of increased clustering starts becoming apparent even though it is not statistically significant at the 3rd day; at the 7th however, it shows a statistical distancing from the immediate effects caused by the mid-leg amputation (15min vs 7d post-amp.: $P \leq 0,01$) although none is shown when compared to the control (Unamp vs 7d post-amp.: $P \leq 0,0001$).

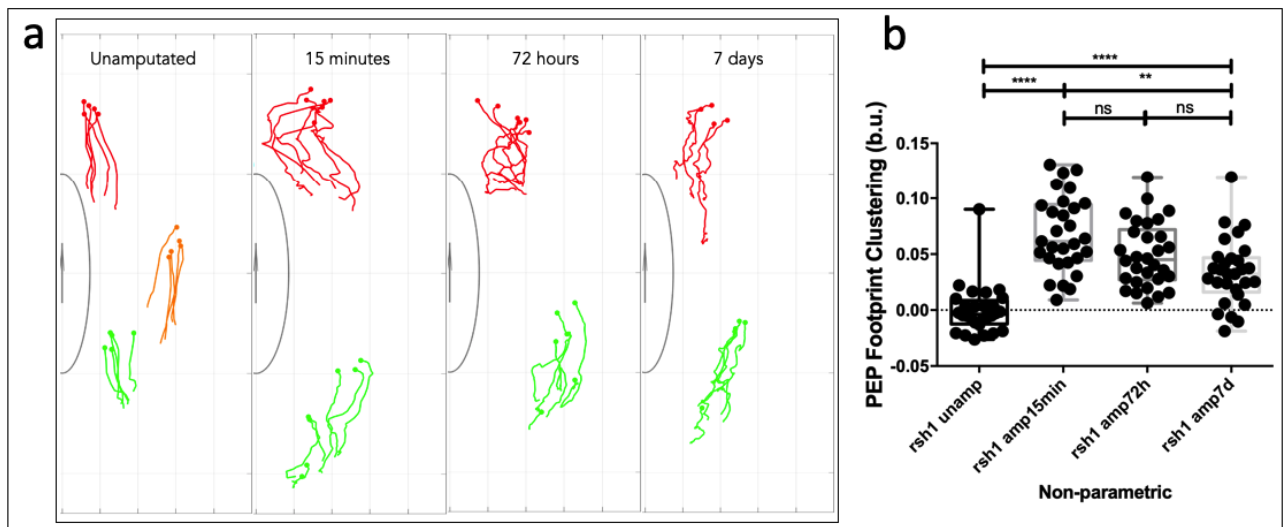


FIGURE 26. *radish*¹ Spatial parameters. **A)** *radish*¹ visual representation of AEP footprint clustering and stance traces for single flies within the median value of AEP footprint clustering for the analysed groups: Unamputated; 15minutes, 72 hours and 7days post-amputation. Body size represents a body unit. **B)** Quantification of *radish*¹'s footprint clustering of posterior Extreme Positions (body units) via residual analysis vs unamputated control group. **Data distribution** assessed by D'Agostino Pearson and Shapiro-Wilk normality tests. **Multiple comparison** tests performed according to patterns of data distribution, either parametric (One-Way ANOVA for normally distributed data; Holm-Sidak's test for multiple comparisons) or non-parametric (Kruskal-Wallis test for abnormally distributed data and Dunn's test for multiple comparisons). **Statistical significances** resulting from multiple comparison tests are as follows: ****, $P \leq 0,0001$; ***, $P \leq 0,001$; **, $P \leq 0,01$; *, $P \leq 0,05$; ns, $P > 0,05$. **Box-plot positioning**, either above or below the x-axis, reflects a respective increase or decrease of the analyzed parameter vs the unamputated control group.

SUMMARY

From the (Fig. 27) produced for the recovery of the *radish*¹ mutant, we can observe that four locomotor parameters show **recovery** – all with no statistically significant difference from the unamputated control. These are the swing speed – a step parameter; the body path, onset ratio and average are of all configurations – stability parameters.

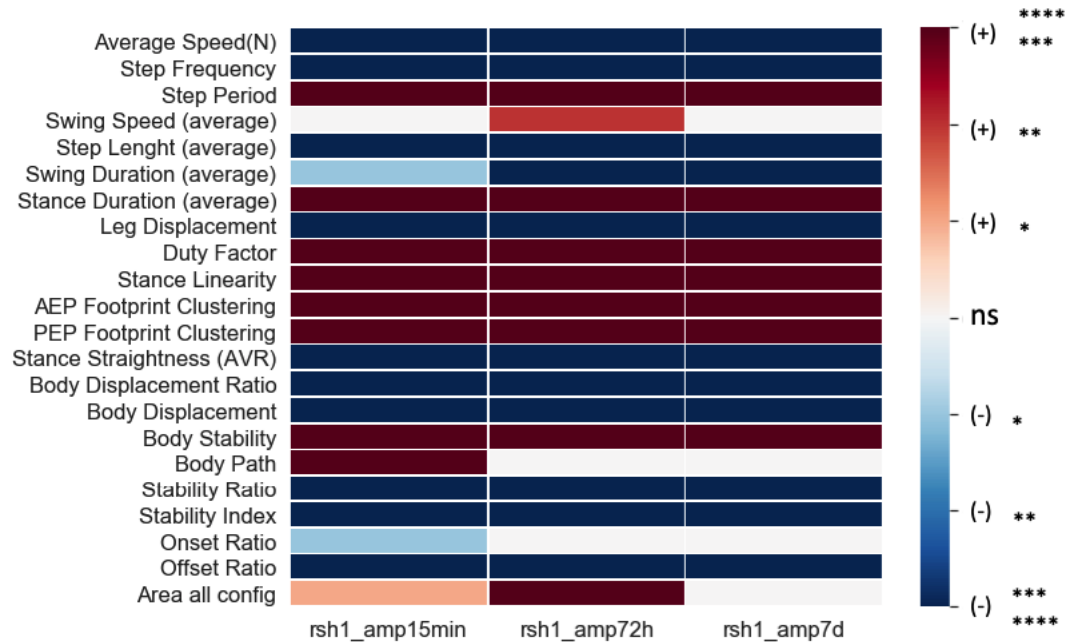


FIGURE 27. *radish*¹ heatmap of all residual data from comparison to unamputated flies of the same genotype. tested locomotor parameters in the following order: Step, Spatial and Stability parameters. **Data distribution** assessed by D’Agostino Pearson and Shapiro-Wilk normality tests. **Multiple comparison** tests performed according to patterns of data distribution, either parametric (One-Way ANOVA for normally distributed data; Holm-Sidak’s test for multiple comparisons) or non-parametric (Kruskal-Wallis test for abnormally distributed data and Dunn’s test for multiple comparisons). Bonferroni **correction** was applied to the multiple comparisons. **Statistical significances** resulting from multiple comparison tests are as follows: ****, P≤0,0001 and ***, P≤0,001, deep red and deep blue; **, P≤0,01, red and blue; *, P≤0,05, pale red and pale blue; ns, P>0,05, white.

THE EFFECTS OF CYCLOHEXIMIDE ON MOTOR LEARNING

To understand if *de novo* protein synthesis is necessary for the recovery phenotype we have been describing thus far, and having clear examples of flies which show none, we used Cycloheximide (CHX) to globally inhibit protein translation. The mixture was administered orally to Canton-S flies and was composed of Cycloheximide dissolved in ethanol – used as a vehicle and as a negative control – water and sugar, so that the flies would feel enticed to feed on this mixture. Flies were kept for three days on the mixture in cycles of [10h treatment / 30 mins in regular food / 1h30min starvation] and motor behavior was assessed at the end.

The third day was defined as the last timepoint as we previously observed that, at this time, Canton-S flies already show early signs of recovery; besides as CHX is toxic, survivability was at stake and our usual 7 days of recovery simply seemed too ambitious as the protocol was very challenging to perform as is.

EFFECTS OF CYCLOHEXIMIDE ON MOTOR BEHAVIOR

To understand if CHX and the vehicle, ethanol (EtOH), alone cause changes in locomotor behavior, we first tested unamputated flies on the feeding protocol.

From the produced heatmap (Fig. 28), both mixtures clearly show an effect on locomotion.

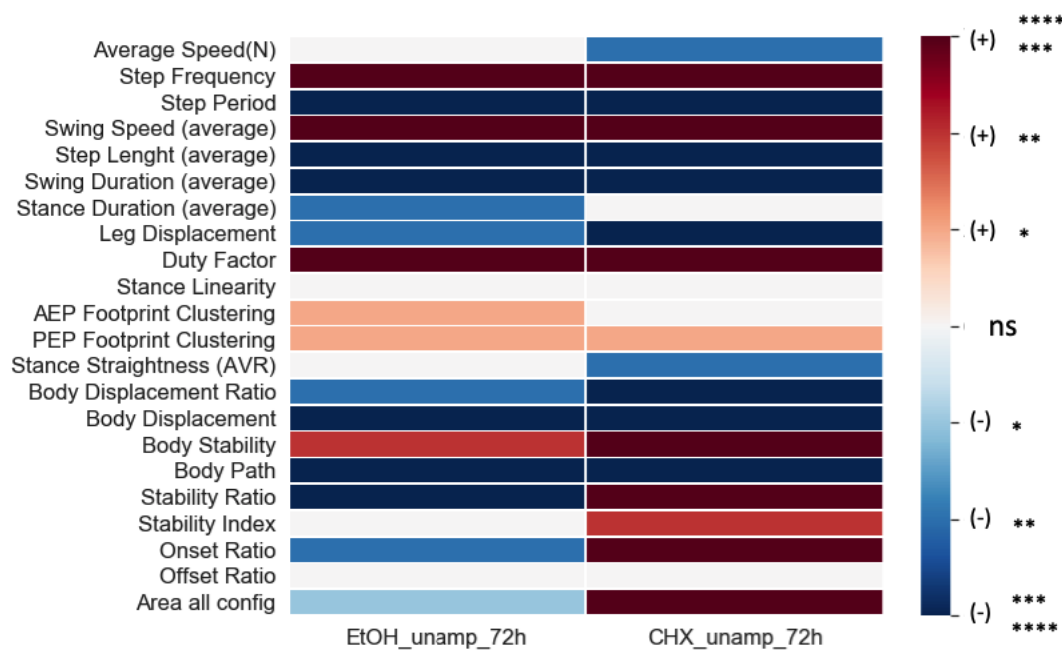


FIGURE 28. Cycloheximide's and Empty vehicle's effect on unamputated flies heatmap of all residual data from comparison to Canton-S untreated and unamputated flies. Tested locomotor parameters in the following order: Step, Spatial and Stability parameters. **Data distribution** assessed by D'Agostino Pearson and Shapiro-Wilk normality tests. **Multiple comparison** tests performed according to patterns of data distribution, either parametric (One-Way ANOVA for normally distributed data; Holm-Sidak's test for multiple comparisons) or non-parametric (Kruskal-Wallis test for abnormally distributed data and Dunn's test for multiple comparisons). Bonferroni **correction** was applied to the multiple comparisons. **Statistical significances** resulting from multiple comparison tests are as follows: ****, $P \leq 0,0001$ and ***, $P \leq 0,001$, deep red and deep blue; **, $P \leq 0,01$, red and blue; *, $P \leq 0,05$, pale red and pale blue; ns, $P > 0,05$, white.

STEP PARAMETERS

Three step parameters are shown to be **increased** as a result of the 3-day EtOH or EtOH+CHX feeding protocol: the **step frequency**, **swing speed** and **duty factor** – flies perform more step cycles per second as the swings phases are faster. A result of the faster swings is the **decrease** in **swing duration** and **step length** (as there is less time to do them); additionally, and since the step frequency is increased, this is reflected in the **step period** by the decrease in time needed to perform one step cycle. The last parameter that varies and performs similarly in both conditions is the duty factor (percentage of the step cycle spent in stance), displaying an increase – since step cycles are less prolonged and the swing phase is performed with increased speed, this effect is expected: flies spend an increased portion of the step cycle on the stance phase.

Differences between both treatments are reflected on the decrease of the **average speed** and **leg displacement** of CHX treated flies – this may be a sign of its toxic effect.

SPATIAL PARAMETERS

Regarding the four spatial parameters, the biggest notable difference between treatments is in the decrease of **stance straightness** displayed by CHX treated flies; additionally, both show **PEP footprint clustering** which are less clustered together, and EtOH treated flies also show this effect in the **AEP footprint clustering**, probably due to the increase in step frequency and maintaining of their average speed (observed in the step parameters), likely making steps more rushed and less “planed”.

STABILITY PARAMETERS

Here is where clear differences between treatments are the clearest and most disparate. While the **Body displacement ratio**, **-displacement**, **-stability**, **-path** and **offset ratios** show similar effects on both treatments, the presumed effect of CHX is notable on the disparity of three stability parameters: the stability ratio, onset ratio and area of all configurations, all showing opposite effects between the study groups.

While the ethanol alone **decreases** the **stability ratio**, **onset ratio** and **area of all configurations**; the adding of Cycloheximide to the mixture shows the exact opposite: as flies seem to walk slower and with less stance straightness, the effects on their stability are reflected by the need to adopt a bigger support area, the static position of the COM in relation to the area of support and the big increase in their stability ratio. Additionally, we can also observe an effect exclusive to CHX treatment on the body stability, which CHX further accentuates as flies imbibing it appear to be even less stable than vehicle-treated ones – these observations suggest a “lack of confidence” in walking, probably due to CHX’s toxicity which has been built up for three days. While their increase may seem positive, consider that the “drunk” flies can efficiently perform the straight walking bursts with decreased stability, further adding to the argument that CHX treated flies are overcompensating in stability parameters due to the drug’s negative effects.

EFFECTS OF CHX AND ETOH ON MOTOR LEARNING

Considering that, from the previous experiment we realize that our empty vehicle control displays many behavioral changes, all results regarding locomotor recovery from amputation should be taken with caution. We concluded that stability is the parameter most affected by CHX, and from analysis of locomotor recovery (Fig. 29), stability and spatial parameters are those which show the most recovery. We will thus analyze these two in this section – with particular attention to those which CHX affects the most – to study its influence on locomotor adaptation to amputation.

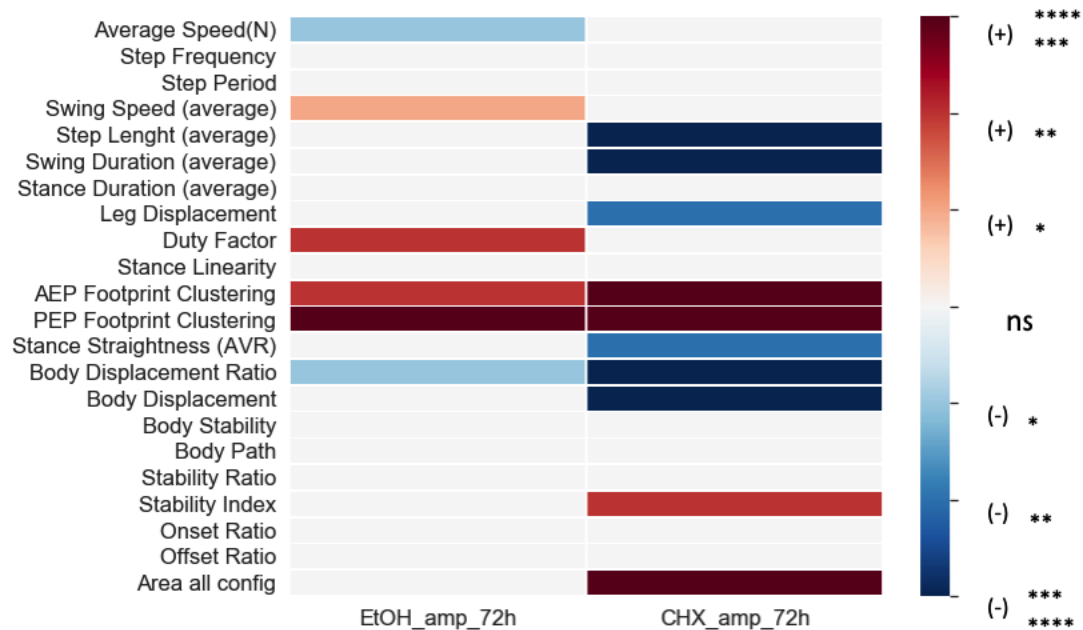


FIGURE 29. Cycloheximide’s and empty vehicle’s effect on locomotor recovery. Heatmap of all residual data from comparison to Canton-S untreated and unamputated flies. Tested locomotor parameters in the following order: Step, Spatial and Stability parameters. **Data distribution** assessed by D’Agostino Pearson and Shapiro-Wilk normality tests. **Multiple comparison** tests performed according to patterns of data distribution, either parametric (One-Way ANOVA for normally distributed data; Holm-Sidak’s test for multiple comparisons) or non-parametric (Kruskal-Wallis test for abnormally distributed data and Dunn’s test for multiple comparisons). Bonferroni **correction** was applied to the multiple comparisons. **Statistical significances** resulting from multiple comparison tests are as follows: ****, $P \leq 0,0001$ and ***, $P \leq 0,001$, deep red and deep blue; **, $P \leq 0,01$, red and blue; *, $P \leq 0,05$, pale red and pale blue; ns, $P > 0,05$, white.

SPATIAL PARAMETERS

Observing the heatmap (Fig. 29) relative to locomotor recovery under treatment with either EtOH alone and CHX+EtOH – compared to Canton-S amputated flies at the 72h timepoint – we observe that the **stance linearity** performs equally in all groups. Regarding the footprint clustering of **AEPs** and **PEPs** and the **stance straightness**, we observe the same pattern as in the previous analysis relative to the effect of the treatment on unamputated flies – no conclusions can be taken from the effect of CHX on their locomotor recovery.

STABILITY PARAMETERS

Regarding stability parameters, only the **Area of all configurations** and **Stability index** show an isolated effect while locomotor adaptation is happening. These two parameters, especially the increase of the area of support, are taken to be effects of CHX; we observe in both an statistical increase, meaning that CHX+EtOH treated flies require a larger support area and that CHX also increases – although less conclusively, EtOH did so too in the previous experiment – their instability.

SUMMARY

Regarding the effect of CHX and the need for *de novo* protein synthesis for locomotor recovery from amputation to occur, we observe that it, alone, affects flies' stability. Regarding these parameters and those reflecting the flies' spatial disposition of the legs – all show a clear readout of recovery (Fig. 29)– we observe that, under the influence of the protein translation inhibitor, the Area of all configurations is affected and worsened. Arguably, CHX seems to slightly dampen locomotor recovery; however, since the control vehicle clearly disturbs it too, no clear conclusions can be extracted from these results.

DISCUSSION

DROSOPHILA MELANOGASTER, *REPLETA* AND *PSEUDOOBSCURA*: PATTERNS OF LOCOMOTOR RECOVERY

From the analyses of the *Drosophila* wild types **Canton-S** and the *Drosophila pseudoobscura* and *repleta* subspecies, patterns emerge: two branches of locomotion systematically adapt to amputation – **spatial** (Figs. 5 and 9) and **stability** (Figs. 4 and 8) parameters – and even though, at times, this adaptation is not enough to lead to a functional recovery – meaning no statistical difference to unamputated flies – these parameters show a clear improvement in performance by approaching control levels while, over time, deviating from their 15-minute post-amputation counterparts. Additionally, it appears to be no coincidence that these behaviors repeat themselves in flies with such a big evolutionary and phylogenetic distance between them. Finally, taking into account the specific kinematic changes occurring during motor adaptation, recovery in these parameters seems like a viable strategy to regain fluidity in motion; stability (**body displacement ratio**, **body path** and the **area of all configurations**) and spatial (**AEP** and **PEP footprint clustering**, **stance straightness** and **linearity**) adaptation of locomotion reflects both a regain in locomotor fluidity (by exerting more control over side-to-side body displacement, as the middle legs which served that purpose can no longer be used) and precision in leg placement, which when working ensemble, also indicate increased coordination. This hypothesis does not, however, exclude the fact that other parameters such as changes in step properties or adoption of new gaits are important for locomotor recovery; these merely suggest that, given the timescale under analysis (7 days), stability and spatial parameters seem to be those that are adapted first, to then pave the way for a full recovery in which coordination is gained by finetuning step parameters and by adopting new gaits compatible with four-legged locomotion. Indeed this favoring of Spatial and Stability parameters seems to happen by abdicating the gain in performance in Step parameters. Taking the example of the Duty factor step parameter (Figs. 7 and 11), which, by showing no alteration during the adaptation period, suggests that this may be an adopted strategy for the stability and spatial parameters to recover – in this way, flies spend a bigger percentage of the step cycle in the stance phase (legs on the ground) maintain body stability as seen by the decrease of the Body paths (Figs. 4D and 8C and D).

Regarding the lack of analysis of gait parameters (besides that done in Canton-S flies), this decision was made as our actual gait parameters seem to be incompatible with this motor recovery scenario. As of now, only the Non-canonical index has a minimal potential of utility to assess the lack of coordination, which can also be done (with more striking results) using the AEP and PEP footprint clustering spatial parameters. The FlyWalker, when analyzing tetrapod flies, substitutes the Tripod and Tetrapod indexes by the Pace and Trot indexes, respectively. These two gaits are indeed gaits normally adopted by quadruped animals; however, these gaits are solely adopted at high speeds, which, given our “newly quadruped flies” is very unlikely to happen, as these gaits require a leap phase (no feet on the ground), which is highly unlikely to happen in insects, particularly while recovering from amputation. Additionally, since flies do not run, they simply walk faster (hence the fluid gait changes between wave, tetrapod and tripod gaits as speed increases), they do not leap but instead increase their step frequency^{10,82}. As an alternative, we must develop a way to measure the “walk” and “amble” gaits, which never have a leap phase and which are adopted at slower speeds by quadruped animals.

Regarding other recovery patterns of Canton-S flies, we see some parameters initially recovering (72h) and then again decreasing in performance at the timepoint at 7 days (AEP footprint clustering (Fig. 5A) and Offset ratio (Fig. 7) show this pattern vs the unamputated control). We have two justifications for

this: 1) the flies may simply get more tired as time goes by; or 2) motor activity during recovery is not stimulated; these flies, while recovering, spent 7 days in isolation in a vial; if we think about this situation in our own lives, it may be awful for some, but even besides the isolation they experienced, other side effects may come to, for example the lack of motor activity fomented by stimulation, which, again doing a parallel with our own species, is essential for motor recovery (take physiotherapy and regular exercise for example). In response to this, flies started to be placed in pairs while recovering and during filming (*Drosophila pseudoobscura* and *repleta* included), guaranteeing that they had a more stimulating environment in both situations. This showed an obvious effect when flies were being filmed, as the “air puff stimulus” to promote walking was much less necessary since flies would bump into each other, thus stimulating walking bouts.

Another observation that must be done, now comparing the degree of locomotor recovery of the subspecies (particularly *pseudoobscura*) vs Canton-S's, we can see that the first displays a slightly better adaptation to the amputation scenario when compared to their own controls regarding parameters such as AEP footprint clustering (Figs. 5B and 9D) and Stance straightness (Figs. 5D and 9F). An explanation that comes to mind is that, like HeLa cells, Canton-S flies have been widely used for many years; this grants both the maintenance of the genetic background, but also pollutes it due to inbreeding. Since these *Drosophila* subspecies come from a more recent lineage, their genetic background should be less compromised having had less time for random mutations to occur. Another explanation is that, since *D.* subspecies are slightly larger than *D. melanogaster*, hence supporting a higher body load, the necessary degree of recovery to regain function may be decreased, therefore requiring a less steep recovery curve.

Overall, this data shows that various *Drosophila* species are capable of recovering functional locomotion after being submitted to a double middle-leg amputation which forces them to learn how to walk on four legs only. Over the course of 7 days, various locomotor parameters are adapted so that this behavioral changes can occur. Since these *Drosophila* species have significant evolutionary distance separating them, we can claim that locomotor adaptation following mid-leg amputation is an evolutionarily conserved behavioral phenotype in the *Drosophilidae* phylogenetic tree.

DISSECTING THE cAMP LEARNING AND MEMORY CASCADE: *AMN*¹, *RUT*¹, *DNC*¹, *RSH*¹ AND *DE NOVO* PROTEIN SYNTHESIS

We start the dissection of the cAMP pathway (Fig. 30A) with the **amnesiac** mutants (*amn*¹) that, as it is inferred from the literature that this is our most upstream target. The *amnesiac*-encoded pre-neuropeptide (thought to be co-released with Acetylcholine (ACh) from DPM cells), to activate *rutabaga*, possibly via GPCR's.

These mutants, very interestingly, showed phenotypical adaptation of motor behavior in all three relevant branches of motor behavior: parameters regarding its Stability, Step and Spatial performance. They *adapt* (meaning, vs the 15min timepoint) in a total of 18/21 locomotor parameters, but only recover in 3 of them, none however, pertain to those that are consistent in wild type recovery. Due to this fact we conclude that they do not recover from amputation, thus suggesting a role for it in motor learning.

The adaptation that we see occurring in so many parameters cannot be ignored. Could these flies actually be recovering, although at a slower rate? Could other sources of input, instead of *amnesiac*'s G protein-coupled receptors, be stimulating the cells affected by the mutation – those that simultaneously express

rutabaga, *dunce* and *radish*? NMDA and AMPA receptors or even inputs from other brain areas could be stimulating the cells affected by the *amnesiac* mutation. It makes sense that many types of inputs must be necessary for such a global behavioral adaptation to occur. This brings forth the thought that, by cutting *amnesiac* out of the equation we may be putting a “bottleneck” on the input to the target cells, while not cutting it out completely. This could somewhat “slow down the time” of recovery on a molecular level, since the necessary cAMP would take longer to be reached, reflecting on the fly’s large locomotor adaptation but inefficient recovery. On the other hand, these flies can simply be showing a slow locomotor adaptation from buildup in muscle strength and not via learning and memory-related neuronal plasticity.

It is important to mention that *amnesiac*, besides olfactory learning, also plays a developmental role in DPM neuron formation and perineurial glial growth. If the mutation compromises the nervous system from the start – which does not seem to happen regarding hexapod locomotor behavior – it may sabotage locomotor recovery from the start. With this effect, and assuming that *amnesiac* plays a role exclusively in olfactory learning, could also explain the absence of recovery due to neuronal malformations, in which *amnesiac* would not play a role anyways.

Regarding *rutabaga*’s mutation (*rut¹*) affecting the pan-neuronally expressed adenylate cyclase – which, by definition, responds to activation by synthesis of cyclic Adenosine Monophosphate (cAMP) – it results in the least effective genotype at locomotor recovery, probably due to its wide expression pattern, indicating that this gene is very likely to play a role in locomotor adaptation. It shows recovery in two locomotor parameters – none of which are from most prominent to recover in the wild types – and only adapts to 5/21 parameters. This is a clear case of no recovery, which is not too surprising given that the mutation affects so much of the nervous system, and doing it so though such a fundamental player in many different pathways – as cAMP is a second messenger in many biological processes and in this pathway it plays a role via PKA downstream activation.

Even though these flies become slightly more stable during the onset and offset phases of the stance (Figs. 18C, 19) increasing their stability ratio (Fig. 18D) – COM inside the area of support – over time their body shows increasingly more displacement (Figs. 18A,B) and no reduction in body path (Fig. 19).

Regarding their step parameters, the swing speed seems to be modulated, returning the duration of swing phase to control levels. Besides these, no parameters that are adapted in wild type conditions show recovery, and even though adaptation can occur through different parameters and still prove functional, it does not happen in the case of these flies; they become, and clearly stay uncoordinated and unable to deal with their body weight – clear from the continuous increase of the displacement of their body.

Regarding general locomotor activity when unamputated, these do not display any type of abnormal walking behavior, a claim made by the observation of how straight their body traces are when the flies walk on six legs.

dunce’s described function serves to balance the rise in intracellular cAMP, degrading it, as it has cAMP-specific phosphodiesterase activity, counteracting *rutabaga* activity; this is an interesting mutant to study since, in this case, the cAMP pathway is exacerbated and would, in theory, overstimulate the L&M pathway.

In response to amputation, this mutant seems to recover better than any of those analyzed up to now – this because it actually shows a statistical approximation to the unamputated control in parameters that

consistently improve in wild type flies (Body path and AEP footprint clustering). Two stability parameters fully recover: at 72h post-amputation the body path (Figs. 20D,23) displays equal levels of performance to the control, which however reverts at 7 days; additionally, the body displacement is the same as the unamputated control at 7 days (Fig. 20C), meaning that all flies, amputated or not, cover the same distance in 5 steps (per leg). Recovery in these two stability parameters, in the AEP footprint clustering – a spatial parameter that reflects precision in leg placement – and in three step parameters (Swing speed, Step length and Stance duration (Fig. 23) indicate that this mutant slightly recovers even if not as efficiently as the wild types.

In total, *dnc*¹ flies adapt 12 out of 21 locomotor parameters, four of them stability, five step and three spatial parameters. These results bring forth the assumption that the indiscriminate rise in cAMP – resulting from the absence of *dunce*'s phosphodiesterase activity – may have promoted some locomotor recovery by exerting an effect on Long Term- and in Anesthesia Resistant Memory (CREB and *radish*, respectively).

The last flies, mutants for the small GTPase *radish*¹, are the most difficult to classify in terms of recovery. While these show a statistical approximation to controls in four stability parameters (Figs. 24C,F,G,H), two of which consistently recover in the wild types (Body path and Area of all configurations), no spatial parameters show recovery. One step parameter recovers (Swing speed, Figs. 25A; 27), whereas the PEP footprint clustering spatial parameter (Fig. 26B) only adapts slightly, not approaching the control.

It can be said is that there is some degree of recovery, although not as the wild types nor as *dunce*'s (Figs. 20A,B and 24A,B), adaptation in walking behavior seems to occur, seemingly driven by an increase in stability. This increase in some stability parameters may be related to the negative change in two step parameters: the Duty factor and Step frequency – over time, flies take steps at a slower rate (Fig. 25C), thus spending increasingly more time in the stance phase (Fig. 25B). This results in wobbly stance traces (Fig. 26A) and leads to the assumption that *radish* mutants take more time between steps in an attempt to stabilize the body; however, even like this, they are unable to take precise steps (AEP footprint clustering in Fig. 27).

This mutation affects our most downstream target of the cAMP pathway, responsible for anesthesia resistant memory (ARM), the protein synthesis independent branch of long term memory. In this case, as ARM and LTM are genetically independent, we must assume that LTM is still occurring even though our mutation prevents ARM – this being a possible explanation for the recovery in two of stability parameters that do so too in WT conditions.

The aforementioned data seems to suggest that, unless *radish* plays an important role during development, the protein synthesis dependent LTM is not enough for locomotor recovery to occur as it does in WTs, suggesting that ARM is also important for this function. Interestingly, studies exploring downstream partners of *radish* suggest that it has binding activity with Rac1⁸³, an important protein described to be upregulated in the act of forgetting⁸⁴. This small GTPase influences neuronal growth and synaptic morphology by regulating cytoskeletal reorganization^{83,85}, reorganization which seems to be regulated by the opposing Raf/Rac1⁶⁸ pathways. In this model Rac1 promotes forgetting and Raf, via MAPK and Non-Muscle Myosin II (NMII), promotes increased memory performance, presumably by cytoskeletal rearrangements that facilitate it (synaptogenesis or other mechanisms of neuronal plasticity?).

A mystery that lingers, however, is that of the binding of *rsh* to Rac1, and if the binding activates or inhibits Rac1 activity. Seeing that our mutant for *rsh* is characterized as ARM-deficient, and since Rac1

upregulation serves as a forgetting mechanism, then *rsh* could bind to Rac1 to inactivate it, promoting instead Raf/MAPK cytoskeletal rearrangements that increase memory performance. This assumption, plus the notion that the *rsh* mutant still possesses LTM, suggests that 1) both LTM and ARM are necessary for normal locomotor learning; and that 2) LTM is contributing to learning with *de novo* protein synthesis and that ARM (acting in a protein-synthesis independent manner) may be promoting learning via cytoskeletal rearrangements which increase the number, size and volume of active zones⁶⁸ – the one contributing with structure, the other with function, in which case the *radish* mutant would only have function and no structural changes accompanying it.

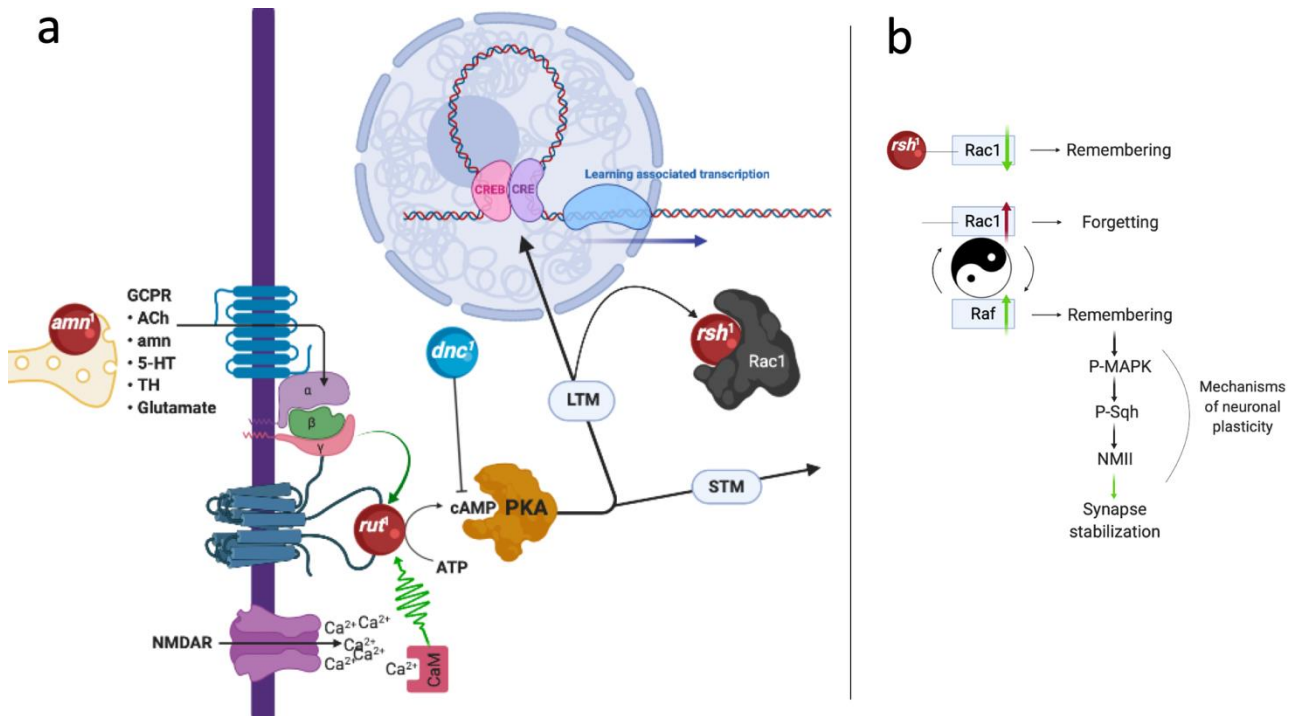


FIGURE 30. A) The cAMP “learning and memory” pathway. Figure design inspired by Waddell, S & Quinn, W. G., Trends Genet., 2001⁵³. **B)** *rsh* and Rac1 interaction and hypothesis of *rsh* influence on learning and memory. Interaction Between Rac1 and Raf described by Zhong, Y. Et al., Neuron, 2018⁶⁸.

Summing up:

- *amnesiac¹* may be an off target for locomotor recovery, as it is the genotype with the most adaptation of locomotor parameters, adaptation which, however, was not sufficient for a functional recovery.
- *rutabaga¹* is pan-neuronally expressed and this mutation shows a huge negative effect on locomotor adaptation; these flies did not display signs of locomotor recovery.
- *dunce²*, by promoting the rise in cAMP in its expressing cells, shows signs of locomotor recovery in two relevant parameters: precision in steps (AEP footprint clustering) and one regarding body stability (Body path).
- *radish¹*, the most downstream target of the pathway – which affects protein-synthesis independent memory formation – recovered on two important parameters that maximizes the fly’s stability (Area of all configurations and Body path).

Regarding the effect of cycloheximide and the need for ***de novo* protein synthesis** for locomotor recovery from amputation to occur, we observe that CHX alone, affects flies’ stability.

Regarding stability parameters and those reflecting the flies' spatial disposition of the legs – our readout for locomotor recovery – we observe that, under the influence of the protein translation inhibitor, the Area of all configurations is affected and worsened. Arguably, CHX seems to slightly dampen locomotor recovery; however, since the control vehicle clearly disturbs it too, no clear conclusions can be extracted from these results.

Literature suggests that cycloheximide should not have an effect in massed and spaced training experiments^{86,55}, a model which resembles our adaptation period. If this is so, if we found a vehicle with no behavioral effects to dissolve CHX, we should observe recovery with and without cycloheximide. Our experiments, however, show that CHX affects recovery in flies to a greater extent than the vehicle alone (EtOH) (Fig. 29), suggesting that motor learning mechanisms are somewhat different from those occurring during massed and spaced training learning paradigms and that *de novo* protein synthesis could play a role in locomotor rehabilitation.

CONCLUSIONS / FUTURE PERSPECTIVES

With the experiments described in this manuscript we show that Canton-S flies and the evolutionary distant *Drosophila repleta* and *pseudoobscura* species are capable of recovering functional locomotor performance in 3 days – in response to a double middle-leg amputation – and that this response is sustained at 7 days post-amputation. Additionally, our data shows that the recovery process occurs by adaptation of several locomotor parameters and that some of these consistently recover in all the tested *Drosophila* species. The parameters that recover consistently across species are those regarding the flies' stability (body displacement ratio, body path and the area of all configurations) and spatial placement of the legs (AEP and PEP footprint clustering, stance straightness and linearity). We can then conclude that, besides the fact that the phenotype of motor recovery seems to have evolutionary conservation in various subspecies of the *Drosophilidae* phylogenetic tree, its mode of action (that being the parameters that show adaptation) is also similar across them, as various parameters regarding stability and spatial positioning of the legs display the same phenotype.

We hypothesized that several genes relevant for learning and memory play a role in the observed locomotor recovery phenotype. To test this hypothesis we went on studying various mutants along the cAMP cascade described for learning and memory. By descending on the pathway we went on affecting less of the memory phases required for consolidated memory, theoretically increasing the chance of memory acquisition as less molecular players were affected. The first two mutants affected either STM (*rutabaga*) or MTM (*amnesiac*) and prevented the occurrence of LTM; this was well reflected on the absence of a recovery phenotype of these mutants, although the one expressed in a more restricted tissue (not, *rutabaga* which is pan-neuronal) showed some adaptation – *amnesiac*. STM was also affected by favoring the rise of cAMP instead of dampening it (*dunce*), yielding a motor performance that resembled recovery – similar to that displayed by wild types – at different timepoints; two locomotor parameters recovered, one reflecting precision in step placement, the other regarding body stability (Body path). When ARM was affected by the *radish* mutation however, we were still enabling STM, MTM and LTM; this reflected on the recovery of two important stability parameters regarding the flies' area of support. These results show that all these mutants seem to play a role in locomotor adaptation and that LTM alone is not sufficient to promote the recovery phenotype.

Interestingly, ARM seems to have an important role in neuronal plasticity, especially taking into account its binding partner Rac1, which has been shown to be extremely important in several learning and memory experiments conducted in *Drosophila*: its upregulation leads to an increase in forgetting^{81,87}, while its downregulation, especially when Raf is simultaneously upregulated leads to a tremendous increase in

memory performance⁸⁸. This is certainly an interesting future experiment to conduct, as well as the manipulation of CREB via a Dominant Negative form driven by a neuronal Gal-4 driver. This would be done to understand the role of *de novo* protein synthesis in the context of learning and memory (UAS-CREB[DN]) in a pertinent tissue (neurons) instead of inhibiting protein synthesis in the whole organism as happens with the administration of Cycloheximide. An additional future experiment which is essential to prove our point – that this pathway somehow mediates motor learning – is the rescue of our phenotype, probably via *rutabaga*, as this is the mutant with the lesser degree of recovery.

BIBLIOGRAPHY

1. Dickinson, M. H. *et al.* How animals move: An integrative view [Review]. *Science (80-.)*. **288**, 100–106 (2000).
2. Arber, S. & Costa, R. M. Connecting neuronal circuits for movement. *Science (80-.)*. **360**, 1403–1404 (2018).
3. Dickinson, M. H. *et al.* How Animals Move: An Integrative View. *Science (80-.)*. **288**, 100–106 (2000).
4. Marder, E. & Bucher, D. Central pattern generators and the control of rhythmic movements. *Curr. Biol.* **11**, R986–R996 (2001).
5. Borgmann, A., Hooper, S. L. & Buschges, A. Sensory Feedback Induced by Front-Leg Stepping Entrain the Activity of Central Pattern Generators in Caudal Segments of the Stick Insect Walking System. *J. Neurosci.* **29**, 2972–2983 (2009).
6. Isakov, A. *et al.* Recovery of locomotion after injury in *Drosophila melanogaster* depends on proprioception. (2016). doi:10.1242/jeb.133652
7. Mendes, C. S., Rajendren, S. V., Bartos, I., Márka, S. & Mann, R. S. Kinematic Responses to Changes in Walking Orientation and Gravitational Load in *Drosophila melanogaster*. *PLoS One* **9**, e109204 (2014).
8. Ofstad, T. A., Zuker, C. S. & Reiser, M. B. Visual place learning in *Drosophila melanogaster*. *Nature* **474**, 204–207 (2011).
9. da Silva, J. A., Tecuapetla, F., Paixão, V. & Costa, R. M. Dopamine neuron activity before action initiation gates and invigorates future movements. *Nature* **554**, 244–248 (2018).
10. Mendes, C. S., Bartos, I., Akay, T., Márka, S. & Mann, R. S. Quantification of gait parameters in freely walking wild type and sensory deprived *Drosophila melanogaster*. *Elife* **2**, e00231 (2013).
11. Sperry, R. W. *HEMISPHERE DECONNECTION AND UNITY IN CONSCIOUS AWARENESS J.*
12. You Are Two - YouTube. Available at: <https://www.youtube.com/watch?v=wfYbgdo8e-8>. (Accessed: 30th September 2019)
13. Smith, M. A., Brandt, J. & Shadmehr, R. Motor disorder in Huntington’s disease begins as a dysfunction in error feedback control. *Nature* **403**, 544–9 (2000).
14. Mazzoni, P., Shabbott, B. & Cortés, J. C. Motor control abnormalities in Parkinson’s disease. *Cold Spring Harb. Perspect. Med.* **2**, a009282 (2012).
15. Vasudevan, E. V. L., Glass, R. N. & Packel, A. T. Effects of Traumatic Brain Injury on Locomotor Adaptation. *J. Neurol. Phys. Ther.* **38**, 172–182 (2014).
16. Darmohray, D. M., Jacobs, J. R., Marques, H. G. & Carey, M. R. Spatial and Temporal Locomotor Learning in Mouse Cerebellum. *Neuron* **102**, 217–231.e4 (2019).
17. Takeoka, A. & Arber, S. Functional Local Proprioceptive Feedback Circuits Initiate and Maintain Locomotor Recovery after Spinal Cord Injury. *Cell Rep.* **27**, 71–85.e3 (2019).
18. Isakov, A. *et al.* Recovery of locomotion after injury in *Drosophila melanogaster* depends on proprioception. *J. Exp. Biol.* **219**, 1760–71 (2016).
19. Kathman, N. D. & Fox, J. L. Representation of haltere oscillations and integration with visual inputs in the fly central complex. *J. Neurosci.* (2019). doi:10.1523/JNEUROSCI.1707-18.2019

20. Pearson-Fuhrhop, K. M., Kleim, J. A. & Cramer, S. C. Brain Plasticity and Genetic Factors. *Top. Stroke Rehabil.* **16**, 282–299 (2009).
21. Xiao, H., Yang, Y., Xi, J. & Chen, Z. Structural and functional connectivity in traumatic brain injury. *Neural Regen. Res.* **10**, 2062 (2015).
22. Pi, Y.-L. *et al.* Motor skill learning induces brain network plasticity: A diffusion-tensor imaging study. *PLoS One* **14**, e0210015 (2019).
23. Kliemann, D. *et al.* Intrinsic Functional Connectivity of the Brain in Adults with a Single Cerebral Hemisphere. *Cell Rep.* **29**, 2398–2407.e4 (2019).
24. Northcutt, A. J. & Schulz, D. J. Molecular Mechanisms of Homeostatic Plasticity in Central Pattern Generator Networks. *Dev. Neurobiol.* dneu.22727 (2019). doi:10.1002/dneu.22727
25. Adkins, D. L., Boychuk, J., Remple, M. S. & Kleim, J. A. Motor training induces experience-specific patterns of plasticity across motor cortex and spinal cord. *J. Appl. Physiol.* **101**, 1776–1782 (2006).
26. Kleim, J. A. *et al.* BDNF val66met polymorphism is associated with modified experience-dependent plasticity in human motor cortex. *Nat. Neurosci.* **9**, 735–737 (2006).
27. Pearson-Fuhrhop, K. M., Kleim, J. A. & Cramer, S. C. Brain Plasticity and Genetic Factors. *Top. Stroke Rehabil.* **16**, 282–299 (2009).
28. Mahley, R. W. & Rall, S. C. A POLIPOPROTEIN E: Far More Than a Lipid Transport Protein. *Annu. Rev. Genomics Hum. Genet.* **1**, 507–537 (2000).
29. Stanne, T. M. *et al.* Genetic variation at the BDNF locus: evidence for association with long-term outcome after ischemic stroke. *PLoS One* **9**, e114156 (2014).
30. Mahley, R. W. & Huang, Y. Apolipoprotein e sets the stage: response to injury triggers neuropathology. *Neuron* **76**, 871–85 (2012).
31. Egan, M. F. *et al.* The BDNF val66met polymorphism affects activity-dependent secretion of BDNF and human memory and hippocampal function. *Cell* **112**, 257–69 (2003).
32. Statton, M. A., Vazquez, A., Morton, S. M., Vasudevan, E. V. L. & Bastian, A. J. Making Sense of Cerebellar Contributions to Perceptual and Motor Adaptation. *The Cerebellum* **17**, 111–121 (2018).
33. Morton, S. M. & Bastian, A. J. Cerebellar Control of Balance and Locomotion. *Neurosci.* **10**, 247–259 (2004).
34. Vassiliadis, P., Derosiere, G. & Duque, J. Beyond Motor Noise: Considering Other Causes of Impaired Reinforcement Learning in Cerebellar Patients. *eNeuro* **6**, ENEURO.0458-18.2019 (2019).
35. Therrien, A. S., Wolpert, D. M. & Bastian, A. J. Effective reinforcement learning following cerebellar damage requires a balance between exploration and motor noise. *Brain* **139**, 101–114 (2016).
36. Zill, S., Schmitz, J. & Büschges, A. Load sensing and control of posture and locomotion. *Arthropod Struct. Dev.* **33**, 273–286 (2004).
37. Wosnitza, A., Bockemühl, T., Dübbert, M., Scholz, H. & Büschges, A. Inter-leg coordination in the control of walking speed in *Drosophila*. 480–491 (2013). doi:10.1242/jeb.078139
38. Creamer, M. S., Mano, O. & Clark, D. A. Visual Control of Walking Speed in *Drosophila*. *Neuron* **100**, 1460–1473.e6 (2018).
39. Wernig, A. & Müller, S. Laufband locomotion with body weight support improved walking in

- persons with severe spinal cord injuries. *Spinal Cord* **30**, 229–238 (1992).
40. Dietz, V., Wirz, M., Curt, A. & Colombo, G. Locomotor pattern in paraplegic patients: training effects and recovery of spinal cord function. *Spinal Cord* **36**, 380–90 (1998).
 41. Hamers, F. P. T., Lankhorst, A. J., van Laar, T. J., Veldhuis, W. B. & Gispens, W. H. Automated Quantitative Gait Analysis During Overground Locomotion in the Rat: Its Application to Spinal Cord Contusion and Transection Injuries. *J. Neurotrauma* **18**, 187–201 (2001).
 42. Ghosh, S. & Hui, S. P. Axonal regeneration in zebrafish spinal cord. *Regen. (Oxford, England)* **5**, 43–60 (2018).
 43. Darmohray, D. M., Jacobs, J. R., Marques, H. G. & Carey, M. R. Spatial and Temporal Locomotor Learning in Mouse Cerebellum. *Neuron* **102**, 217–231.e4 (2019).
 44. van Meer, M. P. A. *et al.* Recovery of Sensorimotor Function after Experimental Stroke Correlates with Restoration of Resting-State Interhemispheric Functional Connectivity. *J. Neurosci.* **30**, 3964–3972 (2010).
 45. Pfeiffer, K. & Homberg, U. Organization and Functional Roles of the Central Complex in the Insect Brain. *Annu. Rev. Entomol.* **59**, 165–184 (2014).
 46. Wolff, T. & Rubin, G. M. Neuroarchitecture of the *Drosophila* central complex: A catalog of nodulus and asymmetrical body neurons and a revision of the protocerebral bridge catalog. *J. Comp. Neurol.* **526**, 2585–2611 (2018).
 47. Triphan, T., Poeck, B., Neuser, K. & Strauss, R. Visual Targeting of Motor Actions in Climbing *Drosophila*. *Curr. Biol.* **20**, 663–668 (2010).
 48. Neuser, K., Triphan, T., Mronz, M., Poeck, B. & Strauss, R. Analysis of a spatial orientation memory in *Drosophila*. *Nature* **453**, 1244–1247 (2008).
 49. Kim, S. S., Hermundstad, A. M., Romani, S., Abbott, L. F. & Jayaraman, V. Generation of stable heading representations in diverse visual scenes. *Nature* **576**, 126–131 (2019).
 50. Fisher, Y. E., Lu, J., D’Alessandro, I. & Wilson, R. I. Sensorimotor experience remaps visual input to a heading-direction network. *Nature* **576**, 121–125 (2019).
 51. Krause, T., Spindler, L., Poeck, B. & Strauss, R. *Drosophila* Acquires a Long-Lasting Body-Size Memory from Visual Feedback. *Curr. Biol.* (2019). doi:10.1016/J.CUB.2019.04.037
 52. Strausfeld, N. J., Hansen, L., Li, Y., Gomez, R. S. & Ito, K. Evolution, discovery, and interpretations of arthropod mushroom bodies. *Learn. Mem.* **5**, 11–37 (1998).
 53. Waddell, S. & Quinn, W. G. What can we teach *Drosophila*? What can they teach us? *Trends Genet.* **17**, 719–726 (2001).
 54. Hige, T. What can tiny mushrooms in fruit flies tell us about learning and memory? *Neurosci. Res.* **129**, 8–16 (2018).
 55. Margulies, C., Tully, T. & Dubnau, J. Deconstructing Memory in *Drosophila*. *Curr. Biol.* **15**, R700–R713 (2005).
 56. Gerber, B., Tanimoto, H. & Heisenberg, M. An engram found? Evaluating the evidence from fruit flies. *Curr. Opin. Neurobiol.* **14**, 737–744 (2004).
 57. Martin, J. R., Ernst, R. & Heisenberg, M. Mushroom bodies suppress locomotor activity in *Drosophila melanogaster*. *Learn. Mem.* **5**, 179–91 (1998).

58. Namiki, S., Dickinson, M. H., Wong, A. M., Korff, W. & Card, G. M. The functional organization of descending sensory-motor pathways in *Drosophila*. *Elife* **7**, (2018).
59. Zacarias, R., Namiki, S., Card, G. M., Vasconcelos, M. L. & Moita, M. A. Speed dependent descending control of freezing behavior in *Drosophila melanogaster*. *Nat. Commun.* **9**, 3697 (2018).
60. Cognigni, P., Felsenberg, J. & Waddell, S. Do the right thing: neural network mechanisms of memory formation, expression and update in *Drosophila*. *Curr. Opin. Neurobiol.* **49**, 51–58 (2018).
61. Zars, T., Fischer, M., Schulz, R. & Heisenberg, M. Localization of a Short-Term Memory in *Drosophila*. *Science (80-.)*. **288**, 672–675 (2000).
62. Feany, M. B. Rescue of the learning defect in *dunce*, a *Drosophila* learning mutant, by an allele of *rutabaga*, a second learning mutant. *Proc. Natl. Acad. Sci.* **87**, 2795–2799 (1990).
63. Scheunemann, L., Plaçais, P.-Y., Dromard, Y., Schwärzel, M. & Preat, T. *Dunce* Phosphodiesterase Acts as a Checkpoint for *Drosophila* Long-Term Memory in a Pair of Serotonergic Neurons. *Neuron* **98**, 350-365.e5 (2018).
64. Davis, R. L. & Dauwalder, B. The *Drosophila dunce* locus: learning and memory genes in the fly. *Trends Genet.* **7**, 224–9 (1991).
65. Yasuyama, K., Meinertzhagen, I. A. & Schürmann, F.-W. Synaptic connections of cholinergic antennal lobe relay neurons innervating the lateral horn neuropile in the brain of *Drosophila melanogaster*. *J. Comp. Neurol.* **466**, 299–315 (2003).
66. Tempel, B. L., Livingstone, M. S. & Quinn, W. G. Mutations in the dopa decarboxylase gene affect learning in *Drosophila*. *Proc. Natl. Acad. Sci.* **81**, 3577–3581 (1984).
67. Johnson, O., Becnel, J. & Nichols, C. D. Serotonin receptor activity is necessary for olfactory learning and memory in *Drosophila melanogaster*. *Neuroscience* **192**, 372–381 (2011).
68. Zhang, X., Li, Q., Wang, L., Liu, Z.-J. & Zhong, Y. Active Protection: Learning-Activated Raf/MAPK Activity Protects Labile Memory from Rac1-Independent Forgetting. *Neuron* **98**, 142-155.e4 (2018).
69. Schwaerzel, M. *et al.* Dopamine and octopamine differentiate between aversive and appetitive olfactory memories in *Drosophila*. *J. Neurosci.* **23**, 10495–502 (2003).
70. Margulies, C., Tully, T. & Dubnau, J. Deconstructing memory in *Drosophila*. *Curr. Biol.* **15**, R700-13 (2005).
71. Guan, Z., Buhl, L. K., Quinn, W. G. & Littleton, J. T. Altered gene regulation and synaptic morphology in *Drosophila* learning and memory mutants. *Learn. Mem.* **18**, 191–206 (2011).
72. Turrel, O., Goguel, V. & Preat, T. Amnesiac Is Required in the Adult Mushroom Body for Memory Formation. *J. Neurosci.* **38**, 9202–9214 (2018).
73. Tully, T. & Quinn, W. G. Classical conditioning and retention in normal and mutant *Drosophila melanogaster*. *J. Comp. Physiol. A.* **157**, 263–77 (1985).
74. Yin, J. C. P. *et al.* Induction of a dominant negative CREB transgene specifically blocks long-term memory in *Drosophila*. *Cell* **79**, 49–58 (1994).
75. Tully, T., Preat, T., Boynton, S. C. & Del Vecchio, M. Genetic dissection of consolidated memory in *Drosophila*. *Cell* **79**, 35–47 (1994).
76. Folkers, E., Drain, P. & Quinn, W. G. *Radish*, a *Drosophila* mutant deficient in consolidated

- memory. *Proc. Natl. Acad. Sci. U. S. A.* **90**, 8123–7 (1993).
77. Folkers, E., Waddell, S. & Quinn, W. G. The *Drosophila* radish gene encodes a protein required for anesthesia-resistant memory. *Proc. Natl. Acad. Sci. U. S. A.* **103**, 17496–500 (2006).
 78. LaFerriere, H., Speichinger, K., Stromhaug, A. & Zars, T. The Radish Gene Reveals a Memory Component with Variable Temporal Properties. *PLoS One* **6**, e24557 (2011).
 79. Szczecinski, N. S., Bockemühl, T., Chockley, A. S. & Büschges, A. Static stability predicts the continuum of interleg coordination patterns in *Drosophila*. *J. Exp. Biol.* **221**, jeb189142 (2018).
 80. Davis, R. L. Rac in the Act of Forgetting. *Cell* **140**, 456–458 (2010).
 81. Shuai, Y. *et al.* Forgetting Is Regulated through Rac Activity in *Drosophila*. *Cell* **140**, 579–589 (2010).
 82. Büschges, A., Akay, T., Gabriel, J. P. & Schmidt, J. Organizing network action for locomotion: Insights from studying insect walking. *Brain Res. Rev.* **57**, 162–171 (2008).
 83. Formstecher, E. *et al.* Protein interaction mapping: a *Drosophila* case study. *Genome Res.* **15**, 376–84 (2005).
 84. Liu, Y. *et al.* Hippocampal Activation of Rac1 Regulates the Forgetting of Object Recognition Memory. *Curr. Biol.* **26**, 2351–2357 (2016).
 85. Folkers, E., Waddell, S. & Quinn, W. G. The *Drosophila* radish gene encodes a protein required for anesthesia-resistant memory. *Proc. Natl. Acad. Sci.* **103**, 17496–17500 (2006).
 86. Tully, T., Preat, T., Boynton, S. C. & Del Vecchio, M. Genetic dissection of consolidated memory in *Drosophila*. *Cell* **79**, 35–47 (1994).
 87. Liu, Y. *et al.* Hippocampal Activation of Rac1 Regulates the Forgetting of Object Recognition Memory. *Curr. Biol.* **26**, 2351–2357 (2016).
 88. Zhang, X., Li, Q., Wang, L., Liu, Z.-J. & Zhong, Y. Active Protection: Learning-Activated Raf/MAPK Activity Protects Labile Memory from Rac1-Independent Forgetting. *Neuron* doi:10.1016/j.neuron.2018.02.025